Distribution Agreement

In presenting this thesis or dissertation as a partial fulfillment of the requirements for an advanced degree from Emory University, I hereby grant to Emory University and its agents the non-exclusive license to archive, make accessible, and display my thesis or dissertation in whole or in part in all forms of media, now or hereafter known, including display on the world wide web. I understand that I may select some access restrictions as part of the online submission of this thesis or dissertation. I retain all ownership rights to the copyright of the thesis or dissertation. I also retain the right to use in future works (such as articles or books) all or part of this thesis or dissertation.

Signature:

_____ _____

Jessica Hartmann Belle Date

Advanced gap-filling techniques in satellite-based $PM_{2.5}$ exposure models and their applications in air pollution epidemiology

By

Jessica Hartmann Belle
Doctorate of Philosophy

Environmental Health Sciences

_____

Yang Liu
Advisor

_____

Howard Chang
Committee Member

_____

James Mulholland
Committee Member

_____

Matthew Strickland
Committee Member

Accepted:

_____

Lisa A. Tedesco, Ph.D.
Dean of the James T. Laney School of Graduate Studies

_____

Date

Advanced gap-filling techniques in satellite-based $PM_{2.5}$ exposure models and their applications in air pollution epidemiology

By

Jessica Hartmann Belle
MSPH, Emory University, 2013
B.A., Augustana College, 2009

Advisor: Yang Liu, PhD, MS

An abstract of
A dissertation submitted to the Faculty of the
James T. Laney School of Graduate Studies of Emory University
in partial fulfillment of the requirements for the degree of
Doctor of Philosophy
in Environmental Health Sciences
2018

Abstract

Advanced gap-filling techniques in satellite-based $PM_{2.5}$ exposure models and their applications in air pollution epidemiology
By Jessica Hartmann Belle

Satellite-based models relating the satellite-derived parameter aerosol optical depth (AOD) to ground-level $PM_{2.5}$ have a number of advantages over more traditional approaches to exposure characterization. Namely, observations are available, via satellite, at a daily level over areas that lack traditional ground monitors. However, satellite-based models are also subject to cloud and snow-driven missingness which may bias results in unpredictable ways, particularly when satellite-derived $PM_{2.5}$ estimates are further used in human health studies. This dissertation focuses on the problem of missing observations in satellite retrievals. In chapter 1 we characterize the scope of the missing data problem in the daily Moderate resolution imaging spectroradiometer (MODIS) Aqua AOD product, finding that observations were only present in the United States on an average of 30% of possible days with the remaining 70% missing as a result of cloud-cover and surface brightness. In chapter 2 we strive to understand drivers, in terms of cloud cover properties and correlated meteorological conditions, behind differences between cloudy and non-cloudy $PM_{2.5}$ observations. We found that changes in temperature, wind speed, relative humidity, planetary boundary layer height, convective available potential energy, precipitation, cloud effective radius, cloud optical depth, and cloud emissivity were all associated with changes in $PM_{2.5}$ concentrations and composition at two sites, one in Atlanta, and one in San Francisco. A case study at the San Francisco site confirmed that accounting for cloud-cover and associated meteorological conditions could alter average concentrations and the predicted spatial distribution of daily $PM_{2.5}$ concentrations. In chapter 3, we aim to develop and compare the ability of different gap-filling methods to eliminate bias resulting from missing AOD observations in human health studies. We find that different gap-filling models produce comparable odds ratios in a study on the relationship between emergency department visits for asthma or wheeze, otitis media, and upper respiratory infection. However, when gap-filling was not used, odds ratios were attenuated towards the null for two of the three possible outcomes. This dissertation highlights the importance of understanding and correcting for missing observations in satellite retrievals when estimating $PM_{2.5}$ concentrations.

Advanced gap-filling techniques in satellite-based $PM_{2.5}$ exposure models and their applications in air pollution epidemiology

By

Jessica Hartmann Belle
MSPH, Emory University, 2013
B.A., Augustana College, 2009

Advisor: Yang Liu, PhD, MS

A dissertation submitted to the Faculty of the
James T. Laney School of Graduate Studies of Emory University
in partial fulfillment of the requirements for the degree of
Doctor of Philosophy
In Environmental Health Sciences
2018

Table of contents

List of Tables and Figures

Introduction

The first part of the 20th century was marked by two world wars, baby booms, economic booms, and economic busts. It was also a period of significant scientific and technological advancement. Between 1900 and 1950, Einstein proposed his theory of relativity, Niels Bohr his model of the atom, and, in 1953, Crick and Watson the structure of DNA. It became increasingly possible to measure, and thus, to understand, the world around us in more ways and with greater precision than ever before. The modern mass spectrometer was developed in 1918. The electron microscope in 1926. The spectrophotometer and the radiosonde also hail from this era, enabling an understanding of the physics and chemistry of the atmosphere, and, scientific weather predictions. Nations began or expanded information collection, routinely collecting and preserving information on their populations and environments. It was also during this period, and using these same tools, that we began to experience and understand the drawbacks of industrialization. Smog, a combination of smoke and fog, became a regularly occurring public nuisance, accompanied by watery eyes, poor visibility, sickness, and death.

Some of the earliest concrete scientific evidence for the detrimental impact of smog on human health and wellbeing was presented to the Royal Academy of Medicine in Belgium in 1931. A panel of experts had been appointed by the Royal Prosecutor of Liege to determine the cause of the deadly smog which had settled on the narrow Meuse valley and, over a period of 3 days, killed at least 60 and caused severe respiratory illness in many more. Evidence from necropsy of the victims showed damage to the respiratory tract, and within the lungs, the researchers noted that, "Pure carbon dust particles of 0.5-1.35 μm diameter were seen free within the alveoli or engulfed in polynuclear leucocytes." Meteorological

analyses described a temperature inversion over the valley, a meteorological phenomenon where warm air settles over the top of cooler air, effectively acting as a blanket and trapping any emitted smoke from the factories and homes within. Chemical analyses of emissions from industrial plants within the valley, measured after the episode, determined that Sulphur from coal burning was the most prominent substance and the panel concluded that this had likely been responsible for the deaths. [1] The combined evidence proved convincing for many and the report was widely read.

A similar incident occurred seventeen years later in Donora Pennsylvania, southeast of Pittsburgh. Patients, stricken with difficulty breathing, chest pain, nausea and vomiting, flooded local hospitals, exhausting supplies. Twenty died. Again, a panel was convened to determine the cause, with the conclusion that the deadly smog had been the result of the combination of another temperature inversion and emissions from local industrial plants. The likely chemical complicit in the deaths being Sulphur dioxide, specifically that carried on particulate matter (PM). [2]

These episodes, however, merely presaged the horror to come. In December of 1952, a heavy fog covered London for 4 days. 4,000 died. Concentrations of smoke and Sulphur dioxide were 3-10 times their normal values. [3] In a report, published in the Lancet in 1953, it was stated that, "death-rates attained a level that has been exceeded only rarely during the past hundred years – for example, at the height of the cholera epidemic of 1854 and the influenza epidemic of 1918-19." [4] Later reports noted that mortality had remained elevated for months after the episode, during which period an estimated 8,000 additional persons died. [3]

A smog problem of a different nature was brewing simultaneously in sunny Los Angeles, from the same ingredients that went into the deadly fogs; industrial pollution and meteorological conditions. Damage, in the form of silvering and bleaching of vegetation, particularly leafy vegetables, was first noted in the Los Angeles area in 1944. With each passing year, it got worse. At the behest of the Los Angeles Chamber of Commerce Agricultural committee and the Los Angeles County Air Pollution Control District, a research program was begun to determine the cause. After measuring trace gases and organic compounds in the air and running experiments on the effect each had on plants, they attributed the damage to oxidants, specifically peroxides formed from a reaction between ozone and hydrocarbon, also noting that photo-oxidation of hydrocarbons with NO_2 produced a similar effect. [5] Later work would confirm the ozone was the true culprit, and that it could be formed from the photo-oxidation of hydrocarbons with NO_2. The authors additionally confirmed that the Sulphur dioxides and particulates thought to be behind deadly smogs were not responsible for this type of damage to the vegetation. Interest grew in understanding air pollution in its various forms and, in the U.S., funds were allocated for its study in 1955.

Worried about smog events on the scale of what had happened in London, the county of Los Angeles began a monitoring program for warning purposes, appointing planning committees in 1954. [6] The result was an automated monitoring system, similar in concept to the stations in use today, with individual monitors placed throughout the city for meteorological information, carbon monoxide, sulfur dioxide, nitrogen dioxide, oxidants or ozone, and what we now know as black carbon. Two distinct patterns emerged from the resulting data, termed Type I and Type II contaminants. Concentrations of Type I contaminants, carbon monoxide, nitrogen dioxide, black carbon, and Sulphur dioxide, now

known as primary air pollutants, peaked twice daily, during the morning and evening rush hours when emissions were highest. Concentrations of Type II contaminants, oxidants and plant damage from oxidants, peaked once daily in the afternoon and were typically highest during the fall months. Type II contaminants, now known as secondary air pollutants, are the products of chemical reactions in the atmosphere involving sunlight and primary air pollutants. [7] Thus, by 1960 it was known that there were two distinct air pollution problems of similar origins.

As the human health and economic impacts of air pollution became increasingly obvious, governments began to introduce legislation to mitigate the problem, although efforts were primarily focused on contaminants known to directly impact human health and wellbeing. In 1963 the Clean Air Act (CAA) was passed in the U.S., allocating funds for research into the measurement and control of ambient air pollution concentrations. In 1967 the Air Pollution Control Act was passed to begin regulating concentrations of the air pollutants found in the two types of smog, based on the fact that they were damaging to human health, agriculture, and well-being. In 1970, the CAA was amended and revised to provide for the establishment, and enforcement, of state and federal standards for ozone, nitrogen dioxide, sulphur dioxide, particulate matter, and carbon monoxide. Standards were to be achieved through the regulation, by states, of emissions from a variety of sources, and compliance was measured using the network of ground-based monitors that had expanded from Los Angeles since the 1950's with the help of funds from the 1955, 1963, and 1967 air pollution control acts. In 1977, the CAA was again amended, this time to increase enforcement in areas unable or unwilling to achieve the 1970 standards. By 1980, the network of air pollution monitors used to measure compliance had been nationally standardized, and comparisons could be made between different areas in the United States. In 1990, the final set of amendments to

the clean air act were passed, expanding the enforcement authority of the federal government, and adding acid rain, depletion of the ozone layer by ChloroFluoroCarbons (CFCs), and hazardous air pollutants, including heavy metals, to the list of regulated air pollutants.

Research on the human health effects of air pollution continued over the time period corresponding to the regulatory ramp-up that started in 1955 and went through 1990. Follow-up work in Donora 10 years after the incident demonstrated that those sickened by the smog, particularly those with pre-existing chronic conditions such as asthma and cardio-pulmonary disease, had higher rates of morbidity and mortality from a range of conditions over the 10 years following the deadly smog. [8] A study on asthmatics in Los Angeles in 1961 demonstrated that asthma attacks were more likely on days with oxidant levels high enough to cause watery eyes or plant damage. [9] By the 1970's concentrations of particulate matter and sulfur dioxide had declined from the extremely high concentrations experienced during the 1950's and 1960's that led to the deadly smogs. [10] However, research on human health impacts continued, now often focused on more sensitive indicators, such as lung function and respiratory disorders or on vulnerable populations such as the elderly, asthmatics, and children. However, studies of daily fluctuations in mortality over long time series, conducted with the aid of ground-based monitors, dominated the literature, with the majority of work concentrated in New York City and London. [10]

Over this time-period, from 1955 through 1990, there was also a ramping up of statistical methods and the volume of data that could be handled as computers became more widely available. The earliest studies calculated simple correlations between air pollutant concentration and deviations from a moving average of mortality counts, used to remove

seasonal effects. [11] By the late 1970's, sophisticated time series models were common, particularly regression analyses, including more advanced models such as ridge regression and constrained least squares. [12] By the 1990's multi-stage log-linear and Poisson models were in use, and in the 2000's you start to see generalized additive models (GAM), and Bayesian statistics. Both pollution and mortality are correlated with season, climate, demographic characteristics, availability of physician care, smoking status, and home heating and cooking methods, confounding results, particularly at lower concentrations. [13] There was also substantial debate over collinearity between different pollutant effects, and the exact nature of the exposure-response relationship, which would continue until the present day. Specifically, debate on the exposure response relationship centered on whether or not there was a threshold below which negative impacts were not observed, and which could be used for regulatory purposes. [14] [12]

A majority of studies were population-based, or ecological in nature, with all of the population under study typically exposed to some extent, contributing to issues with understanding the nature of the exposure response curve. Although, the widespread exposure misclassification and the fact that a minority of studies relied on any consistent definition of particulate matter and Sulphur oxide measurement [10] didn't help either. Thus, while studies published up to 1980 were sufficient to demonstrate that sulfate-based smog was broadly damaging to respiratory health at high concentrations, the precise definition of a 'high concentration,' and how best to go about measuring it, proved elusive. [13,15] The next leap forward in air pollution research came in the early 1990's, with the publication of the Harvard Six Cities and American Cancer Society (ACS) cohort studies, conducted in the 1970's and 80's. These studies established that fine particulate matter was associated with a

small, but significant, increased risk of death, specifically that from cardiovascular disease and respiratory illness.

Particulate matter and human mortality

The Harvard Six Cities (HSC) study came first. Begun in 1974, the authors deployed monitors for a variety of pollutant measures at centralized locations in the study areas both prior to enrolling cohorts of participants and throughout the duration of the cohort study. [16] Separate, comparable, cohorts consisting of a few thousand children and adults were enrolled and followed for over 12 years in 6 U.S. cities: Watertown, MA; Kingston and Harriman, TN; Steubenville, OH; St. Louis, MO; Portage, WI; and Topeka, KS. [17] While the study began as an investigation into the respiratory health of children and adults exposed to air pollutants, as measured using tests of lung function and vital status, the design mitigated many of the issues associated with previous studies and by the end, a number of other causes had jumped on the bandwagon. Dozens of studies have been published on the Harvard Six Cities cohort, including multiple landmark studies that remain relevant to this day. A feat of study design in and of itself.

More to the point, the HSC study was instrumental in providing a more nuanced understanding of what air pollution was, as well as how and at what concentrations it was relevant to human health. Much of the development focused on particulate matter (PM). Sticky balls of molecules that roll around in the air, picking up other molecules of whatever they collide with: water, soot, dust, pollen, smoke, heavy metals, and condensable products of chemical reactions between gases in the atmosphere. Particulates range in size from a few

nanometers to several hundred micrometers (μm) across, or from the size of a single molecule of sugar to that of an amoeba.

At the beginning of the HSC study, measurement and regulation of particulate concentrations was typically done via the Total Suspended Particulates (TSP) method. Most monitors for particulate matter work by drawing air in through an inlet at a prespecified rate, catching any particulate mass on a filter, and then using the change in the weight of the filter and the rate of air flow to it to determine the concentration in the air over a period of time. TSP samplers have the largest inlets, allowing particles up to 100 μm in diameter through to the filter. The issue with this, as it relates to human health, is that our respiratory tracts are quite effective at filtering out these larger particles, which also tend to be heavier than smaller particles. TSP sampler-based concentrations, therefore, include a large, but highly variable proportion of mass in the concentration that is not relevant to human health. This reduces the signal-to-noise ratio in any health studies based off of the TSP metric, and for regulatory purposes, unfairly penalizes areas that tend to have more soil, dust, and sand in the air as a result of natural causes. To handle this problem, monitors were developed with smaller inlets that would allow only particles below a certain size to accumulate on the filters.

This led to the development of the modern concepts of PM_{10} and $PM_{2.5}$, or coarse particulate matter (PM) below 10 μm in diameter (PM_{10}) and fine particulate matter below 2.5 μm in diameter ($PM_{2.5}$). These designations roughly correspond to the particle sizes that, in humans, are able to penetrate into the upper respiratory tract (PM_{10}) and into the lungs ($PM_{2.5}$). The HSC study, as part of its experimentation with the measurement of particulate matter, was an early adopter of the newer, size-selective samplers. While the original study design had called for the use of TSP when sampling for particulate matter, additional

sampling for $PM_{2.5}$ and PM_{15} (PM less than 15 μm in diameter) began in the 6 cities in the late 1970's, and for PM_{10} in 1984. [18] As a result of the early adoption of newer measurement techniques, many of which were developed at Harvard, researchers with the HSC were able to examine health associations with TSP, PM_{10}, and $PM_{2.5}$ over the course of more than a decade. Of the methods available to measure peoples' exposure to particulate matter, $PM_{2.5}$ showed the strongest associations with human mortality. [19] A reanalysis of the same data in 1996 and again in 2000, additionally demonstrated that there was little to no additional information relevant to human mortality in the PM_{10} metric that could not be explained by $PM_{2.5}$ concentrations. [20,21] Following this research, in 1987 the US EPA updated the particulate standards to be based off of PM_{10} standard, and in 1997, added an additional $PM_{2.5}$ standard for human health. [22] [23]

The HSC study also examined the more relevant exposure in terms of the composition, as well as the size of the particulates. Particulate matter tends to have average compositions that reflect local emissions and the typical size of the molecules and other particles that have been added to them. For instance, larger particles are more likely to be primarily composed of soil or sand, while smaller particles are more likely to be composed of condensed gases. Hundreds of different compounds can be found in PM. However, at the time of the HSC study, the acidity of the particulates was a matter of great concern, as PM provided a mechanism where strong acids could be delivered straight to tissues in the respiratory tract, including the lungs. What makes a particle acidic though? The short answer is sulfate and nitrate, both products of fossil fuel combustion. The long answer is more complicated and is something we're still fleshing out. [24] Monitoring for aerosol acidity as part of the HSC study began in 1985 and continued through 1987. They estimated that, after accounting for ventilation rates, time activity patterns, and deposition rates in the various parts of the

respiratory tract, children were receiving a dose of acid to their lungs of between 1,240 and 3,240 nanomoles every 12 hours. [25] This was within the range that, in controlled studies in adults, caused respiratory symptoms. Health studies found that aerosol acidity was associated with increased symptoms in asthmatics, and with increased rates of bronchitis in children. [26,27] Contemporary studies had found that aerosol acidity beat out black smoke at predicting adult mortality in London. [28] HSC, however, found that total $PM_{2.5}$ was more strongly associated with human mortality than aerosol acidity [19] Specifically, mortality resulting from cardiopulmonary diseases, and lung cancer. This set the stage for the publication of the American Cancer Society study.

The American Cancer Society (ACS) study was very different in both design and purpose. The ACS Cancer Prevention Study II (CPS-II) is a (still) ongoing mortality study of 1.2 million volunteers, enrolled in the fall of 1982 during a national campaign in the United States, and followed until death. Pope et al. relied on the network of EPA monitors to measure participants' exposure to $PM_{2.5}$ and sulfate in and around 1980, then compared mortality rates, adjusted for age, sex, race, smoking status, exposure to passive smoke, occupational exposure, education, BMI, and alcohol use, from the most polluted cities to those from the least polluted cities. They found that increased rates of death from all causes together and cardiopulmonary disease specifically were associated with living in an area with high concentrations of sulfate and $PM_{2.5}$. Living in an area with high concentrations of sulfate was also associated with increased rates of death from lung cancer. [29] These results, along with others, eventually confirmed the causal association between chronic exposures to air pollution and human mortality, particularly that from cardiopulmonary disease and lung cancer.

The reanalyses and extensions

However, voices outside of, and within, the Harvard cohort responsible for most of the mortality research noted problems with the studies. Academic debates raged for decades, some continue to this day, over key issues; the harvesting effect, the shape of the exposure response curve, confounders, effect modifiers, co-pollutants, and the ecological fallacy. In response, the HSC and ASC studies, in particular, were replicated, audited, extended and reanalyzed to within an inch of their lives.

First came the replication, performed by the independent Health Effects Institute (HEI) in 2000, accompanied by an extensive sensitivity analysis. [30] The HEI investigators found that the original HSC and ACS study results were robust to changes in the confounders that were included, the model used, or the population subgroup studied, with one exception. The exception had to do with educational level, which HEI found modified the effect of air pollution on mortality, effectively showing that the effect was stronger among the less educated. This was important because they also investigated the impact of spatial correlation on the results, finding both that they were unable to completely control for it and that it impacted the results, decreasing the magnitude of the effect found. The shape of the exposure-response relationship was investigated as well. They found that it was linear over most of the exposure distribution, but there were indications of non-linearity at the extremes. They additionally examined co-pollutants and the impact of considering them on the results, finding that sulfate had an impact on mortality that was independent of PM. They additionally considered the impact of changes in air pollution levels over time on the relationship between PM and mortality. HEI found that the risk of death associated with PM

was lessened when concentrations decreased. [30] The authors of the HEI report followed up on this with a separate publication in 2002, concluding that decreases in concentrations were associated with a decreased risk of death, and that the timing of the exposure relative to the timing of death was irrelevant. [31]

A second validation, replication and sensitivity analysis effort was published in 2004 and 2005, also by the HEI authors. This involved an audit of the medical records, which found that around 1% of the records were inaccurate, but the results were robust to this type of error. [32] [33] This sensitivity analysis was more extensive than the last, including examination of previously unconsidered confounders, changes in confounders over time, and occupational exposures. [34] They again found that the results were robust to everything except effect modification by educational level.

Follow-up on the HSC cohort by the original authors at Harvard was eventually extended through to 2009. Two studies were published on the extended follow-up. One in 2006, and a second in 2012. Both found comparable results to those in the original study, an increase in all-cause, cardiovascular, and respiratory mortality of 14%, 26%, and 37%, respectively in the 2012 follow-up study. They additionally concluded that reductions in $PM_{2.5}$ concentrations were associated with reductions in mortality. Of particular interest in these later studies was the relevant time period of exposure to that of death and the shape of the exposure-response function.

Cohorts galore

While the reanalyses of the HSC and ACS studies were being conducted, more cohorts were assembled to look at the problem. The first published was the California Seventh-day Adventists study, in 1999 and 2000. They found that, in males, PM_{10} and $PM_{2.5}$

concentrations were associated with increased all-cause, respiratory, and lung cancer mortality, with increases in the individual risk of mortality of 22%, 64%, and 123%, respectively, for a 24.3 $\mu g/m^3$ increase in $PM_{2.5}$ concentrations in the non-smoking Seventh-day Adventist population. The author's additionally concluded that chronic exposures were more relevant than exposure within the past month, and that $PM_{2.5}$ was responsible for most of the associations with PM_{10}. [35]

Next, in 2007 from the University of Washington, came the Women's health initiative study results. A cohort of ~66,000 post-menopausal women in 36 U.S. cities, all of whom with no preexisting cardiovascular disease, was assembled. It was a huge study involving multiple arms, of which the air pollution study was simply a small part. They found that the risk of a cardiovascular event increased by 24% for each 10 $\mu g/m^3$ increase in annual average pollutant concentrations from the nearest regulatory monitor and that the risk of death from cardiovascular disease was increased by 76% for the same change in pollutant concentrations. [36] Associations specific to stroke were slightly higher, 35% increase in risk of a stroke and an 83% increase in the risk of death from a stroke. This demonstrated that air pollution concentrations were associated with both the development of cardiovascular disease and with increased rates of death from cardiovascular disease, specifically disease assumed to be atherosclerotic. The study additionally looked at the contribution of within and between-city variability in air pollution concentrations, finding that within-city contrasts were often greater than between-city contrasts in air pollution concentration and, thus, cardiovascular risk. This same issue of within versus between city contrasts in air pollution and their relevance to public health was studied in a Dutch cohort in 2008. The Netherlands Cohort Study on Diet and Cancer (NLCS), begun in 1986, was co-opted for the purposes of studying the impact air pollution on human health, specifically at levels below current

standards, estimated using land use models and traffic intensity data. Their results were not statistically significant, but were slightly positive, and were comparable in magnitude to those found in the ACS cohort in the U.S., although, in the Dutch cohort they additionally found associations between respiratory mortality and traffic intensity, supporting the importance of within-city variability. [37]

The nurses' health study was also co-opted to respond to the women's health initiative results. By this point, 2009, within-city models of air pollution concentrations had gotten far more sophisticated than the simple across-monitor averages used in HSC and ACS studies, and the nearest monitor averages used in the WHI study. The Nurse's Health study used a GAMM model to interpolate monitor observations within cities, with the help of meteorological data, road networks, and land use, to get estimates of pollutant concentrations at residential addresses. They found increased risks of all-cause and coronary heart disease-related mortality, of, respectively, 26% and 102% for each 10 $\mu g/m^3$ increase in annual average $PM_{2.5}$ concentrations at the patient's residence, comparable to results from the HEI study. [38] This was followed by the Health professionals' follow-up study in 2011, a male-only cohort. They used the same methods as the nurses' health study, but found no significant associations with air pollution in their population of affluent males. [39] This lent credence to the idea that not all populations were equally affected by air pollutant concentrations, with effects concentrated among the less educated or less affluent members of a population.

The multi-city studies

Following the HSC and ACS studies were a number of other large, multi-city mortality studies that were important in the literature and bear mentioning before we move on from mortality studies, which only give us some insight into how air pollution impacts people through inducing an early death, to morbidity and mechanisms of action. The first was the Air Pollution and Health: a European Approach (APHEA) project, published in 1997. [40] In 15 European cities spread out over 10 countries, the researchers compared concentrations of Sulphur dioxide, black smoke, and PM_{10} concentrations from regulatory monitors to mortality rates across cities using city-specific auto-regressive Poisson time-series models, and pooling effects across cities by means of a weighted average. They found overall increases in daily mortality associated with a 50 $\mu g/m^3$ increase in sulfur dioxide, black smoke, and PM_{10}, respectively, of 2%. 1%, and 2%.

The second was the John's Hopkins 20 city study, published in 2000. Similar in concept to the APHEA study, the 20 city study looked at associations between concentrations of ozone, PM_{10}, nitrogen dioxide, sulfur dioxide, and carbon monoxide, measured using regulatory ground-monitors, and mortality in 20 of the most populous US cities. They used a slightly more sophisticated two-stage log-linear regression model, where the first stage was fit to each city, and the second stage combined estimates across cities. After adjusting for concentrations of co-pollutants, ozone, nitrogen dioxide, sulfur dioxide, and carbon monoxide, a 10 $\mu g/m^3$ increase in PM_{10} concentrations was associated with a 0.3-0.6% increase in daily mortality. Like in the Harvard 6 cities study, they found slightly higher mortality increases associated with respiratory and cardiovascular than all-cause mortality.[41] NMMAPS, a 90 city extension of the John Hopkin's 20 city study by the same authors, but funded by the HEI institute, found similar results, about a 5% increase in daily mortality for each 10 $\mu g/m^3$ increase in PM10.

The last was a combined study, called APHENA, published in 2007, that included the APHEA cities, NMMAPS cities, and a set of Canadian cities that had also been studied previously. Using a common protocol to analyze data from all 124 cities included in the study, APHENA pooled results. They found that cardiovascular mortality was elevated among the elderly (>75 years of age) by 1.3% in the Canadian cities, 0.5% in the European cities, and 0.5% in the U.S. cities for each 10 $\mu g/m^3$ increase in PM_{10} concentrations on the day preceding the death.

Estimates for the impact of PM on mortality differed between the multi-city studies highlighted here and the HSC study and its reanalyses. The HSC extensions found increases in the risk of mortality of 14% for all-cause, 26% for cardiovascular, and 37% for lung cancer between the most and least polluted cities. APHENA found increases of ~0.5% for cardiovascular mortality for the same increase in pollutant concentrations, 10 $\mu g/m^3$. Apart from the differences in study design, the HSC and APHENA studies were very different in terms of the time frames over which they looked for these effects. HSC looked at chronic exposures, or concentrations experienced over long time-periods, and relied on annual averages when calculating their effects. APHENA and the studies that composed it, looked at acute exposures, or concentrations experienced in the day or so preceding the mortality event. The two are related, areas that tend to have high annual average concentrations also tend to have high daily concentrations, but are not the same, and differ in terms of the effects they have on the human body. Thus, the multi-city studies are only capturing deaths that occur as a result of short-term, acute exposures to high concentrations of PM, and ignoring deaths that may have occurred as a result of chronic exposure to lower levels of PM.

Taken together, the multi-city studies along with the HSC and ACS cohorts, conducted largely at Harvard, University of Athens, and John's Hopkins University, established that short-term and long-term increases in PM concentrations were associated with a small, but significant, increased risk of death, specifically that from cardiovascular disease and respiratory illness. They also established that this effect was consistent across different populations of people.

PM and hospitalizations

While mortality is useful as a health endpoint, it often represents the tip of the iceberg. The latter half of the 1990's saw an increasing number of studies focused on the link between air pollution and hospitalizations for various causes, particularly since by this time medical billing for Medicaid made hospital billing records both a standardized and widely available indicator of morbidity in the elderly, a particularly vulnerable population. [42] There was existing evidence for this link, mass hospitalizations had contributed to the extreme incidents in Meuse valley and Donora. By August of 2000, 12 studies on the topic had been published. [43] Admissions for congestive heart failure and ischemic heart disease were associated with PM_{10} exposure, increasing around 0.7% for each 10 $\mu g/m^3$ increase in PM_{10}, comparable to the increased mortality estimates seen in the multi-city studies.

A 2006 analysis of 11.5 million medicare enrollees in the 204 most populous U.S. counties found increased hospitalization rates associated with same-day, previous day, or two days previous concentrations of $PM_{2.5}$ for all health outcomes excepting injuries. They found a 1.28% increase in the hospitalization rates for heart failure, and noticed heterogeneity in effect estimates across the United States, with higher estimates in the East.

PM mechanisms of action

The thick stew of studies on air pollution and human health was, combined with toxicological studies done in animals and people, sufficient by 2010 to flesh out a number of mechanisms through which PM could act on the human body to adversely affect cardiovascular health. Namely by inducing pulmonary and systemic inflammation and oxidative stress, increasing thrombosis and coagulation, increasing systemic and pulmonary arterial BP, altering vascular function, worsening atherosclerosis, reducing heart rate variability, inducing cardiac ischemia and repolarization abnormalities, inducing epigenetic changes, and worsening insulin resistance. [44] Similarly, mechanisms were fleshed out whereby PM had direct impacts on respiratory health; by increasing symptoms and medication use in children with asthma, reducing pulmonary function, inducing pulmonary inflammation and oxidative stress, inducing pulmonary injury and allergic responses, activating host defenses, and inducing lung cancer mortality. [45] This, rather horrifying, list bolstered the evidence base for both chronic and acute impacts of PM exposure on human cardiac and respiratory health, although some of the details are still being fleshed out.

The body's response to particulate matter starts with a breath of less than fresh air. Whether or not a particle ends up in the lungs depends on the size of the particle. A large fraction of particles between around 1 and 0.1 μm, and a smaller fraction of larger and smaller particles, are never deposited in the respiratory tract, but leave the body during expiration. [45] During inspiration, the air enters through the nose and larynx, within which particle deposition varies in efficiency between 10 and 0.5 μm, nearly all particles 10-15 μm in size or larger and few to none of particles 0.5 μm or less are deposited. In mouth breathers, few to no particles

are deposited of a diameter 2 μm or less and deposition efficiencies increase to 90% for particles 10 μm in diameter. [46] [47] The aerosols not filtered out by the nose and larynx continue down through the trachea to the bronchi, which filter out a small number of particles between 0.5 and 15 μm in diameter and an increasingly large proportion of particles less than 0.5 μm, such that around 30% of particles of 0.01 μm across are deposited in the bronchi. [47] The remaining particulates, which tend to be smaller in size on average, make it into the alveoli. The alveoli, in contrast to the bronchi, trachea, larynx, nose, and mouth, lack an efficient way to remove particles from the body before they can cause harm, a process called clearance. [45]

Once the particles have deposited in the alveoli they interact with lung and immune cells, as well as their protective secretions. [44] The exact response by the body's cells is determined by a number of factors, including anti-oxidant levels in the host and the size, charge, potential ability to produce reactive oxygen species (ROS), and solubility of the particles. [44] Some particles are eventually cleared from the lung, some stay, or are engulfed within immune cells and digested, some of the smallest particles pass directly into the circulatory or lymphatic systems. [48] Some will activate nerve cells, designed to detect irritant particles and gases, and activate the autonomic nervous system. If the ROS potential of the particulates, such as those containing metals, organic compounds, Polycyclic Aromatic Hydrocarbons (PAHs), and semi-quinones, which tend to have the greatest ROS potential, is greater than the antioxidant potential in the cells and protective secretions of the lungs, a state of oxidative stress ensues. This state triggers a local inflammatory response, releasing cytokines and other chemicals to recruit immune cells to the site. [49] These same types of particles are also capable of directly facilitating an inflammatory response. This inflammatory response can trigger a worsening of the original oxidative stress which can trigger additional

inflammation, and so on. This cycle, involving oxidative stress and inflammation, combined with activation by particulates of the automatic nervous system (ANS), is central to the body's response to particulates, and ultimately begets many of the bodily responses to PM.

This pulmonary inflammation and oxidative stress, and the resulting immune response, can injure delicate lung tissues, activating additional host defenses and intensifying the cycle of oxidative stress and immune escalation. Pulmonary injury can also induce airway hyperresponsiveness, a key marker of asthma patients and contributor to findings of decreased lung function following PM exposure. Injury or irritation increases the permeability of the tissues lining the airway and capillaries within the alveoli, allowing passage of PM components, oxidative compounds, and inflammatory mediators into the general circulation. This can then set off or worsen an existing systemic cycle of inflammation and oxidative stress, a fact supported by epidemiological evidence showing elevated levels of inflammatory biomarkers, most consistently C-reactive protein, following PM exposure. If the host has been sensitized by repeated exposures, allergic responses can be activated both systemically and within the pulmonary system. Rogue oxidative compounds of the right size have been shown to enter the nuclei of cells and damage DNA, ultimately resulting in possible lung cancer. [45]

Systemically, the combination of spillover of inflammatory mediators and oxidative compounds from the lungs into the circulatory system, passage of the smallest particles and soluble compounds into the circulatory system, and ANS activation by particulates, are largely responsible for the cardiovascular effects of PM. Systemic oxidative stress and inflammation leads to increased coagulation and thrombosis of the blood, while ANS activation and PM in the circulatory system can both lead to platelet aggregation. Meanwhile,

PM, ANS activation, and systemic inflammation all led to vasoconstriction, endothelial dysfunction, and increases in an individual's reactive oxygen species (ROS) potential. ANS activation, along with indirect effects from vasoconstriction, has been shown to lead to increased blood pressure and heart rate. Systemic inflammation and oxidative stress is associated with atherosclerosis and metabolic changes that induce dyslipidemia and insulin resistance.

These cellular and, ultimately, systemic effects on the human body ultimately explain increased acute mortality from cardiovascular and respiratory causes, as well as increased rates of emergency room use, particularly by asthmatics and others with pre-existing disease. Chronic impacts are derived from these acute insults, but additionally involve the body's response to repetitive injury. As such, chronic impacts on the cardiopulmonary system include: atherosclerosis, blood coagulation, systemic inflammation and oxidative stress, venous thromboembolism, metabolic syndromes, changes in cardiac mass and output, coronary heart disease, stroke, pulmonary injury, pulmonary inflammation, allergic responses and increased mortality. Much of the epidemiologic research has focused on elderly or pediatric populations, as these populations are particularly vulnerable to the effects of air pollution.

Pregnant women, are another population of concern. The basic cellular mechanisms through which harm may be caused to the fetus are thought to be the same, however, with the inflammation/oxidative stress cycle at the center. Epidemiological associations have been found with a variety of birth outcomes, including restricted growth, pre-term birth, low birth weight, birth defects, and infant mortality. [45] Of these, low birth weight, restricted growth,

and pre-term birth are interrelated in that low birth weight can result from either restricted growth or pre-term birth.

Remote sensing of aerosols

Remote sensing entered the field of $PM_{2.5}$ research in 2003, when Jun Wang and Sundar Christopher at the University of Alabama published an "Intercomparison between satellite-derived aerosol optical thickness and $PM_{2.5}$ mass: Implications for air quality studies." [50] This paper focused on large positive correlations between MODIS aerosol optical depth (AOD), and $PM_{2.5}$ measurements at seven locations in Jefferson County, AL, demonstrating that MODIS AOD was correlated with $PM_{2.5}$ mass at ground-level stations with R=0.7. In 2004, Jill Engel-Cox et al published a national-scale paper looking at correlations between AOD and $PM_{2.5}$ concentrations at ground monitors throughout the United States, relating PM2.5 concentrations to AOD with a simple linear model to get the equation: $PM_{2.5}$(daily) = 7.54 + 18.66*AOD. [51]. By the summer of 2004, EPA scientists, working with scientists at NASA and NOAA, were able to build a satellite-based forecasting program for operational use through the AIRNow website. [52]

Over the next few years, a number of other studies published on correlations between various satellite's AOD products, and there was a ramping up of statistical methods. [53] [54] Models moved from the linear scale to the log-linear scale. [55] The addition of various meteorological parameters, such as relative humidity and planetary boundary layer height improved model fits. By 2009, complex two-stage GAM models were in use. [56] In 2011, a linear mixed effects model was proposed with random intercepts for each day in the year

and random slopes for AOD. [57]. Finally, in 2017 you start to see machine learning models. [58].

Works Cited

1. Nemery, B.; Hoet, P.H.; Nemmar, A. The meuse valley fog of 1930: An air pollution disaster. *The Lancet* **2001**, *357*, 704-708.
2. Schrenk, H.H.; Heimann, H.; Clayton, G.D.; Gafafer, W.M.; Wexler, H. *Air pollution in donora, pa. Epidemiology of the unusual smog episode of october 1948. Preliminary report*. Wash: 1949; p ix+173 pp.
3. Wilkins, E. Air pollution and the london fog of december, 1952. *Journal of the Royal Sanitary Institute* **1954**, *74*, 1-21.
4. Logan, W. Mortality in the london fog incident, 1952. *The Lancet* **1953**, *261*, 336-338.
5. Haagen-Smit, A.; Darley, E.F.; Zaitlin, M.; Hull, H.; Noble, W. Investigation on injury to plants from air pollution in the los angeles area. *Plant Physiology* **1952**, *27*, 18.
6. Chass, R.L.; Pratch, M.; Atkisson, A.A. The air pollution disaster—prevention program of los angeles county. *Journal of the Air Pollution Control Association* **1958**, *8*, 72-86.
7. Hamming, W.J.; Macphee, R.D.; Taylor, J.R. Contaminant concentrations in the atmosphere of los angeles county. *Journal of the Air Pollution Control Association* **1960**, *10*, 7-16.
8. Ciocco, A.; Thompson, D.J. A follow-up of donora ten years after: Methodology and findings. *American Journal of Public Health and the Nations Health* **1961**, *51*, 155-164.

9. Schoettlin, C.E.; Landau, E. Air pollution and asthmatic attacks in the los angeles area. *Public Health Reports* **1961**, *76*, 545.

10. Ware, J.H.; Thibodeau, L.A.; Speizer, F.E.; Colóme, S.; Ferris Jr, B.G. Assessment of the health effects of atmospheric sulfur oxides and particulate matter: Evidence from observational studies. *Environmental Health Perspectives* **1981**, *41*, 255.

11. Martin, A. Mortality and morbidity statistics and air pollution. SAGE Publications: 1964.

12. Schimmel, H. Evidence for possible acute health effects of ambient air pollution from time series analysis: Methodological questions and some new results based on new york city daily mortality, 1963-1976. *Bulletin of the New York Academy of Medicine* **1978**, *54*, 1052.

13. Lebowitz, M.D. Utilization of data from human population studies for setting air quality standards: Evaluation of important issues. *Environmental health perspectives* **1983**, *52*, 193.

14. Schimmel, H.; Murawski, T.J. The relation of air pollution to mortality. *Journal of Occupational and Environmental Medicine* **1976**, *18*, 316-333.

15. Whittemore, A.S. Air pollution and respiratory disease. *Annual review of public health* **1981**, *2*, 397-429.

16. Speizer, F.E. Studies of acid aerosols in six cities and in a new multi-city investigation: Design issues. *Environmental health perspectives* **1989**, *79*, 61.

17. Speizer, F.E. Asthma and persistent wheeze in the harvard six cities study. *CHEST Journal* **1990**, *98*, 191S-195S.

18. Ferris Jr, B.; Speizer, F.; Spengler, J.; Dockery, D.; Bishop, Y.; Wolfson, M.; Humble, C. Effects of sulfur oxides and respirable particles on human health: Methodology

and demography of populations in study 1–3. *American Review of Respiratory Disease* **1979**, *120*, 767-779.

19. Dockery, D.W.; Pope, C.A.; Xu, X.; Spengler, J.D.; Ware, J.H.; Fay, M.E.; Ferris Jr, B.G.; Speizer, F.E. An association between air pollution and mortality in six us cities. *New England journal of medicine* **1993**, *329*, 1753-1759.

20. Klemm, R.J.; Mason Jr, R.M.; Heilig, C.M.; Neas, L.M.; Dockery, D.W. Is daily mortality associated specifically with fine particles? Data reconstruction and replication of analyses. *Journal of the Air & Waste Management Association* **2000**, *50*, 1215-1222.

21. Schwartz, J.; Dockery, D.W.; Neas, L.M. Is daily mortality associated specifically with fine particles? *Journal of the Air & Waste Management Association* **1996**, *46*, 927-939.

22. Haines, J. Revisions to the national ambient air quality standards for particulate matter. Division, S.a.A.S., Ed. Federal Register, 1987; Vol. 52, pp 24634-24669.

23. Haines, J. National ambient air quality standards for particulate matter. Division, A.Q.S.a.S., Ed. EPA: Federal Register, 1997; Vol. 62, pp 38652-38760.

24. Weber, R.J.; Guo, H.; Russell, A.G.; Nenes, A. High aerosol acidity despite declining atmospheric sulfate concentrations over the past 15 years. *Nature Geoscience* **2016**.

25. Spengler, J.; Keeler, G.; Koutrakis, P.; Ryan, P.; Raizenne, M.; Franklin, C. Exposures to acidic aerosols. *Environmental health perspectives* **1989**, *79*, 43.

26. Dockery, D.W.; Cunningham, J.; Damokosh, A.I.; Neas, L.M.; Spengler, J.D.; Koutrakis, P.; Ware, J.H.; Raizenne, M.; Speizer, F.E. Health effects of acid aerosols on north american children: Respiratory symptoms. *Environmental health perspectives* **1996**, *104*, 500.

27. Ostro, B.D.; Lipsett, M.J.; Wiener, M.B.; Selner, J.C. Asthmatic responses to airborne acid aerosols. *American journal of public health* **1991**, *81*, 694-702.

28. Thurston, G.D.; Ito, K.; Lippmann, M.; Hayes, C. Reexamination of london, england, mortality in relation to exposure to acidic aerosols during 1963-1972 winters. *Environmental health perspectives* **1989**, *79*, 73.

29. Pope III, C.A.; Thun, M.J.; Namboodiri, M.M.; Dockery, D.W.; Evans, J.S.; Speizer, F.E.; Heath Jr, C.W. Particulate air pollution as a predictor of mortality in a prospective study of us adults. *American journal of respiratory and critical care medicine* **1995**, *151*, 669-674.

30. Krewski, D.; Burnett, R.T.; Goldberg, M.S.; Hoover, K.; Siemiatycki, J. Special report reanalysis of the harvard six cities study and the american cancer society study of particulate air pollution and mortality part ii: Sensitivity analyses appendix c. Flexible modeling of the effects of fine particles. *Health Effects Institute. Cambridge, MA* **2000**, *246*.

31. Villeneuve, P.J.; Goldberg, M.S.; Krewski, D.; Burnett, R.T.; Chen, Y. Fine particulate air pollution and all-cause mortality within the harvard six-cities study: Variations in risk by period of exposure. *Annals of Epidemiology* **2002**, *12*, 568-576.

32. Krewski, D.; Burnett, R.T.; Goldberg, M.S.; Hoover, K.; Siemiatycki, J.; Abrahamowicz, M.; White, W.H. Validation of the harvard six cities study of particulate air pollution and mortality. *New England Journal of Medicine* **2004**, *350*, 198-199.

33. Krewski, D.; Burnett, R.; Goldberg, M.; Hoover, K.; Siemiatycki, J.; Abrahamowicz, M.; White, W. Reanalysis of the harvard six cities study, part i: Validation and replication. *Inhalation toxicology* **2005**, *17*, 335-342.

34. Krewski, D.; Burnett, R.; Goldberg, M.; Hoover, K.; Siemiatycki, J.; Abrahamowicz, M.; Villeneuve, P.; White, W. Reanalysis of the harvard six cities study, part ii: Sensitivity analysis. *Inhalation toxicology* **2005**, *17*, 343-353.

35. McDonnell, W.F.; Nishino-Ishikawa, N.; Petersen, F.F.; Chen, L.H.; Abbey, D.E. Relationships of mortality with the fine and coarse fractions of long-term ambient pm10 concentrations in nonsmokers. *Journal of Exposure Science and Environmental Epidemiology* **2000**, *10*, 427.

36. Miller, K.A.; Siscovick, D.S.; Sheppard, L.; Shepherd, K.; Sullivan, J.H.; Anderson, G.L.; Kaufman, J.D. Long-term exposure to air pollution and incidence of cardiovascular events in women. *N Engl j Med* **2007**, *2007*, 447-458.

37. Beelen, R.; Hoek, G.; van Den Brandt, P.A.; Goldbohm, R.A.; Fischer, P.; Schouten, L.J.; Jerrett, M.; Hughes, E.; Armstrong, B.; Brunekreef, B. Long-term effects of traffic-related air pollution on mortality in a dutch cohort (nlcs-air study). *Environmental health perspectives* **2008**, *116*, 196.

38. Puett, R.C.; Hart, J.E.; Yanosky, J.D.; Paciorek, C.; Schwartz, J.; Suh, H.; Speizer, F.E.; Laden, F. Chronic fine and coarse particulate exposure, mortality, and coronary heart disease in the nurses' health study. *Environmental health perspectives* **2009**, *117*, 1697.

39. Puett, R.C.; Hart, J.E.; Suh, H.; Mittleman, M.; Laden, F. Particulate matter exposures, mortality, and cardiovascular disease in the health professionals follow-up study. *Environmental health perspectives* **2011**, *119*, 1130.

40. Katsouyanni, K.; Touloumi, G.; Spix, C.; Schwartz, J.; Balducci, F.; Medina, S.; Rossi, G.; Wojtyniak, B.; Sunyer, J.; Bacharova, L. Short term effects of ambient sulphur

dioxide and particulate matter on mortality in 12 european cities: Results from time series data from the aphea project. *Bmj* **1997**, *314*, 1658.

41. Samet, J.M.; Dominici, F.; Curriero, F.C.; Coursac, I.; Zeger, S.L. Fine particulate air pollution and mortality in 20 us cities, 1987–1994. *New England journal of medicine* **2000**, *343*, 1742-1749.
42. Schwartz, J.; Morris, R. Air pollution and hospital admissions for cardiovascular disease in detroit, michigan. *American journal of epidemiology* **1995**, *142*, 23-35.
43. Morris, R.D. Airborne particulates and hospital admissions for cardiovascular disease: A quantitative review of the evidence. *Environmental health perspectives* **2001**, *109*, 495.
44. Brook, R.D.; Rajagopalan, S.; Pope, C.A.; Brook, J.R.; Bhatnagar, A.; Diez-Roux, A.V.; Holguin, F.; Hong, Y.; Luepker, R.V.; Mittleman, M.A. Particulate matter air pollution and cardiovascular disease. *Circulation* **2010**, *121*, 2331-2378.
45. EPA, D. Integrated science assessment for particulate matter. *US Environmental Protection Agency Washington, DC* **2009**.
46. Heyder, J.; Gebhart, J.; Rudolf, G.; Schiller, C.F.; Stahlhofen, W. Deposition of particles in the human respiratory tract in the size range 0.005–15 μm. *Journal of Aerosol Science* **1986**, *17*, 811-825.
47. Lippmann, M. Regional deposition of particles in the human respiratory tract. *Comprehensive Physiology* **1977**.
48. Møller, P.; Jacobsen, N.R.; Folkmann, J.K.; Danielsen, P.H.; Mikkelsen, L.; Hemmingsen, J.G.; Vesterdal, L.K.; Forchhammer, L.; Wallin, H.; Loft, S. Role of oxidative damage in toxicity of particulates. *Free radical research* **2010**, *44*, 1-46.

49. Mühlfeld, C.; Rothen-Rutishauser, B.; Blank, F.; Vanhecke, D.; Ochs, M.; Gehr, P. Interactions of nanoparticles with pulmonary structures and cellular responses. *American Journal of Physiology-Lung Cellular and Molecular Physiology* **2008**, *294*, L817-L829.

50. Wang, J.; Christopher, S.A. Intercomparison between satellite-derived aerosol optical thickness and pm2. 5 mass: Implications for air quality studies. *Geophysical research letters* **2003**, *30*.

51. Engel-Cox, J.A.; Holloman, C.H.; Coutant, B.W.; Hoff, R.M. Qualitative and quantitative evaluation of modis satellite sensor data for regional and urban scale air quality. *Atmospheric environment* **2004**, *38*, 2495-2509.

52. Al-Saadi, J.; Szykman, J.; Pierce, R.B.; Kittaka, C.; Neil, D.; Chu, D.A.; Remer, L.; Gumley, L.; Prins, E.; Weinstock, L.*, et al.* Improving national air quality forecasts with satellite aerosol observations. *Bulletin of the American Meteorological Society* **2005**, *86*, 1249-1262.

53. Green, M.; Kondragunta, S.; Ciren, P.; Xu, C. Comparison of goes and modis aerosol optical depth (aod) to aerosol robotic network (aeronet) aod and improve pm2. 5 mass at bondville, illinois. *Journal of the Air & Waste Management Association* **2009**, *59*, 1082-1091.

54. Gupta, P.; Christopher, S.A.; Wang, J.; Gehrig, R.; Lee, Y.; Kumar, N. Satellite remote sensing of particulate matter and air quality assessment over global cities. *Atmospheric Environment* **2006**, *40*, 5880-5892.

55. Liu, Y.; Sarnat, J.A.; Kilaru, V.; Jacob, D.J.; Koutrakis, P. Estimating ground-level pm2. 5 in the eastern united states using satellite remote sensing. *Environmental science & technology* **2005**, *39*, 3269-3278.

56. Liu, Y.; Paciorek, C.J.; Koutrakis, P. Estimating regional spatial and temporal variability of pm2. 5 concentrations using satellite data, meteorology, and land use information. *Environmental health perspectives* **2009**, *117*, 886.

57. Lee, H.; Liu, Y.; Coull, B.; Schwartz, J.; Koutrakis, P. A novel calibration approach of modis aod data to predict pm2. 5 concentrations. *Atmos. Chem. Phys* **2011**, *11*, 7991-8002.

58. Hu, X.; Belle, J.H.; Meng, X.; Wildani, A.; Waller, L.A.; Strickland, M.J.; Liu, Y. Estimating pm2. 5 concentrations in the conterminous united states using the random forest approach. *Environmental Science & Technology* **2017**, *51*, 6936-6944.

Chapter 1: Evaluation of Aqua MODIS collection 6 AOD parameters for air quality research over the continental United States

Remote Sens. **2016**, *8*(10), 815; doi:10.3390/rs8100815

Article

Evaluation of Aqua MODIS Collection 6 AOD Parameters for Air Quality Research over the Continental United States

J. H. Belle and Yang Liu *

Department of Environmental Health, Rollins School of Public Health, Emory University, Atlanta, GA 30322, USA

*

Correspondence: Tel.: +1-404-727-8744

Academic Editors: Jun Wang, Omar Torres, Alexander A. Kokhanovsky, Richard Müller and Prasad S. Thenkabail

Received: 18 July 2016 / Accepted: 26 September 2016 / Published: 1 October 2016

Abstract:

Satellite-retrieved aerosol optical depth (AOD) has become an important predictor of ground-level particulate matter (PM) and greatly empowered air pollution research worldwide. We evaluated the AOD parameters included in the Collection 6 aerosol product of the Moderate Resolution Imaging Spectroradiometer (MODIS) for two key factors affecting their applications in air quality research—coverage and accuracy—over the continental US. For the high confidence retrievals (QAC 3), the 10 km DB-DT combined AOD has the best coverage nationwide (29.7% of the days in a year in any given 12 km grid cell). While the Eastern US generally had more successful AOD retrievals, the highest

Note: This chapter has been published in the journal, Remote Sensing, and has been formatted according to journal guidelines.

spatial coverage of AOD parameters were found in California (>55%) and other vegetated parts of the Western US. If lower QAC retrievals were included, the coverage of the 10 km DB AOD was dramatically increased to 49.6%. In the Eastern US, the QAC 3 retrievals of all four AOD parameters are highly correlated with AERONET observations (correlation coefficients between 0.80 and 0.92). In the Western US, positive retrieval errors existed in all MODIS AOD parameters, resulting in lower correlations with AERONET. AOD retrieval errors showed significant dependence on flight geometry, land cover type, and weather conditions. To ensure appropriate use of these AOD values, air quality researchers should carefully balance the needs for coverage and accuracy, and develop additional data screening criteria based on their study design.

Keywords:

MODIS; AOD; remote sensing; United States; retrieval accuracy; satellite coverage

1. Introduction

Aerosol optical depth (AOD) is 'the single most comprehensive variable to remotely assess the aerosol burden in the atmosphere' [1]. It is used to characterize ambient aerosols, either for land-based remote sensing applications where it is used to remove atmospheric influences, or directly, to assess atmospheric pollution, primarily fine particulate matter, and its impacts on the climate, ecosystems, and human populations. Exposure to fine particulate matter ($PM_{2.5}$, airborne particles with an aerodynamic diameter of 2.5 micrometers or less) was identified as a leading risk factor for global disease burden with an estimated 2.9 million attributable deaths in the year 2013 [2]. Historically, the estimation of population exposure to $PM_{2.5}$ depends on filter-based ground monitors. However,

because of its high operation and maintenance costs, these ground-based monitoring networks do not achieve comprehensive spatial coverage. With its comprehensive spatial coverage, spatial models driven by MODIS AOD are able to estimate the $PM_{2.5}$ exposure levels in many parts of the world where ground observations are sparse or nonexistent [3]. The MODerate Resolution Imaging Spectroradiometer (MODIS) instruments on board the Aqua and Terra satellite platforms have been providing daily, near-global satellite coverage since 2000 and 2002, respectively [4]. MODIS-retrieved aerosol optical depth (AOD) has been used extensively in estimating ground-level fine particulate matter ($PM_{2.5}$) concentrations [5]. Over the past decade, various MODIS-driven $PM_{2.5}$ exposure models have been developed, from relatively simple linear regressions [6] to complex multi-level spatial models [7] and Bayesian hierarchical models [8]. Because $PM_{2.5}$ is linked to adverse health outcomes even at the low concentrations commonly observed in the cities of North America [9], $PM_{2.5}$ models based on MODIS retrievals have been used to extend ground air quality monitoring networks to cover the suburban and rural populations in the U.S. [10] and Canada [11].

Accuracy and coverage are the most important factors affecting the application of satellite AOD in air quality research. The retrieval error in AOD has a major influence in the $PM_{2.5}$ prediction error, as AOD is often used as the primary predictor in various $PM_{2.5}$ exposure models. If the AOD retrieval error varies by season or with land use types, the $PM_{2.5}$ prediction error will also display spatiotemporal patterns. This is especially true at the low AOD levels, typically below 0.2, commonly observed in developed countries [12]. On the one hand, availability of AOD data coverage determines whether satellite-driven models are feasible for a given study region. On the other hand, it plays an important role

in determining the design of $PM_{2.5}$ health effect studies [13]. For example, the health effect of short-term $PM_{2.5}$ exposure such as asthma exacerbation is often evaluated in a time series model where temporal missingness of exposure estimates can substantially limit model performance [10]. Cohort studies designed for associating long-term $PM_{2.5}$ exposure with cardiovascular morbidity and mortality would benefit from complete spatial coverage [14].

The most recent MODIS collection 6 (C6) aerosol products include enhanced Dark-Target (10 km DT) and Deep-Blue (10 km DB) AOD present in collection 5 (C5), a 'merged' DB-DT parameter (10 km DB-DT) and a 3 km AOD based off of the 10 km DT retrieval algorithm (3 km DT) [15,16]. The MODIS science team has conducted a few global validation studies to document the collective impact of these changes and differences between the various parameters [12,16,17,18]. These studies mainly focused on estimating the AOD retrieval errors by comparing with collocated measurements from the Aerosol Robotic Network (AERONET) at the global scale. Because of the large spatial differences in aerosol loading, global performance metrics such as regression slopes and correlation coefficients are often driven by regions of high AOD values. To date, only a handful of evaluation studies were reported in North America, none of which had both accuracy and coverage as their primary research objectives [19,20]. Therefore, there remains a need for detailed validation studies in dominantly low-AOD regions to investigate issues related to surface reflectance treatment and extreme events [12]. In addition, the accuracy and potential usability of lower quality retrievals needs to be better characterized, and could have important implications on the coverage issue in air quality applications of MODIS data.

Note: This chapter has been published in the journal, Remote Sensing, and has been formatted according to journal guidelines.

In the current analysis, we focused on characterizing the accuracy and coverage of various MODIS AOD parameters in the continental US, a dominantly low-AOD area. We focused on examining the degree to which changes in surface properties and retrieval conditions, such as viewing angle and land use, affect AOD retrieval error. In addition to the highest quality AOD data, we evaluate the impact of including lower quality AOD values on the spatial and temporal coverage statistics. Additionally, we use a case study to demonstrate the practical implications of including lower-quality retrievals and accounting for major sources of bias on the ability of each AOD parameter to accurately estimate ground-level $PM_{2.5}$ concentrations. Finally, we summarize the strengths and weaknesses of these AOD parameters in the context of air quality research.

2. Materials and Methods

2.1. Satellite and Ground Datasets

We collected Aqua MODIS level 2 AOD data [21] between 1 January 2004 and 31 December 2013 in the Continental US. Level 2 cloud-screened and quality assured AOD retrievals from 120 permanent AERONET stations and 73 temporary stations from the Distributed Regional Aerosol Gridded Observation Networks (DRAGON) were collected to validate MODIS retrievals. Out of the 120 permanent AERONET stations, 48% had been in operation for less than one year (Figure 1). Total column precipitable water estimates were also collected from these stations to evaluate their impact on MODIS AOD retrieval error. Since AERONET does not directly measure AOD at the 0.55 μm wavelength reported by MODIS, values were interpolated to this wavelength with a quadratic fit in log-log space based on valid AOD values at a minimum of 4 of any of the 15 wavelengths potentially reported by AERONET [22]. Ancillary datasets were collected

for identifying surface properties and retrieval conditions that could have affected MODIS retrieval accuracy. The MODIS 16-day gridded NDVI parameter at 1 km spatial resolution [23] was used to calculate NDVI values at individual MODIS level 2 AOD pixels. The National Land Cover Database (NLCD) with a 30 m spatial resolution was used for land cover type calculation at individual MODIS level 2 AOD pixels [24]. The 2006 NLCD was used for collocations occurring prior to 2009 and the 2011 NLCD was used for collocations occurring after 2009. Information on scattering, viewing, and solar angles for each AOD retrieval was obtained for each MODIS pixel from the MODIS AQUA level 2 Aerosol product [21].

2.2. Coverage

Since MODIS pixels are created relative to each satellite view and the MODIS instrument exhibits a fish-eye effect, the size and location of individual pixels is not constant from one day to the next. To compensate for this, a 12 km grid commonly used in the Community Multi-scale Air Quality (CMAQ) modeling system was created for our coverage calculation (a total of 55,031 cells). The grid size roughly corresponds to the nadir resolution of the MODIS 10 km AOD parameters and represents an important application of the MODIS data, where AOD observations are assimilated into air quality models to improve model performance [25]. MODIS pixels were determined to be within a grid cell if, for the 10 km DT, 10 km DB, and 10 km DB-DT AOD, the polygon representing the pixel area, reconstructed from the pixel centroids using a Voronoi tessellation algorithm [26], lay at least partially within the grid cell. Pixels from the 3 km DT parameter were determined to be within a grid cell if the centroid of the 3 km pixel fell within the grid cell, allowing the

increased resolution of the 3 km DT parameter relative to the grid to compensate for the lack of smoothing between cells that the Voronoi tessellation would have provided. The percentage of days with a valid, QAC 3 retrieval were calculated for each grid cell and parameter. Results were interpreted relative to averages over the continental U.S. (CONUS) for each parameter. Coverage statistics were also calculated for QAC 1, 2, and 3 retrievals together to provide an accounting of the gains in coverage by including lower confidence retrievals in an analysis.

2.3. Accuracy

AERONET observations were collocated with each MODIS AOD parameter respectively, so that a temporal average of AERONET observations within ±30 min of the MODIS pass was compared to the spatial average of MODIS pixels within a ~25 km radius for the 10 km DT, DB and DB-DT AOD, and a ~7.5 km radius for the 3 km DT AOD [17]. Following previous work, a collocation was only considered valid if a minimum of three MODIS pixels, two AERONET measurements, and at least 20% of the total number of MODIS pixels included in the 25/7.5 km radius had valid values with a QAC code of 3 assigned to the pixel [27]. AERONET stations were categorized as either being in the East or the West, using the 100° W longitude line [16]. The east/west division was necessary because previous work had found large differences in MODIS performance between the two regions [25]. Retrieval error, or the difference between MODIS and AERONET AOD at each collocation ($\tau_M - \tau_A$) and the percentage of MODIS observations within the 10 km DT expected error envelope (EE_{DT})—defined as $\pm(0.05 + 0.15)\tau$—[16] were calculated and linear regression models were used to quantify retrieval errors. In order to evaluate the QAC code assignments as indicators of retrieval errors, independent collocations were created for

QAC 1 and QAC 2 retrievals with AERONET, using the same criteria as for the QAC 3 collocations. Finally, for each AOD parameter, retrieval error in MODIS AOD relative to AERONET was examined within quintiles of the surface and retrieval parameters. These parameters include median NDVI, total column precipitable water from AERONET, land-cover type mode, mean solar zenith, sensor zenith, and scattering angles. Linear regression models were used to identify any significant linear trends in retrieval error for each surface and retrieval parameter.

3. Results

During our study period, 193 ground stations reported a total of 286,055 observations that could be interpolated to AOD at 550 nm. Of these, 262,491 originated from a permanent AERONET station and 23,564 were recorded during a DRAGON campaign. In the Eastern US, the number of valid collocations at the 127 stations with high confidence MODIS retrievals ranges from 5616 for 3 km DT to 6617 for 10 km DB observations. AERONET AOD ranged from 0.0005 to 1.26, with mean values of 0.12, 0.12, 0.12, and 0.10 for collocations with the high confidence 3 km DT, 10 km DT, 10 km DB-DT and 10 km DB parameters, respectively. MODIS AOD ranged from −0.05 to 2.77, with mean values of 0.13, 0.13, 0.13, and 0.11 for these four AOD parameters, respectively. In the Western US, the number of valid collocations at 66 AERONET stations with high confidence MODIS retrievals ranges from 6251 for 3 km DT to 11,590 for 10 km DB-DT AOD. AERONET AOD values ranged from 0.0003 to 1.43, with mean values of 0.09, 0.09, 0.08, and 0.08 for collocations with the high confidence 3 km DT, 10 km DT, 10 km DB-DT, and 10 km DB parameters, respectively. MODIS AOD values ranged from −0.05 to 2.35, with mean values of 0.09, 0.12, 0.10, and 0.08 for these parameters, respectively. In

both regions, and for all four products, the majority of collocations occurred in the fall and summer, while the fewest occurred in winter months.

3.1. Coverage of High-Confidence Retrievals

Table 1 shows that on average, a valid AOD retrieval was available on 25%–30% of days in any given grid cell. However, there is considerable spatial heterogeneity in coverage rates for each parameter (Figure 1). The highest rates of coverage are found on the western coast, near the large cities of Los Angeles and San Francisco, and in California's central valley. In these areas, all four AOD parameters achieve coverage rates of over 55%, and in the area right around Los Angeles, coverage rates are above 70%. Similarly high coverage rates, between 50% and 60%, are also observed over the national forests north of Phoenix in Arizona and rates of 40%–50% are observed over the south-central plains covering the areas of central Texas, Oklahoma, and Kansas. A north-to-south and elevation gradient in coverage rates can also be observed in Figure 2. The lowest coverage rates were observed over the Great Salt Lake desert, where a few locations had no valid retrieval. Outside of the Rockies, average coverage rates in the northern parts of the CONUS—an area that includes the large cities of Chicago and New York—were typically only 10%–20%. Coverage rates further south were 30%–40%, slightly higher than the CONUS-wide average. This north-south and elevation-based gradient in coverage rates can be linked to seasonal snow-cover occurring primarily at higher latitudes and elevations.

The 3 km DT AOD, with a CONUS-wide coverage rate of 28.2%, is comparable to the 10 km AOD parameters in terms of coverage. In contrast to the 10 km products, the 3 km DT AOD excels over areas where the surface is more complex but not arid, such as the Pacific Northwest, and over the Carolinas. It achieves slightly higher coverage rates on the

eastern coast than the 10 km parameters, and retrieves at higher rates at high to moderate latitudes and elevations than the 10 km AOD parameters (Figure 2a). The most likely explanation for these higher coverage rates at higher elevations and latitudes would be an increased ability, on the part of the higher resolution parameter, to retrieve aerosols over patchy snow-cover. However, while it has been previously noted that the higher resolution parameter is able to retrieve aerosol information at higher rates over complex landscapes, coastlines, and between clouds, the extension of this ability to complex snow-cover has not been investigated [17,19]. The 10 km merged AOD has the highest overall coverage, averaging 29.7% for the CONUS. This parameter aims to maximize the number of high-confidence AOD retrievals by using AOD values from the 10 km DT algorithm over locations where the NDVI is higher and to use 10 km DB AOD values over locations where NDVI is lower and the 10 km DT algorithm is less likely to accurately retrieve AOD. The result is that the spatial patterns of coverage for the merged AOD are similar to 10 km DT AOD, but without the gaps in coverage over the arid southwest. The coverage of 10 km DB AOD along the east coast is lower than the other three AOD parameters especially in the summer months (see Supplementary Figure S1) and over Florida, and balances out the additional coverage gained in the west and south-central plains (Figure 2). The reasons for this are currently unknown, but slight differences exist between the DT and DB retrieval processes in the tests used to identify cloud-cover and distinguish it from aerosols and this could explain summertime differences in coverage over the highly vegetated Eastern CONUS [15,16].

3.2. Coverage Gains with Lower-Quality Retrievals

Note: This chapter has been published in the journal, Remote Sensing, and has been formatted according to journal guidelines.

When lower-quality retrievals were included, coverage rates increased for all AOD parameters. However, there were large differences in relative increases between products, reflective of differences in QAC code assignments among AOD parameters. On the one hand, coverage rates for the 3 km DT AOD increased only slightly from 28.2% to 28.9%, similar to that observed for the 10 km DB-DT AOD. Coverage rates for the 10 km DT parameter increased substantially from 24.3% to 32.8%. On the other hand, coverage of the 10 km DB AOD increased dramatically from 28.9% to 49.6% when lower-confidence retrievals were included. Of the four AOD parameters, the 10 km merged AOD provides the highest overall coverage over the CONUS if only high-confidence retrievals are considered. Coverage patterns are similar to those observed for high confidence observations (Supplementary Figure S2). Previous studies have examined how AOD missingness impacts the representativeness of the sample within the CONUS, with mixed results [28,29]. For some applications, the typical coverage rates from high quality retrievals of ~30% may be too low to preserve study power, and investigators may seek to boost coverage rates through the use of noisier, lower-confidence observations. In this instance, the 10 km DB AOD offers the greatest potential gains in coverage.

3.3. Accuracy of High-Confidence Retrievals

Error statistics for all four AOD parameters, broken down by region, are presented in Table 2. In the eastern region, 76% of QAC 3 3 km DT AOD retrievals were within pre-launch expectations with a mean retrieval error of 0.01, and the correlation coefficient between AERONET and MODIS values was 0.89. However, the slope of a regression line fit between the two was 1.24, indicating over-prediction. In the western region, 49% of 3 km DT observations were within the EE and the slope of a line relating AERONET AOD

values to MODIS observations was 1.41. The QAC 3 10 km DT AOD retrievals in the East had a slightly positive, but near 0 retrieval error, and its correlation coefficient with AERONET observations (0.92) was the highest of the four parameters. Over-prediction was a problem in the western region, but was more problematic at low AOD levels. The performance of the 10 km DB-DT AOD across accuracy metrics was nearly identical to the 10 km DT AOD in the Eastern US, but it had an additional 341 QAC 3 collocations. In the western region, it was the most highly correlated with AERONET (0.73). The QAC 3 10 km DB AOD had somewhat uneven performance across accuracy metrics relative to findings from global validations [12]. It had the highest percentage of observations within EE_{DT}(87% in the East, 83% in the West). Correlation coefficients, however, were lower than the other three parameters (0.80 in the East, 0.63 in the West) and global estimates [12]. Median retrieval error estimates in both regions were low (0.01 in the East, −0.00 in the West), but intercepts from regression modeling were higher (0.03 in the East, 0.02 in the West) and slopes were below 1 (0.79 in the East, 0.75 in the West). When assessed together, these metrics indicated over-prediction at lower AOD values and under-prediction at higher AOD values. Previous global validations have found similar patterns for 10 km DB retrievals, but over-prediction was more severe in the Western US than was noted in the global studies.

3.4. Accuracy Assessment of Lower-Confidence Retrievals

The more mature 10 km DB and 10 km DT AOD had 20,306 and 6924 valid lower-confidence collocations, respectively. In contrast, the less mature 3 km DT and 10 km DB-DT products had only 1429 and 2259 valid lower-confidence collocations, respectively. As expected, lower confidence collocations for the 10 km DB and 10 km DT AOD were

noisier and had larger retrieval errors when compared to QAC 3 observations (Table 2). For both parameters, a lower proportion of low-confidence observations were within EE_{DT}, ranging from 40% to 68% of retrievals, median retrieval error estimates were higher, ranging from 0.02 to 0.09, and correlation coefficients were lower, ranging from 0.52 to 0.88. There were a substantial number of valid QAC 1 10 km DB collocations with a positive retrieval error at lower AOD values. This is typically attributable to cloud contamination, and so it may be possible to use some of these observations in an analysis with caution and additional cloud screening procedures [25]. Accuracy statistics for lower-confidence 3 km DT and 10 km merged AOD, on the other hand, were comparable with high confidence retrievals (Table 2). The 3 km DT AOD had a high percentage of observations within EE_{DT}, 83 and 90% for the eastern and western regions, respectively, and strong correlations (0.79 in the East, 0.85 in the West). All low-confidence 10 km DB-DT AOD except QAC 2 retrievals in the eastern region (only 16 valid collocations) met pre-launch expectations, having between 70% and 90% of retrievals within EE_{DT}. The QAC code assignments for the two new AOD parameters do not seem to accurately reflect retrieval errors in the same way as for the more mature AOD parameters.

3.5. Dependence of Retrieval Errors on Flight Geometry and Land Cover Type

Figure 3 illustrates the dependence of AOD errors on the scattering, solar zenith, and viewing angles for QAC 3 retrievals. Scattering angle was associated with a statistically significant, positive trend in retrieval error in all four parameters in both regions. This trend is most pronounced for 3 km DT AOD in the western region with a median retrieval error of 0.12 for the highest quintile, and 0.04 for the lowest quintile of scattering angle. The median retrieval errors of 10 km DT, DB, and DB-DT AOD in both regions, and 3 km DT

observations in the eastern region increase slightly with scattering angle (but remain below 0.04). This type of dependence could be related to issues with accounting for anisotropy in the surface reflectance over the CONUS [30]. Our findings in the CONUS disagree with those presented in global evaluations, which found tendencies of median retrieval error with scattering angle to be small and negative [12]. Our findings on the association between retrieval errors and solar zenith angles are only partially consistent with Sayer et al. [12] which found solar zenith angles below 20 degrees to have positive retrieval errors for the 10 km DT parameter and negative retrieval errors for the 10 km DB parameter, but retrievals at angles greater than 20 to be relatively unbiased. In the Eastern US, our results show a similar pattern to those present in Sayer et al. [12] for 10 km DB retrievals relative to 10 km DT retrievals, but with a slight positive retrieval error for 10 km DB. Additionally, we observed fairly substantial retrieval errors at solar zenith angles greater than 20 degrees. In the Western US, we observed negative retrieval errors in 10 km DB observations spanning solar zenith angles from 25 to 43 degrees, while the first quintile, containing observations with solar zenith angles less than 25 degrees, was relatively unbiased. This finding runs contrary to previous observations which have suggested that it is primarily low solar zenith angles that are problematic [12,25]. AOD retrieval error shows a small negative trend with sensor zenith angle for the 10 km DB AOD in both regions and for the 3 km DT in the West, and a small positive trend for the 10 km DT, 10 km DB-DT, and 3 km DT AOD in the East. The largest change was for 10 km DB observations in the East, where the median retrieval error estimate in AOD within the first quintile of sensor zenith angle, near the nadir, was 0.024 and the median retrieval error in the highest quintile was −0.005.

Note: This chapter has been published in the journal, Remote Sensing, and has been formatted according to journal guidelines.

We assessed AOD retrieval errors by six land cover types, i.e., developed, forest, shrub, grass, cultivated, and wetland (see Supplementary Figure S3). All AOD parameters showed positive retrieval errors over developed areas, particularly in the Western US (0.03 for 10 km DB, and 0.21 for 3 km DT AOD). Small but consistent positive errors were also observed over wetlands in the Eastern US (mean retrieval errors of 0.04 for 3 km DT, 0.03 for 10 km DT, 0.03 for 10 km DB-DT, and 0.02 for 10 km DB). The 3 km DT and, to a lesser degree, 10 km DT AOD also showed significant positive errors over shrub lands in the Western US (mean retrieval errors were 0.10 and 0.06 for 3 km DT and 10 km DT, respectively). The best agreement between MODIS and AERONET was over forests, grasslands, and cultivated lands. Overall, the 10 km DB AOD had the least retrieval errors across all land cover types (<0.03), followed by the 10 km DB-DT AOD (greatest mean retrieval error of 0.10 over developed areas in the Western US). Previous studies have identified high retrieval error in AOD retrievals over developed areas, and the retrieval error in DT products over poorly vegetated surfaces to which 10 km DB retrievals are more robust [16,20,31].

3.6. Dependence of Retrieval Errors on Season and Weather Conditions

Figure 4 summarizes monthly retrieval errors from each AOD parameter. Median retrieval errors in the 10 km DT, 10 km DB-DT, and 3 km DT parameters were the highest in the summer months. The 3 km DT AOD had the widest fluctuation of retrieval errors over the course of the year (0.009 in December to 0.056 in May). The 10 km DB product had a more even distribution over time, from −0.01 in August to 0.01 in February. The reasons for the increased positive retrieval error in the DT-based AOD parameters in the summer months is unclear, and has not been well-characterized in previous work on this collection. However, despite the fact that collocations in summer months are associated with increased mean

NDVI values, which typically result in better accuracy statistics for DT products, collocations in these months also have higher scattering angles, lower solar zenith angles, and higher values of total column precipitable water, all factors that result in positive retrieval errors over the CONUS.

As mentioned above, lower NDVI has been associated with increased retrieval error and noise in MODIS AOD retrievals, particularly for DT-based products, in previous works [16]. In the West, this is clearly shown in the 3 km DT AOD, and to a lesser degree in 10 km DT AOD (Figure 5). The 10 km DB AOD in the Western US was unbiased in the lowest three quintiles of NDVI, but was negatively biased in the upper two quintiles (up to −0.03 in the highest quintile). This pattern was observed in the global validations as well [12] and it likely points to an overestimation of the surface reflectance over vegetated areas in the eastern US. In the East, AOD retrieval errors are less dependent on NDVI, and the negative retrieval error observed for DB at higher NDVI values was not observed. Both humidity and potential cloud contamination have been shown to bias MODIS observations, and total column precipitable water (TCPW) can be a marker for both factors [32]. Figure 5 shows a complex relationship between AOD retrieval errors and TCPW. In the Western US, TCPW has little impact on the retrieval errors of 10 km DB and DB-DT AOD, but both very high or very low TCPW values are associated with positive retrieval errors in the 3 km and 10 km DT AOD. In the Eastern US, the 10 km DB AOD is negatively associated with TCPW. However, the impact of TCPW is generally small for all AOD parameters, except at very high levels where both the 3 km and 10 km DT AOD showed a small positive retrieval error. At higher TCPW values, this bias is likely indicative of cloud contamination, and the lack of retrieval error in 10 km

Note: This chapter has been published in the journal, Remote Sensing, and has been formatted according to journal guidelines.

DB product under these conditions fits with our coverage results, which suggests more conservative cloud screening procedures for this product.

4. Case Study

We conducted a case study over the Atlanta Metropolitan Area from 1 January 2004 to 31 December 2013. The study area stretched from 32°N to 36°N latitude and from 83°W to 86°W longitude, and included 23 ground-level $PM_{2.5}$ monitors in 19 distinct grid cells from the same ~12 km × 12 km grid used in the coverage analysis. This case study compared the ability of each of the four MODIS AOD products to predict ground-level $PM_{2.5}$ in a widely used linear mixed effect (LME) model framework [33]. Three AOD datasets were generated for each of the four MODIS AOD products: (1) AOD values with only QAC = 3; (2) AOD values with the highest available QAC (1, 2 or 3); and (3) filtered and corrected AOD values using the relationships examined in Section 3.5 and Section 3.6 prior to inclusion in the model. To produce the filtered and corrected dataset, AOD values from dataset #2 with scattering angles over 165° or solar zenith angles less than 15° were first eliminated. This removed ~9% of observations while some were additionally lost in the matching process. This filtered dataset was then corrected, using a linear regression model fit to the dataset of matched AERONET and MODIS AOD observations in the Eastern CONUS, used in the accuracy analysis, for QAC value, land use type, sensor zenith angle, total column precipitable water, and NDVI. All 12 combinations of AOD were fit using the LME model, of the form: $PM_{2.5,s,t} = (b_0 + b_{0,t}) + (b_1 + b_{1,t})AOD_{s,t}$, where b_0 is the fixed intercept, $b_{0,t}$ the random intercept for each day, b_1 the fixed slope, and $b_{1,t}$ the random slope for each day [33]. These results are presented in Table 3.

Note: This chapter has been published in the journal, Remote Sensing, and has been formatted according to journal guidelines.

For the parameters where the number of observations increased with the addition of lower QAC valued observations, 10 km DB and 10 km DT, R^2 values for a model relating ground-level $PM_{2.5}$ concentrations to AOD actually increased slightly. Increasing from 0.80 to 0.83 for 10 km DB and from 0.72 to 0.75 for 10 km DT. When AOD values were filtered and corrected to remove potentially biased observations, model fits for the 10 km DT product decreased slightly, from 0.77 to 0.75 and remained the same for the 10 km DB product. For the parameters with relatively few lower quality observations, 10 km DB-DT and 3 km DT, neither the number of observations included in the model nor the resulting R^2 values changed when lower confidence observations were included in the model. When filtering and correction was applied, model fits, as measured by the R^2 values, actually decreased by 0.01 relative to the 'best of' models. These results run counter to what would be expected: that R^2 values for all four parameters would decrease slightly with the inclusion of lower-confidence retrievals, given the fact that the lower confidence observations for the 10 km DB and 10 km DT parameters are noisier. However, in this case study, the additional number of observations appears to have offset the additional noise introduced via these observations in the model and resulted in better prediction of ground-level $PM_{2.5}$ via this simple model. Despite the smaller sample sizes, the models using the corrected and filtered AOD values achieved similar R^2 values as the uncorrected AOD models.

These results illustrate some of the key points made in this paper, namely that coverage is an often-overlooked but important factor, when considering AOD accuracy statistics, and that, because of the role played by coverage, the inclusion of lower-quality AOD observations in a model can provide some benefit. These results additionally highlight our

observation that the lower confidence designations for the newer products, 10 km DB-DT and 3 km DT, are very few in number. The utility of correcting for major sources of bias or error in the AOD values was demonstrated in this limited example by greater fixed effect regression slopes, indicating greater sensitivity of the corrected and filtered AOD values to $PM_{2.5}$ concentrations.

5. Conclusions

We conducted a detailed analysis on the coverage and accuracy of Collection 6 MODIS AOD parameters in the CONUS. With their applications in air quality research in mind, we examined the benefits and risks of including lower QAC retrievals in order to improve data coverage, as well as how AOD retrieval errors depend on various factors. Our recommendation is that, for inexperienced users who are beginning to explore MODIS AOD data for air quality research, the QAC 3 10 km DB-DT AOD is their best choice. For more experienced users, the ideal AOD parameter could depend on the purpose as well as domain of their study. The coverage of QAC 3 retrievals is comparable among all four AOD parameters, ranging from 25% to 30%. The Eastern US in general had higher and more consistent data coverage. However, much higher coverage rates were found in highly developed Southern California and over the south-central plains with limited ground-level air pollution monitoring, a surprising fact since these areas are traditionally regarded as having too high of surface brightness for DT to retrieve reliably. These findings are promising to researchers interested in conducting regional air quality assessments in these regions. Including lower QAC retrievals marginally improved coverage for the 3 km DT and 10 km DB-DT AOD. However, since these QAC assignments do not appear to reflect retrieval accuracy and are few in number, including lower QAC retrievals of these two

parameters is probably beneficial, and unlikely to be harmful. On the other hand, lower QAC retrievals could increase the coverage of 10 km DT AOD by ~20% and that of 10 km DB AOD by ~70% on average. Caution must be given when including them to enhance coverage as these retrievals are often noisier, as shown in Table 2. However, as demonstrated in the case study, sufficient daily sample sizes can sometimes be more important than retaining only the high quality AOD values for the purposes of improving prediction errors with ground-level $PM_{2.5}$. To take advantage of the dramatic coverage gain offered by these lower QAC retrievals, retrieval error correction steps using local AERONET observations could be valuable [7].

In terms of data accuracy, the 10 km DB-DT AOD had the best performance in terms of correlation and linear model fit statistics, although QAC 3 retrievals for all but the 3 km DT AOD over the Western US met pre-launch expectations for the percentage of collocations within EE_{DT}. However, the 10 km DB product performs well in the context of a prediction model and may be an understudied AOD parameter in the US, where the 10 km DT product is currently used more frequently. The robustness of this product to major sources of bias additionally makes it an attractive option in the Western United States. The noisier 3-km DT AOD, however, can be valuable over dark targets in the Eastern US, particularly over areas where it tends to retrieve at higher rates than the lower-resolution products, such as in the Northeast and Northern Midwest, over the South Central plains in Texas, and over Southern Florida. The errors in MODIS AOD parameters vary in time and space, and are dependent on various retrieval conditions. Additional data screening and retrieval error correction steps should be considered other than simply relying on the QAC values, particularly in the Western United states, where these biases tend to have a larger

impact. For example, AOD retrievals associated with high scattering angles and lower solar zenith angles may be excluded to avoid data contamination. Such parameters can be found in the operational MODIS aerosol product. In addition, categorical variables of land cover types as well as time trends can be introduced in $PM_{2.5}$exposure models to control for the systematic retrieval errors in DT-based AOD retrievals. NDVI and TCPW had statistically significant, distinct impacts on all AOD parameters in the Western US, and therefore are probably worth considering when analyzing AOD data. Since they must be extracted from separate MODIS data products, users would need to consider the nontrivial time and computational demands associated with dealing with these large datasets.

Supplementary Materials

The following are available online at www.mdpi.com/2072-4292/8/10/815/s1, Figure S1: Seasonal coverage for high confidence retrievals, Figure S2: Seasonal coverage for all-confidence retrievals, Figure S3: AOD retrieval errors by land cover type.

Acknowledgments

This work was partially supported by the NASA Applied Sciences Program (grant No. NNX11AI53G, PI: Liu). In addition, this publication was made possible by the AERONET principal investigators and their staff for establishing and maintaining the 193 sites used in this investigation. The original MODIS AOD, AERONET AOD, land use, and MODIS NDVI data used in this paper are available free through the links referenced in Section 2 of the paper. We have additionally made our processing and analysis code, gridded coverage estimates, and MODIS and AERONET collocations produced for this analysis available on GitHub (https://github.com/jhbelle/MODIS_C6_Evaluation_over_the_CONUS).

Note: This chapter has been published in the journal, Remote Sensing, and has been formatted according to journal guidelines.

Author Contributions

J.H.B. and Y.L. conceived and designed the experiments; J.H.B. performed the experiments; J.H.B. analyzed the data; J.H.B. and Y.L. contributed reagents/materials/analysis tools; J.H.B. and Y.L. wrote the paper.

Conflicts of Interest

The authors declare no conflict of interest.

References

1. Holben, B.; Tanre, D.; Smirnov, A.; Eck, T.; Slutsker, I.; Abuhassan, N.; Newcomb, W.; Schafer, J.; Chatenet, B.; Lavenu, F. An emerging ground-based aerosol climatology: Aerosol optical depth from aeronet. *J. Geophys. Res. Atmos.* **2001**, *106*, 12067–12097. [Google Scholar] [CrossRef]
2. Brauer, M.; Freedman, G.; Frostad, J.; Van Donkelaar, A.; Martin, R.V.; Dentener, F.; Dingenen, R.V.; Estep, K.; Amini, H.; Apte, J.S. Ambient air pollution exposure estimation for the global burden of disease 2013. *Environ. Sci. Technol.***2015**, *50*, 79–88. [Google Scholar] [CrossRef] [PubMed]
3. Van Donkelaar, A.; Martin, R.V.; Brauer, M.; Boys, B.L. Use of satellite observations for long-term exposure assessment of global concentrations of fine particulate matter. *Environ. Health Perspect.* **2015**, *123*, 135–143. [Google Scholar] [CrossRef] [PubMed]
4. Remer, L.A.; Kaufman, Y.; Tanré, D.; Mattoo, S.; Chu, D.; Martins, J.V.; Li, R.-R.; Ichoku, C.; Levy, R.; Kleidman, R. The MODIS aerosol algorithm, products, and validation. *J. Atmos. Sci.* **2005**, *62*, 947–973. [Google Scholar] [CrossRef]

Note: This chapter has been published in the journal, Remote Sensing, and has been formatted according to journal guidelines.

5. Hoff, R.M.; Christopher, S.A. Remote sensing of particulate pollution from space: Have we reached the promised land? *J. Air Waste Manag. Assoc.* **2009**, *59*, 645–675. [Google Scholar] [PubMed]

6. Gupta, P.; Christopher, S.A.; Wang, J.; Gehrig, R.; Lee, Y.; Kumar, N. Satellite remote sensing of particulate matter and air quality assessment over global cities. *Atmos. Environ.* **2006**, *40*, 5880–5892. [Google Scholar] [CrossRef]

7. Ma, Z.; Hu, X.; Sayer, A.M.; Levy, R.; Zhang, Q.; Xue, Y.; Tong, S.; Bi, J.; Huang, L.; Liu, Y. Satellite-based spatiotemporal trends in $PM_{2.5}$ concentrations: China, 2004–2013. *Environ. Health Perspect.* **2015**, *124*, 184–192. [Google Scholar] [CrossRef] [PubMed]

8. Chang, H.H.; Hu, X.; Liu, Y. Calibrating MODIS aerosol optical depth for predicting daily $PM_{2.5}$ concentrations via statistical downscaling. *J. Expo. Sci. Environ. Epidemiol.* **2014**, *24*, 398–404. [Google Scholar] [CrossRef] [PubMed]

9. Smith, K.R.; Jantunen, M. Why particles? *Chemosphere* **2002**, *49*, 867–871. [Google Scholar] [CrossRef]

10. Strickland, M.; Hao, H.; Hu, X.; Chang, H.; Darrow, L.; Liu, Y. Pediatric emergency visits and short-term changes in $PM_{2.5}$ concentrations in the US State of Georgia. *Environ. Health Perspect.* **2015**, *124*, 690–696. [Google Scholar] [CrossRef] [PubMed]

11. Crouse, D.L.; Peters, P.A.; van Donkelaar, A.; Goldberg, M.S.; Villeneuve, P.J.; Brion, O.; Khan, S.; Atari, D.O.; Jerrett, M.; Pope, C.A., III. Risk of nonaccidental and cardiovascular mortality in relation to long-term exposure to low concentrations of fine particulate matter: A Canadian national-level cohort study. *Environ. Health Perspect.* **2012**, *120*, 708–714. [Google Scholar] [CrossRef] [PubMed]

Note: This chapter has been published in the journal, Remote Sensing, and has been formatted according to journal guidelines.

12. Sayer, A.; Munchak, L.; Hsu, N.; Levy, R.; Bettenhausen, C.; Jeong, M.J. MODIS Collection 6 aerosol products: Comparison between Aqua's e-deep blue, dark target, and "merged" data sets, and usage recommendations. *J. Geophys. Res. Atmos.* **2014**, *119*. [Google Scholar] [CrossRef]
13. Liu, Y. New directions: Satellite driven $PM_{2.5}$ exposure models to support targeted particle pollution health effects research. *Atmos. Environ.* **2013**, *68*, 52–53. [Google Scholar] [CrossRef]
14. Kloog, I.; Ridgway, B.; Koutrakis, P.; Coull, B.A.; Schwartz, J.D. Long-and short-term exposure to $PM_{2.5}$ and mortality: Using novel exposure models. *Epidemiology* **2013**, *24*, 555–561. [Google Scholar] [CrossRef] [PubMed]
15. Hsu, N.; Jeong, M.J.; Bettenhausen, C.; Sayer, A.; Hansell, R.; Seftor, C.; Huang, J.; Tsay, S.C. Enhanced deep blue aerosol retrieval algorithm: The second generation. *J. Geophys. Res. Atmos.* **2013**, *118*, 9296–9315. [Google Scholar] [CrossRef]
16. Levy, R.; Mattoo, S.; Munchak, L.; Remer, L.; Sayer, A.; Hsu, N. The collection 6 MODIS aerosol products over land and ocean. *Atmos. Meas. Tech.* **2013**, *6*, 2989–3034. [Google Scholar] [CrossRef]
17. Remer, L.; Mattoo, S.; Levy, R.; Munchak, L. MODIS 3 km aerosol product: Algorithm and global perspective. *Atmos. Meas. Tech. Discuss.* **2013**, *6*, 69–112. [Google Scholar] [CrossRef]
18. Sayer, A.; Hsu, N.; Bettenhausen, C.; Jeong, M.J. Validation and uncertainty estimates for MODIS collection 6 "deep blue" aerosol data. *J. Geophys. Res. Atmos.* **2013**, *118*, 7864–7872. [Google Scholar] [CrossRef]
19. Livingston, J.; Redemann, J.; Shinozuka, Y.; Johnson, R.; Russell, P.; Zhang, Q.; Mattoo, S.; Remer, L.; Levy, R.; Munchak, L. Comparison of MODIS 3 km and 10 km resolution

aerosol optical depth retrievals over land with airborne sunphotometer measurements during arctas summer 2008. *Atmos. Chem. Phys.* **2014**, *14*, 2015–2038. [Google Scholar] [CrossRef]

20. Munchak, L.; Levy, R.; Mattoo, S.; Remer, L.; Holben, B.; Schafer, J.; Hostetler, C.; Ferrare, R. MODIS 3 km aerosol product: Applications over land in an urban/suburban region. *Atmos. Meas. Tech.* **2013**, *6*, 1747–1759. [Google Scholar] [CrossRef]
21. Levy, R. Collection 006 (C6) MODIS Atmosphere l2 Aerosol Product, 6th ed.LAADS Web, 2014. Available online: https://ladsweb.nascom.nasa.gov/data/search.html (accessed on 15 July 2014). [Google Scholar]
22. Slutsker, I.; Kinne, S. Wavelength dependence of the optical depth of biomass burning, urban, and desert dust aerosols. *J. Geophys. Res.* **1999**, *104*, D24. [Google Scholar]
23. Carroll, M.; DiMiceli, R.; Sohlberg, R.; Townshend, J. *1 km MODIS Normalized Difference Vegetation Index*, 5th ed.; University of Maryland, LAADS Web: College Park, MD, USA, 2015. [Google Scholar]
24. Fry, J.A.; Xian, G.; Jin, S.; Dewitz, J.A.; Homer, C.G.; Limin, Y.; Barnes, C.A.; Herold, N.D.; Wickham, J.D. Completion of the 2006 national land cover database for the conterminous United States. *Photogramm. Eng. Remote Sens.* **2011**, *77*, 858–864. [Google Scholar]
25. Hyer, E.; Reid, J.; Zhang, J. An over-land aerosol optical depth data set for data assimilation by filtering, correction, and aggregation of MODIS collection 5 optical depth retrievals. *Atmos. Meas. Tech.* **2011**, *4*, 379–408. [Google Scholar] [CrossRef]

Note: This chapter has been published in the journal, Remote Sensing, and has been formatted according to journal guidelines.

26. Turner, R. Deldir: Delaunay Triangulation and Dirichlet (Voronoi) Tessellation. 2009. R Package Version 0.0-8. Available online: http://cran.r-project.org/web/packages/deldir (accessed on 31 July 2014).

27. Petrenko, M.; Ichoku, C.; Leptoukh, G. Multi-sensor aerosol products sampling system (MAPSS). *Atmos. Meas. Tech.***2012**, *5*, 913–926. [Google Scholar] [CrossRef]

28. Yu, C.; Di Girolamo, L.; Chen, L.; Zhang, X.; Liu, Y. Statistical evaluation of the feasibility of satellite-retrieved cloud parameters as indicators of $PM_{2.5}$ levels. *J. Exposure Sci. Environ. Epidemiol.* **2015**, *25*, 457–466. [Google Scholar] [CrossRef] [PubMed]

29. Christopher, S.A.; Gupta, P. Satellite remote sensing of particulate matter air quality: The cloud-cover problem. *J. Air Waste Manag. Assoc.* **2010**, *60*, 596–602. [Google Scholar] [CrossRef] [PubMed]

30. Levy, R.C.; Remer, L.A.; Mattoo, S.; Vermote, E.F.; Kaufman, Y.J. Second-generation operational algorithm: Retrieval of aerosol properties over land from inversion of moderate resolution imaging spectroradiometer spectral reflectance. *J. Geophys. Res. Atmos.* **2007**, *112*, D13. [Google Scholar] [CrossRef]

31. Tao, M.; Chen, L.; Wang, Z.; Tao, J.; Che, H.; Wang, X.; Wang, Y. Comparison and evaluation of the MODIS collection 6 aerosol data in China. *J. Geophys. Res. Atmos.* **2015**, *120*, 6992–7005. [Google Scholar] [CrossRef]

32. Ford, B.; Heald, C.L. Aerosol loading in the southeastern united states: Reconciling surface and satellite observations. *Atmos. Chem. Phys.* **2013**, *13*, 9269–9283. [Google Scholar] [CrossRef]

Note: This chapter has been published in the journal, Remote Sensing, and has been formatted according to journal guidelines.

33. Lee, H.; Liu, Y.; Coull, B.; Schwartz, J.; Koutrakis, P. A novel calibration approach of MODIS aod data to predict $PM_{2.5}$ concentrations. *Atmos. Chem. Phys.* **2011**, *11*, 7991–8002. [Google Scholar] [CrossRef]

Note: This chapter has been published in the journal, Remote Sensing, and has been formatted according to journal guidelines.

Chapter 2: The potential impact of satellite-retrieved cloud parameters on ground-level $PM_{2.5}$ mass and composition

Int. J. Environ. Res. Public Health **2017**, *14*(10), 1244; doi:10.3390/ijerph14101244

Article

The Potential Impact of Satellite-Retrieved Cloud Parameters on Ground-Level $PM_{2.5}$ Mass and Composition

Jessica H. Belle [1], Howard H. Chang [2], Yujie Wang [3], Xuefei Hu [1], Alexei Lyapustin [3] and Yang Liu [1,*]

[1]

Department of Environmental Health, Emory University, Atlanta, GA 30322, USA

[2]

Department of Biostatistics and Bioinformatics, Emory University, Atlanta, GA 30322, USA

[3]

NASA Goddard Space Flight Center, Greenbelt, MD 20771, USA

*

Correspondence: Tel.: +1-404-727-2131

Received: 27 July 2017 / Accepted: 10 October 2017 / Published: 18 October 2017

Abstract:

Satellite-retrieved aerosol optical properties have been extensively used to estimate ground-level fine particulate matter ($PM_{2.5}$) concentrations in support of air pollution health effects

Note: This chapter has been published in the journal, International Journal of Environmental Research and Public Health, and has been formatted according to journal guidelines.

research and air quality assessment at the urban to global scales. However, a large proportion, ~70%, of satellite observations of aerosols are missing as a result of cloud-cover, surface brightness, and snow-cover. The resulting $PM_{2.5}$ estimates could therefore be biased due to this non-random data missingness. Cloud-cover in particular has the potential to impact ground-level $PM_{2.5}$concentrations through complex chemical and physical processes. We developed a series of statistical models using the Multi-Angle Implementation of Atmospheric Correction (MAIAC) aerosol product at 1 km resolution with information from the MODIS cloud product and meteorological information to investigate the extent to which cloud parameters and associated meteorological conditions impact ground-level aerosols at two urban sites in the US: Atlanta and San Francisco. We find that changes in temperature, wind speed, relative humidity, planetary boundary layer height, convective available potential energy, precipitation, cloud effective radius, cloud optical depth, and cloud emissivity are associated with changes in $PM_{2.5}$ concentration and composition, and the changes differ by overpass time and cloud phase as well as between the San Francisco and Atlanta sites. A case-study at the San Francisco site confirmed that accounting for cloud-cover and associated meteorological conditions could substantially alter the spatial distribution of monthly ground-level $PM_{2.5}$ concentrations.

Keywords:

$PM_{2.5}$; MAIAC AOD; non-random missingness; cloud properties; RUC/RAP

1. Introduction

Satellite observations of aerosol optical properties, such as the aerosol optical depth (AOD), are increasingly being used to infer spatial and temporal patterns of fine-mode particulate matter, $PM_{2.5}$, for health studies [1]. However, significant challenges associated

Note: This chapter has been published in the journal, International Journal of Environmental Research and Public Health, and has been formatted according to journal guidelines.

with the use of these observations remain. A large proportion of satellite observations are missing (estimated at ~70% in the 10 km AOD products), chiefly as a result of cloud-cover, snow-cover, and surface brightness [2,3]. Previous work to address this gap-filling problem has largely assumed that the observed aerosols are comparable to aerosols that could not be observed [4,5]. Contradicting this assumption, global and US-centric studies have estimated that missing satellite observations result in an underestimation of true $PM_{2.5}$ concentrations, by an average of 20% in the US [6,7]. Additional work has demonstrated that missing satellite data results in over-prediction of ground-level $PM_{2.5}$ concentrations in the summer months and under-prediction in the winter months at higher latitudes [8,9]. More recent work has gone beyond this to examine the contribution of certain drivers, namely the impact of cloud-cover, on $PM_{2.5}$concentrations at ground level and associated changes in the composition of particulates [10]. The authors found that increased quantities of cloud-cover and increased cloud optical depth were associated with both compositional changes in $PM_{2.5}$ and an overall decrease in concentrations in the southeastern US. These findings suggest that cloud-cover is associated with changes in ground-level $PM_{2.5}$ concentrations and composition. Non-random missingness in satellite retrievals, if not accounted for during exposure estimation of $PM_{2.5}$, can bias health effect estimates in subsequent analyses [11].

Through complex physical and chemical processes, clouds influence the composition, vertical distribution, diurnal patterns, size distribution, and mass concentration of the aerosols beneath them [12]. At the macro scale, clouds are associated with meteorological conditions that govern the micro- and macro-physical properties of both clouds and aerosols, as well as temperature, humidity, wind speed, vertical convection, and planetary

Note: This chapter has been published in the journal, International Journal of Environmental Research and Public Health, and has been formatted according to journal guidelines.

boundary layer height [13,14]. All of these can influence particulate concentrations at the ground level by altering rates of deposition, vertical distributions, emissions, and rates of secondary aerosol formation [15]. Relative humidity and temperature additionally interact to influence rates of both cloud and aerosol formation, the properties and phase of the clouds, and gas-particle partitioning of aerosol components [13,15,16,17]. On a more localized scale, clouds, particularly thunderstorms, alter vertical and horizontal convection, block light, and occasionally rain. Changes in convection directly influence vertical distributions of aerosols beneath the cloud, as well as rates of dry deposition [18,19]. Light blockage alters rates of the photochemical reactions responsible for secondary aerosol formation from gaseous precursors in the atmosphere, indirectly altering aerosol composition and concentrations nearer the ground [20,21]. A small fraction of clouds precipitate, in the process depositing airborne aerosols within and beneath the cloud to the ground [22,23]. Near and within the actual cloud, aerosols participate in the process of cloud formation via nucleation scavenging, and can reduce the effective radius of the cloud particles and alter precipitation efficiency [24,25]. Taken together, the result is a complex tangle of interrelationships between clouds, aerosols, and meteorology which results in different aerosol concentrations and composition beneath cloud-cover relative to that observed when the sky is clear.

The combined impact of these processes on ground-level $PM_{2.5}$ has not been directly studied or linked to measurable properties of the clouds themselves. The current study aims to advance our understanding of whether satellite-retrieved cloud properties are associated with changes in ground-level $PM_{2.5}$ concentration and composition, and the extent to which cloud properties are associated with these changes. We examine the empirical relationship

Note: This chapter has been published in the journal, International Journal of Environmental Research and Public Health, and has been formatted according to journal guidelines.

between cloud properties and the meteorological conditions associated with cloud presence and ground-level concentrations of $PM_{2.5}$ from area ground monitors over two urban sites in the US: Atlanta and San Francisco, two sites chosen as representative of different aerosol and meteorological regimes. We additionally apply these relationships to account for cloud-cover related missing $PM_{2.5}$ estimates when using AOD to predict ground-level $PM_{2.5}$. We compare results from a model which assumes that the reason for the missing AOD observation is random, to one that accounts specifically for cloud-cover missingness as a distinct phenomenon.

2. Materials and Methods

Environmental Protection Agency (EPA) ground observations of 24-h total and speciated $PM_{2.5}$ concentrations between 1 April 2007 and 31 March 2015, were obtained from the EPA's AirData website [26]. Daily ground observations were used to represent the daily gravimetric mass concentrations at individual stations. Mass reconstruction was used to calculate concentrations of organic carbon (OC), sulfate, and nitrate, elemental carbon (EC), sea salt, and soil to account for unmeasured molecules in the speciation information and ensure that changes in the speciated masses, and model estimates, would be comparable to changes in the matched gravimetric measurements [27]. This aids interpretation by allowing direct comparison of changes in component masses to changes in gravimetric masses. Results are only presented in the paper for the reconstructed OC, sulfate and nitrate mass concentrations. The Chemical Speciation Network (CSN) EC and OC carbon fractions were additionally corrected for differences between Total Optical Transmittance (TOT) and Total Optical Reflectance (TOR) monitors, following previous work [28].

Note: This chapter has been published in the journal, International Journal of Environmental Research and Public Health, and has been formatted according to journal guidelines.

Monitors located within the study areas surrounding San Francisco and Atlanta, displayed in Figure 1, were collocated with additional data products. The 1 × 1 km twice-daily MAIAC AOD product, with a retrieval accuracy that is comparable to the ±(0.05 + 0.15)*AOD error envelope of the 10 km MODIS AOD products in validation studies, was used to obtain information on AOD and cloud presence/absence, as calculated using the slightly different screening criteria used for aerosol products relative to cloud products [29,30]. The twice-daily MODIS collection 6, daytime cloud product (M*D06) was used to obtain information on cloud emissivity, cloud optical depth (OD), cloud effective radius, and cloud phase [31]. Of these, cloud emissivity, comparable to cloud fraction, and cloud phase are available at 5 km resolution at nadir, while cloud radius and cloud optical depth are available at 1 km resolution at nadir. The 13 × 13 km hourly rapid update cycle (RUC) and its successor the RAPid refresh (RAP) model [32,33] was used to obtain meteorological data on convective available potential energy (CAPE), wind speed, relative humidity (RH), planetary boundary layer (PBL) height, temperature, and precipitation rates in the pixel nearest to each EPA monitoring station during the hours in which twice-daily MODIS pass times from Terra and Aqua occurred. The RUC/RAP meteorological model represents a continuous time-series of moderate resolution assimilated meteorological data, and is known to accurately reproduce vertical profiles of temperature, humidity, and wind speed, all of particular importance to this application [33]. Collocations of satellite and modeled products with EPA observations were processed in a stepwise fashion, starting with MAIAC, so that AOD missingness could be defined separately from its associated climatic conditions and to account for differences in the spatial resolution of each product. First, each 24-h gravimetric EPA observation was matched to the nearest MAIAC pixel within 1

Note: This chapter has been published in the journal, International Journal of Environmental Research and Public Health, and has been formatted according to journal guidelines.

km of the station and defined as AOD missing or present. Using the Quality Assurance (QA) code we further defined each missing AOD value as missing as a result of cloud or other reason, such as snow-cover or fire hot spot. Observations with AOD missing as a result of cloud-cover were then matched to MODIS cloud parameters averaged within a 10 km radius of each EPA observation, and the nearest RUC/RAP observation. Observations where discrepancies existed between the MODIS cloud parameters and the RUC/RAP results on precipitation rate were classified as possibly cloudy, with the remaining cloudy pixels classified according to the cloud phase information from MODIS. This collocation process was repeated separately for both Aqua and Terra MODIS overpasses. Observations were categorized into five categories: definitively uncloudy, possibly cloudy, definitively cloudy but with no phase determination for the cloud, ice clouds, and water clouds. The possibly cloudy and cloudy but of an uncertain phase categories were collapsed in the later analysis into the possibly cloudy category, and definitively uncloudy observations were not analyzed.

In preliminary analyses, a linear mixture modeling approach was used to examine the nature of the relationship between ground-level $PM_{2.5}$ and cloud properties [34,35]. A number of categorical variables were tested as conditioning variables for grouping $PM_{2.5}$ values into sub-populations. The conditional variables included cloud top height, cloud phase, multi-layered cloud flag, the interaction of cloud phase and cloud height and the interaction of multi-layered cloud flag and cloud top height. Of these, the lowest AIC (Akaike information criterion) value was obtained when using cloud phase as the conditioning variable. Since a mixture model with hard separation of components using a categorical variable is statistically very similar to a set of independent models. The final

Note: This chapter has been published in the journal, International Journal of Environmental Research and Public Health, and has been formatted according to journal guidelines.

results presented here correspond to simpler, linear mixed effects models run independently for each modeling category.

Specifically, four separate models for the two cloud phases (ice and water), to all observations where AOD was not missing, as well as to all other observations where AOD was missing as a result of possible cloud-cover, were fit to the natural log of the 24-h $PM_{2.5}$ mass concentration at each study location and for each overpass time, making a total of 16 independent models. $PM_{2.5}$ concentrations were log-transformed to normalize the data distribution for these linear models. Results for the possibly cloud models are presented only in the supplementary materials. All models included as predictors RH, wind speed, temperature, PBL height, CAPE, precipitation rate, cloud radius, cloud OD, and cloud emissivity. The model fit to observations where AOD was not missing were fit only to the meteorological parameters RH, wind speed, temperature, PBL height and CAPE. All models additionally included random intercepts for each day of the study period to control for seasonal effects. The equation for this model, used throughout the paper, is given in Equation (1). Here, the natural log of the $PM_{2.5}$ observation at each location (j) and time (i), is modeled using a random intercept for each day (β_i), and a fixed effect slope (γ_k) for each of k predictors (X), plus a random Normal error component (ε).

$$\ln(PM_{2.5;\,i,j}) = Day_{i,j} * \beta_i + \sum X_{i,j,k} * \gamma_k + \varepsilon \qquad (1)$$

The same linear mixed effects models (Equation (1)) used to model the impact of cloud cover and meteorological conditions on $PM_{2.5}$ mass were used to model the various $PM_{2.5}$ components, with the goal of identifying the individual component's relative impacts

on the change in total mass. Models were fitted to the natural log of the reconstructed mass of three largest components: sulfate, nitrate, and organic carbon.

We then conducted a case study using a MAIAC AOD-PM model to estimate daily $PM_{2.5}$ where AOD was available. When AOD was not available, values missing in the ungap-filled model were filled in using Equation (3) in the Harvard gap-filling model and were filled in using Equation (1) in the Cloud gap-filling model. We examined differences between the ungap-filled, Harvard gap-filled, and Cloud gap-filled models in the spatial distribution of aerosols from an example monthly estimate choosing January 2012 at the San Francisco site and using a models fit to EPA data over the time period from 2012 to 2014 to predict $PM_{2.5}$. We compared daily predictions made using an ungap-filled model to one that assumes missingness is random (Harvard gap-filled) and to one that assumes cloud-driven missingness (Cloud gap-filled). To accomplish this, the MODIS cloud product and RUC/RAP observations were gridded to the 1 × 1 km MAIAC grid used as the predictive surface for $PM_{2.5}$. The MODIS cloud product was gridded using a method that reconstructs the MODIS polygons using a Voronoi tessellation algorithm from the midpoint locations for each pixel in a granule [3]. These reconstructed polygons were then matched to the MAIAC grid by area to account for the fisheye effect, where pixels towards the edges of the granule are larger than those in the center, still present in the MODIS cloud product. The 1 × 1 km MAIAC grid cells were then matched to the nearest ~13 × 13 km RUC/RAP observation. For pixels where AOD was present a standard prediction model, published in previous works (Equation (2)), was used to predict $PM_{2.5}$ from AOD [36].

Note: This chapter has been published in the journal, International Journal of Environmental Research and Public Health, and has been formatted according to journal guidelines.

$$PM_{st}=(\alpha+u_t)+(\beta'_1+v_t)AOD_{st}+(\beta'_{2k})MetVars_{stk}+\beta'_3Elevation_s+\beta'_4MajorRoads_s+\beta'_5ForestCover_s$$
$$+\beta'_6PointEmissions_s+\varepsilon'_{st}(u_t, v_t, w_t)\sim N[(0,0,0), \psi] \quad (2)$$

Where MAIAC AOD was absent, Equation (1) was used to impute the missing $PM_{2.5}$ values. We additionally compared results to those obtained over cloudy pixels from an adaptation of the gap-filling model developed by researchers at Harvard, which assumes that all types of missing AOD observations are comparable (Equation (3)) [5,37]. All three models fit a first-stage model to obtain ground-level $PM_{2.5}$ estimates over all times and locations where AOD exists (Equation (2)). In Equation (2), daily $PM_{2.5}$ is modeled using a mixed effects model with fixed (a) and daily random intercepts (u_t), fixed (β'_1, β'_{2k}) and daily random slopes (v_t) for AOD. We additionally included fixed slopes for each of k meteorological variables (MetVars), which included RH, PBL height, temperature, and wind speed as well as fixed slopes (β'_{3-6}) for spatial variables including road length, forest cover percentage, point emissions, and elevation. Equation (2) additionally accounts for error in space and time ($\varepsilon'_{st}(u_t,v_t,w_t)$), assuming a multivariate normal distribution centered at 0 $N[(0,0,0), \psi]$. The Harvard gap-filled model predicts missing $PM_{2.5}$ via the use of Equation (3), while the gap-filling model utilized in this work accounts for cloud cover by predicting missing $PM_{2.5}$ using Equation (1). Equation (3) predicts the square root of $PM_{2.5}$ concentrations at each location (s) and time (t), to constrain estimates to be positive, fitting a model with an intercept (a'), slope for the square root of the daily mean $PM_{2.5}$ concentration over the study area (β''_1), and using a spatial smoother ($s(X_s, Y_s)$) fit for each month in the year, predicts the value at each location using the daily mean, assuming

random error (ε''_{st}). The R statistical computing language was used to fit all models, relying on the packages mgcv, and lme4 [38].

$$\sqrt{PredPM_{st}} = \alpha' + \beta''_1\sqrt{MeanPM_t} + s(X_s, Y_s)_k + \varepsilon''_{st} \quad (3)$$

3. Results

3.1. Study Area Characteristics

As shown in Table 1 and Figure 1, the Atlanta site contained 23 monitoring sites that collected a total of 26,369 24-h gravimetric observations between 1 April 2007 and 31 March 2015. Study area characteristics for this site are presented in Table 1. Figure 1 shows the spatial distribution of average monitor values. $PM_{2.5}$ concentrations ranged from 2 to 212.5 $\mu g/m^3$, with an average concentration of 11.7 $\mu g/m^3$. Concentration values decreased with time, from an average of 15.9 $\mu g/m^3$ in 2007 to an average of 9.2 $\mu g/m^3$ in 2015, and exhibited seasonal patterns, with higher concentrations in the summer months. Out of the 23 monitoring sites, six additionally collected speciated measurements, which totaled 2410 sets of observations. The largest fraction, both on average and throughout the year, was organic carbon, followed by sulfate.

Of the 26,369 EPA observations, 21,700 could be matched to an Aqua MAIAC pixel, and 21,359 were matched to a Terra MAIAC pixel. Of these, 14,470 (67%) of the Aqua matches and 13,050 (61%) of the Terra matches had a missing AOD observation. For Aqua and Terra the vast majority, were marked as missing due to cloud-cover. This implies that cloud-cover was slightly more common in the mornings in Atlanta. Speciated collocations of monitors and MAIAC pixels followed a similar pattern. Of the 2410 speciated

observations, 1997 were matched to an Aqua MAIAC pixel and 1982 to a Terra MAIAC pixel. Of the 1997 matched to Aqua MAIAC, 1313 had AOD missing, while of the 1982 matched to Terra MAAIC, 1192 has AOD missing. For both Aqua and Terra, all observations with missing AOD were marked as missing due to cloud cover.

At the time of the Aqua overpass, the majority (5860) of observations with AOD missing were possibly cloudy, implying disagreement between parameters of products regarding the presence of a cloud in the vicinity of the EPA station. At the time of the Terra overpass, 3556 were marked as possibly cloudy. When cloud presence was definitive at the Aqua overpass time, 4719 were marked as water clouds, 2725 as ice clouds, and 1100 as clouds of an undetermined phase. When cloud presence was definitive at the Terra overpass, 4269 were classified as water clouds, 3210 as ice clouds, and 1994 as clouds of an undetermined phase. Speciated observations followed a similar pattern. These categorizations are additionally presented in Table 2.

As shown in Table 1 and Figure 1, the San Francisco study site contained 28 monitoring stations that recorded a total of 23,357 24-h observations of $PM_{2.5}$ mass concentration over the study period. Concentration values ranged from 2 to 190.2 $\mu g/m^3$ and had a mean value of 9.5 $\mu g/m^3$. Concentrations had no clear trend by year, but varied seasonally from springtime lows of 6 $\mu g/m^3$ to winter highs of 13.6 $\mu g/m^3$. Of the 28 monitoring stations that recorded total mass, 10 additionally recorded speciated mass fractions (2853 sets of observations). The dominant fraction, throughout the year, was organic carbon. In the summer months, this was followed by sulfate, and in the winter months by nitrate.

Of the 23,357 EPA observations in San Francisco, 19,388 were matched to Aqua MAIAC and 19,390 to Terra MAIAC. Nearly 8000 from Aqua and Terra, separately, were missing

Note: This chapter has been published in the journal, International Journal of Environmental Research and Public Health, and has been formatted according to journal guidelines.

AOD, 5000 to 6000 fewer than at the Atlanta site. Speciated results followed similar patterns. As can be seen in Table 2, after combination with MODIS cloud and RUC/RAP products, observations within categories of ice cloud, clouds of an uncertain phase, and possibly cloudy were comparable in number to those observed at the Atlanta site. However, water clouds were far fewer in number at the San Francisco site. Similar patterns were observed in the categorization of the speciated results and are presented in Table 2.

3.2. Clouds and 24-Hour Gravimetric Mass

Linear mixed effect models relating ground-level $PM_{2.5}$ to meteorological conditions and cloud properties on days and at locations where the MAIAC AOD was missing, separately run for each combination of study site, overpass time, and cloud phase, revealed differences between these categories and dependence of these differences on the cloud phase and the associated variables. As Table 3 demonstrates, cloud-phase specific models outperformed the more ambiguous category containing possible clouds and clouds of an undetermined phase in both sites. Water cloud models also consistently outperformed ice cloud models on this metric, a fact which we ascribe to the fact that the ice cloud category, which includes both thunderstorms and high cirrus clouds, contains a broader range of cloud and meteorological conditions likely to influence aerosol concentrations than the water cloud category, which is more homogenous.

Regression coefficients relating meteorological variables to $PM_{2.5}$ under various cloud conditions are presented in Figure 2 and Supplementary Table S4. With a few exceptions, model results were generally consistent with those from the possibly cloudy and uncloudy observations. Intercepts were all positive, indicating average concentrations in each category that were greater than 1 $\mu g/m^3$. Consistency was also the case for wind speed and

Note: This chapter has been published in the journal, International Journal of Environmental Research and Public Health, and has been formatted according to journal guidelines.

PBL height, both of which were associated with decreases in $PM_{2.5}$ concentrations in nearly all models. An increase in RH was associated with a decrease in the $PM_{2.5}$ concentration when clouds were present, with no clear trends by cloud category, site, or overpass. However, in the no cloud model where AOD values were present, RH was associated with an increase in $PM_{2.5}$ concentrations. Higher temperature was associated with a slight increase in ln($PM_{2.5}$) concentrations in Atlanta, where summertime concentrations tended to be higher, and with a slight decrease in San Francisco, where wintertime concentrations tended to be higher (see Table 1). CAPE, which increases with increasing vertical convection, was strongly negative but not statistically significant at the San Francisco site and slightly positive at the Atlanta site and in the no cloud models at both sites. Precipitation was generally associated with a decrease in ground-level $PM_{2.5}$ at both sites, although this decrease was larger in magnitude at the San Francisco site, where estimates clustered around 0.2 to 0.3, than in Atlanta, where estimates were not significantly different from 0 during the morning overpass. At both sites, precipitation was associated with significant decreases in 24-h $PM_{2.5}$ concentrations when falling in during the afternoon overpass, but with less consistently significant decreases in concentration when falling during the morning overpass.

Cloud properties such as emissivity, radius, and OD, obtained from the MODIS cloud product were also associated with changes in the ground-level $PM_{2.5}$. At the Atlanta site, cloud OD was associated with a significant decrease in $PM_{2.5}$concentrations when ice clouds were present in the morning and afternoon and with an increase when water clouds were present in the mornings. However, water and ice cloud OD, emissivity, and radius were primarily associated with positive changes in ground-level $PM_{2.5}$ at the Atlanta site. Cloud-

Note: This chapter has been published in the journal, International Journal of Environmental Research and Public Health, and has been formatted according to journal guidelines.

cover observed during a MODIS overpass had a more significant and more negative impact on $PM_{2.5}$ concentrations at the San Francisco site. When water clouds were present during the morning overpass, cloud OD was associated with a decrease in ground-level $PM_{2.5}$ concentrations, while increasing cloud radius was associated with a decrease in ground-level $PM_{2.5}$. Cloud emissivity was associated with a decrease in concentration when water clouds were present during the afternoon overpass. Results for ice clouds also differed by overpass at the San Francisco site, although the estimates were comparable, cloud emissivity was a better predictor of concentration changes for morning ice clouds, while cloud OD was a better predictor of concentration changes on the ground for afternoon ice clouds.

3.3. Clouds and Speciation of $PM_{2.5}$

Speciated model results are presented in Supplementary Tables S2–S4. An increase in RH was associated with increases in sulfate and nitrate mass at the San Francisco site, with a decrease in nitrate at the Atlanta site, and with decreases in the OC mass at both sites. Increased temperature was associated with an increase in sulfate mass and a decrease in nitrate mass at both sites, and with a decrease in OC mass at the San Francisco site and an increase in OC mass at the Atlanta site. Wind speed was associated with a decrease in mass for all three components, with the exception of sulfate at the San Francisco site. Increases in the PBL height were also associated with decreases in the mass of all components, with one exception for nitrate at the Atlanta site. This same pattern was observed for an increase in CAPE and decreases in component masses with increasing CAPE, with the exception of nitrate in Atlanta. Precipitation was also associated with decreases in component masses for sulfate, nitrate, and OC, particularly when ice clouds were overhead.

Note: This chapter has been published in the journal, International Journal of Environmental Research and Public Health, and has been formatted according to journal guidelines.

Cloud radius was associated with a decrease in the total and sulfate masses at the San Francisco site, but was otherwise not a significant predictor of changes in $PM_{2.5}$ concentrations. Results for sulfate and cloud emissivity or cloud OD at the San Francisco site were mixed, but cloud OD was associated with a decrease in sulfate mass at the Atlanta site. Cloud OD was associated with a decrease in nitrate mass at the San Francisco site and with an increase in nitrate mass at the Atlanta site, although the majority of estimates at the San Francisco site were positive but not significant. Cloud emissivity at the San Francisco site, and Cloud OD at the Atlanta site were associated with increases in OC mass.

3.4. Application to MAIAC-Derived $PM_{2.5}$

We applied the cloud model results within the context of a predictive model relating MAIAC AOD to ground-level $PM_{2.5}$concentrations, comparing results from an ungap-filled AOD to $PM_{2.5}$ model (Equation (2)) with missing observations to those to those from a gap-filling model that ignores cloud-cover, the Harvard gap filling approach (Equation (3)) and a gap-filling model that accounts for cloud properties, the Cloud gap-filling approach (Equation (1)). Results are presented in Figure 3. All three models produce a similar basic spatial pattern for $PM_{2.5}$ concentrations in San Francisco, with higher concentrations in the central valley, lower concentrations over the forested mountains, and higher concentrations on the other side of the mountains near Nevada. However, there are substantial differences in both the monthly averages and spatial patterns between the Harvard and Cloud gap filled results, ranging from −13.14 to 15.52 $\mu g/m^3$ by location. The Harvard gap filled results are considerably smoother than the Cloud gap filled results, also averaging 2.58 $\mu g/m^3$ higher in concentration over the month of January in 2012. It is also worth noting the differences

Note: This chapter has been published in the journal, International Journal of Environmental Research and Public Health, and has been formatted according to journal guidelines.

between the non-gap filled and Cloud gap filled results, which average 2.40 μg/m^3. In Figure 3, the Cloud gap filled monthly average concentrations are lower than the non-gap filled results, particularly over the central valley and metropolitan San Francisco. Cloud fractions (panel E) additionally vary spatially, ranging from 20% to 80%, depending on location.

4. Discussion

We examined the relationship between cloud presence and ground-level $PM_{2.5}$ mass and speciation, linking changes in concentration to cloud properties and meteorological conditions. We found that, overall, cloud presence can lead to fairly substantial over or under-prediction of $PM_{2.5}$ concentrations and differences in the spatial patterns of pollutant concentrations when using satellite-observed AOD to estimate ground-level concentrations.

The impact of relative humidity on $PM_{2.5}$ was both negative and consistent between sites, overpass times, and cloud and type. However, results differed by species, with estimates for RH that were negative and largest in magnitude for organic carbon. This implies that most of the changes in total $PM_{2.5}$ mass that were associated with relative humidity result specifically from a decrease in the organic carbon fraction. A likely explanation for this is an increase in the photo-oxidation rates for aromatic hydrocarbons with decreasing humidity [16]. The fact that this association was stronger for organics at the San Francisco site, where NOx concentrations are higher and relative humidity tends to be lower on average, but stronger for gravimetric $PM_{2.5}$ at the Atlanta site, which is known for its high isoprene emissions, also supports this explanation.

Note: This chapter has been published in the journal, International Journal of Environmental Research and Public Health, and has been formatted according to journal guidelines.

The impact of PBL height and the horizontal wind speed on ground-level concentrations of $PM_{2.5}$ were consistently negative, excepting estimates for the association between PBL height and nitrates in Atlanta, implying that increased wind speeds and PBL heights were associated with decreases in $PM_{2.5}$ concentrations. CAPE, an indicator of vertical stability, was more consistently associated with increases in ground-level concentrations of $PM_{2.5}$ on the ground, implying increases with decreasing convective energy, although this association was not consistent. This, in addition to the nitrate results, suggests that future work on this topic should include consideration of vertical convection and distribution of aerosols, as these may also change under cloudy conditions.

Increasing cloud OD, a marker of light blockage from cloud cover, and cloud emissivity, an indicator of the quantity of cloud present, were significantly associated with changes in nitrate, sulfate, and organic carbon concentrations. At both sites, we observed decreases in sulfate and total mass with increasing cloud OD when ice clouds were present. This is consistent with previous results [10] and with an impact specifically from blockage of light to the surface during sunny/fair weather conditions that would otherwise be conducive to the photochemical production of sulfate from gaseous sulfur dioxide [20,39]. Results for water clouds and for nitrate and OC were not consistent between sites, however, and interpretation of these results is less straightforward. This interpretation is further complicated by the fact that cloud-aerosol interactions go both ways, and aerosols have the potential to reduce cloud droplet radii, and thus alter emissivity and OD [21,24]. We had expected to observe an increase in nitrate concentrations with increasing cloud OD or cloud amount, but instead only observed a decrease in nitrate concentrations under afternoon ice clouds in San Francisco. One possible explanation is noise from precipitation events

associated with darker cloud-cover that were missing from our precipitation variable. Similarly, we observed an increase in the OC mass with morning water cloud OD at the Atlanta site and emissivity at the San Francisco site. The results point to changes in rates of secondary organic aerosol formation associated with light blockage. Similar to nitrate, recent research points to more rapid, nitrate-driven, nighttime oxidation of isoprene and other volatile organic compounds than through the photo-oxidation routes available during daytime and could explain this increase in concentration with increasing light blockage during the morning hours when nitrate could still be present [20].

Precipitation, via the process of wet deposition, is associated with an overall decrease in $PM_{2.5}$ mass that is larger in magnitude for soluble than for non-soluble PM species [40]. This was observed in our data consistently for ice clouds, which tended to precipitate more, and to some extent for water clouds. The impact of precipitation at the time of the overpass in San Francisco was also larger than that observed in Atlanta. Reasons for this could include the fact that we used a precipitation indicator instead of the precipitation rate, and that it rains more frequently in Atlanta than San Francisco, making the capture of rain during a MODIS overpass time less important relative to 24-h pollutant concentrations.

Finally, we observed a few important differences between sites. Overall, cloud-cover properties and observations at the time of the MODIS overpasses had greater explanatory power in San Francisco than in Atlanta. This was evidenced both by the significance of the cloud OD, cloud emissivity, cloud radius, and precipitation predictors in the models, as well as by the R^2 values presented in Table 3. The case study included in our results additionally demonstrates that accounting for cloud-cover in a gap-filling model produces differences

in monthly results that can be substantial. The observed differences may also stem from the frequency of cloud cover.

We had expected a large proportion of MAIAC retrievals for AOD would be missing, however, a smaller proportion than expected had consistent information on cloud properties between products. Hence, this study was only able to investigate associations for around 50% of the missing AOD observations, limiting the generalizability of conclusions. To mitigate this issue, we have made an effort in the discussion to only highlight results that were consistently observed across the models. However, this also underscores the importance of possible cloud contamination as a source of uncertainty in estimation of ground-level $PM_{2.5}$ from satellite retrievals and is a potentially important area for future research.

5. Conclusions

This study demonstrated that clouds are associated with changes in ground-level $PM_{2.5}$ concentration, and these changes are driven by physical and chemical processes associated with cloud cover. We additionally demonstrated that the impact of cloud-driven satellite missingness on our ability to make accurate $PM_{2.5}$ estimates over a surface using this data differs by location. Not accounting for cloud cover and associated meteorological conditions, particularly rainfall, can lead to both over- and under-estimation of $PM_{2.5}$ concentrations. However, additional work is still needed to confirm and clarify the relationships investigated here, particularly into the nature and rationale for the geographic differences observed in these relationships.

Note: This chapter has been published in the journal, International Journal of Environmental Research and Public Health, and has been formatted according to journal guidelines.

Associations between meteorological variables and $PM_{2.5}$ total mass and constituents showed variability across pollutants, cloud types, and locations, but a few important findings stood out. We found that relative humidity is associated with a decrease in the organic component of $PM_{2.5}$ resulting from the humidity dependence of rates of secondary organic aerosol formation. Also, precipitation and changes in rates of secondary aerosol production, indicated by increased cloud OD or cloud emissivity, impact concentration, and speciation of aerosols underneath the clouds.

Our analyses also suggested that not all clouds and locations can be considered equal, and the cloud presence, observed at a specific time of the day, generally matters more in San Francisco than in Atlanta. In San Francisco, we conducted a case study demonstrating changes in spatial patterns of air pollution at the monthly level that were associated with cloud-cover.

Supplementary Materials

The following are available online at www.mdpi.com/1660-4601/14/10/1244/s1, Table S1. Tabulation of numbers of observations within cloud categories by Environmental Protection Agency (EPA) monitoring site in the Atlanta study area; Table S2. Tabulation of numbers of observations within cloud categories by EPA monitoring site in the San Francisco study area; Table S3. Tabulation of observations within cloud categories by season in Atlanta and San Francisco; Table S4. Model results for gravimetric $PM_{2.5}$ mass concentration. All results are presented as the parameter estimate (standard error) with stars indicating significance if the *p*-value was below 0.05; Table S5. Model results for Sulfate. All results are presented as the parameter estimate (standard error) with stars indicating significance if the *p*-value was below 0.05; Table S6. Model results for Nitrate. All results

are presented as the parameter estimate (confidence interval) with stars indicating significance if the *p*-value was below 0.05; Table S7. Model results for organic carbon (OC). All results are presented as the parameter estimate (confidence interval) with stars indicating significance if the *p*-value was below 0.05; Table S8. CV R^2values from San Francisco case study data over time period from 2012 to 2014.

Acknowledgments

The work of Jessica H. Belle and Yang Liu is partially supported by the NASA Applied Sciences Program (Grant # NNX14AG01G and NNX16AQ28G, PI: Liu).

Author Contributions

Jessica H. Belle, Yang Liu, and Howard H. Chang conceived and designed the analysis. Yujie Wang and Alexei Lyapustin contributed data. Jessica H. Belle analyzed the data. Jessica H. Belle and Xuefei Hu contributed analysis tools. Jessica H. Belle wrote the paper.

Conflicts of Interest

The authors declare no conflict of interest.

References

1. Sorek-Hamer, M.; Just, A.C.; Kloog, I. Satellite remote sensing in epidemiological studies. *Curr. Opin. Pediatr.* **2016**, *28*, 228–234. [Google Scholar] [CrossRef] [PubMed]
2. Fasso, A.; Finazzi, F. Statistical Mapping of Air Quality by Remote Sensing. In Proceedings of the Accuracy 2010 Conference, leicester, UK, 20–23 July 2010; Available online: http://www.spatial-accuracy.org/FassoAccuracy2010(accessed on 17 October 2017). [Google Scholar]

Note: This chapter has been published in the journal, International Journal of Environmental Research and Public Health, and has been formatted according to journal guidelines.

3. Belle, J.; Liu, Y. Evaluation of aqua modis collection 6 aod parameters for air quality research over the continental united states. *Remote Sens.* **2016**, *8*, 815. [Google Scholar] [CrossRef]
4. Anderson, T.L.; Charlson, R.J.; Winker, D.M.; Ogren, J.A.; Holmén, K. Mesoscale variations of tropospheric aerosols. *J. Atmos. Sci.* **2003**, *60*, 119–136. [Google Scholar] [CrossRef]
5. Just, A.C.; Wright, R.O.; Schwartz, J.; Coull, B.A.; Baccarelli, A.A.; Tellez-Rojo, M.M.; Moody, E.; Wang, Y.; Lyapustin, A.; Kloog, I. Using high-resolution satellite aerosol optical depth to estimate daily $PM_{2.5}$ geographical distribution in mexico city. *Environ. Sci. Technol.* **2015**, *49*, 8576–8584. [Google Scholar] [CrossRef] [PubMed]
6. Ford, B.; Heald, C. Exploring the uncertainty associated with satellite-based estimates of premature mortality due to exposure to fine particulate matter. *Atmos. Chem. Phys. Discuss.* **2015**, *15*, 25329–25380. [Google Scholar] [CrossRef]
7. Van Donkelaar, A.; Martin, R.V.; Brauer, M.; Boys, B.L. Use of satellite observations for long-term exposure assessment of global concentrations of fine particulate matter. *Environ. Health Perspect.* **2015**, *123*, 135. [Google Scholar] [CrossRef] [PubMed]
8. Christopher, S.A.; Gupta, P. Satellite remote sensing of particulate matter air quality: The cloud-cover problem. *J. Air Waste Manag. Assoc.* **2010**, *60*, 596–602. [Google Scholar] [CrossRef] [PubMed]
9. Gupta, P.; Christopher, S.A. An evaluation of terra-modis sampling for monthly and annual particulate matter air quality assessment over the southeastern united states. *Atmos. Environ.* **2008**, *42*, 6465–6471. [Google Scholar] [CrossRef]

Note: This chapter has been published in the journal, International Journal of Environmental Research and Public Health, and has been formatted according to journal guidelines.

10. Yu, C.; Di Girolamo, L.; Chen, L.; Zhang, X.; Liu, Y. Statistical evaluation of the feasibility of satellite-retrieved cloud parameters as indicators of $PM_{2.5}$ levels. *J. Expo. Sci. Environ. Epidemiol.* **2015**, *25*, 457–466. [Google Scholar] [CrossRef] [PubMed]
11. Strickland, M.; Hao, H.; Hu, X.; Chang, H.; Darrow, L.; Liu, Y. Pediatric emergency visits and short-term changes in $PM_{2.5}$ concentrations in the us state of georgia. *Environ. Health Perspect.* **2015**, *124*, 690–696. [Google Scholar] [CrossRef] [PubMed]
12. Seinfeld, J.H.; Pandis, S.N. *Atmospheric Chemistry and Physics: From Air Pollution to Climate Change*; John Wiley & Sons: New York, NY, USA, 2012. [Google Scholar]
13. Mauger, G.S.; Norris, J.R. Meteorological bias in satellite estimates of aerosol-cloud relationships. *Geophys. Res. Lett.***2007**, *34*. [Google Scholar] [CrossRef]
14. Rossow, W.B.; Schiffer, R.A. Advances in understanding clouds from ISCCP. *Bull. Am. Meteorol. Soc.* **1999**, *80*, 2261–2287. [Google Scholar] [CrossRef]
15. Klein, S.A.; Hartmann, D.L.; Norris, J.R. On the relationships among low-cloud structure, sea surface temperature, and atmospheric circulation in the summertime northeast pacific. *J. Clim.* **1995**, *8*, 1140–1155. [Google Scholar] [CrossRef]
16. Zhang, H.; Surratt, J.; Lin, Y.; Bapat, J.; Kamens, R. Effect of relative humidity on soa formation from isoprene/no photooxidation: Enhancement of 2-methylglyceric acid and its corresponding oligoesters under dry conditions. *Atmos. Chem. Phys.* **2011**, *11*, 6411–6424. [Google Scholar] [CrossRef]
17. Zhou, Y.; Zhang, H.; Parikh, H.M.; Chen, E.H.; Rattanavaraha, W.; Rosen, E.P.; Wang, W.; Kamens, R.M. Secondary organic aerosol formation from xylenes and mixtures of toluene and xylenes in an atmospheric urban hydrocarbon mixture: Water and particle seed effects (II). *Atmos. Environ.* **2011**, *45*, 3882–3890. [Google Scholar] [CrossRef]

Note: This chapter has been published in the journal, International Journal of Environmental Research and Public Health, and has been formatted according to journal guidelines.

18. Morgan, W.; Allan, J.; Bower, K.; Capes, G.; Crosier, J.; Williams, P.; Coe, H. Vertical distribution of sub-micron aerosol chemical composition from north-western europe and the north-east atlantic. *Atmos. Chem. Phys.* **2009**, *9*, 5389–5401. [Google Scholar] [CrossRef]

19. Hicks, B.; Baldocchi, D.; Meyers, T.; Hosker, R.; Matt, D. A preliminary multiple resistance routine for deriving dry deposition velocities from measured quantities. *Water Air Soil Pollut.* **1987**, *36*, 311–330. [Google Scholar] [CrossRef]

20. Ng, N.; Kwan, A.; Surratt, J.; Chan, A.; Chhabra, P.; Sorooshian, A.; Pye, H.O.; Crounse, J.; Wennberg, P.; Flagan, R. Secondary organic aerosol (SOA) formation from reaction of isoprene with nitrate radicals (NO_3). *Atmos. Chem. Phys.***2008**, *8*, 4117–4140. [Google Scholar] [CrossRef]

21. Liao, H.; Adams, P.J.; Chung, S.H.; Seinfeld, J.H.; Mickley, L.J.; Jacob, D.J. Interactions between tropospheric chemistry and aerosols in a unified general circulation model. *J. Geophys. Res. Atmos.* **2003**, *108*. [Google Scholar] [CrossRef]

22. Radke, L.F.; Hobbs, P.V.; Eltgroth, M.W. Scavenging of aerosol particles by precipitation. *J. Appl. Meteorol.* **1980**, *19*, 715–722. [Google Scholar] [CrossRef]

23. Rodhe, H.; Grandell, J. On the removal time of aerosol particles from the atmosphere by precipitation scavenging. *Tellus* **1972**, *24*, 442–454. [Google Scholar] [CrossRef]

24. Fan, J.; Leung, L.R.; Rosenfeld, D.; Chen, Q.; Li, Z.; Zhang, J.; Yan, H. Microphysical effects determine macrophysical response for aerosol impacts on deep convective clouds. *Proc. Natl. Acad. Sci. USA* **2013**, *110*, E4581–E4590. [Google Scholar] [CrossRef] [PubMed]

25. Stevens, B.; Feingold, G. Untangling aerosol effects on clouds and precipitation in a buffered system. *Nature* **2009**, *461*, 607–613. [Google Scholar] [CrossRef] [PubMed]

Note: This chapter has been published in the journal, International Journal of Environmental Research and Public Health, and has been formatted according to journal guidelines.

26. EPA. Aqs Data Mart. Available online: https://aqs.epa.gov/aqsweb/documents/data_mart_welcome.html (accessed on 31 March 2016).

27. Hand, J.; Copeland, S.; Day, D.; Dillner, A.; Indresand, H.; Malm, W.; McDade, C.; Moore, C.; Pitchford, M.; Schichtel, B. Spatial and Seasonal Patterns and Temporal Variability of Haze and Its Constituents in the United States Report V. IMPROVE Reports. Available online: http://vista.cira.colostate.edu/improve/Publications/improve_reports.htm(accessed 11 September 2011).

28. Malm, W.C.; Schichtel, B.A.; Pitchford, M.L. Uncertainties in $PM_{2.5}$ gravimetric and speciation measurements and what we can learn from them. *J. Air Waste Manag. Assoc.* **2011**, *61*, 1131–1149. [Google Scholar] [CrossRef] [PubMed]

29. Levy, R.; Mattoo, S.; Munchak, L.; Remer, L.; Sayer, A.; Hsu, N. The collection 6 modis aerosol products over land and ocean. *Atmos. Meas. Tech.* **2013**, *6*, 2989–3034. [Google Scholar] [CrossRef]

30. Lyapustin, A.; Wang, Y.; Laszlo, I.; Kahn, R.; Korkin, S.; Remer, L.; Levy, R.; Reid, J. Multiangle implementation of atmospheric correction (MAIAC): 2. Aerosol algorithm. *J. Geophys. Res. Atmos.* **2011**, *116*. [Google Scholar] [CrossRef]

31. Platnick, S.; Ackerman, S.; King, M.; Menzel, P.; Wind, G.; Frey, R. *MODIS Atmosphere l2 Cloud Product (06_L2)*; System, N.M.A.P., Ed.; Goddard Space Flight Center: Greenbelt, MD, USA, 2015.

32. Benjamin, S.G.; Dévényi, D.; Weygandt, S.S.; Brundage, K.J.; Brown, J.M.; Grell, G.A.; Kim, D.; Schwartz, B.E.; Smirnova, T.G.; Smith, T.L. An hourly assimilation-forecast cycle: The ruc. *Mon. Weather Rev.* **2004**, *132*, 495–518. [Google Scholar] [CrossRef]

Note: This chapter has been published in the journal, International Journal of Environmental Research and Public Health, and has been formatted according to journal guidelines.

33. Benjamin, S.G.; Weygandt, S.S.; Brown, J.M.; Hu, M.; Alexander, C.R.; Smirnova, T.G.; Olson, J.B.; James, E.P.; Dowell, D.C.; Grell, G.A. A north american hourly assimilation and model forecast cycle: The rapid refresh. *Mon. Weather Rev.* **2016**, *144*, 1669–1694. [Google Scholar] [CrossRef]

34. Grün, B.; Leisch, F. Fitting finite mixtures of generalized linear regressions in R. *Comput. Stat. Data Anal.* **2007**, *51*, 5247–5252. [Google Scholar] [CrossRef]

35. Leisch, F. Flexmix: A General Framework for Finite Mixture Models and Latent Glass Regression in R. *J. Stat. Softw.***2004**, *11*, 1–18. [Google Scholar] [CrossRef]

36. Hu, X.; Waller, L.A.; Lyapustin, A.; Wang, Y.; Al-Hamdan, M.Z.; Crosson, W.L.; Estes, M.G.; Estes, S.M.; Quattrochi, D.A.; Puttaswamy, S.J. Estimating ground-level $PM_{2.5}$ concentrations in the southeastern united states using maiac aod retrievals and a two-stage model. *Remote Sens. Environ.* **2014**, *140*, 220–232. [Google Scholar] [CrossRef]

37. Kloog, I.; Ridgway, B.; Koutrakis, P.; Coull, B.A.; Schwartz, J.D. Long-and short-term exposure to $PM_{2.5}$ and mortality: Using novel exposure models. *Epidemiology* **2013**, *24*, 555. [Google Scholar] [CrossRef] [PubMed]

38. Team, R.C. R: A Language and Environment for Statistical Computing. *R Foundation for Statistical*. Available online: https://www.R-project.org/ (accessed on 17 October 2017).

39. Stockwell, W.R.; Calvert, J.G. The mechanism of the HO-SO_2 reaction. *Atmos. Environ.* **1983**, *17*, 2231–2235. [Google Scholar] [CrossRef]

40. Chamberlain, A. *Aspects of Travel and Deposition of Aerosol and Vapour Clouds*; Atomic Energy Research Establishment: Harwell/Berks, UK, 1953.

Note: This chapter has been published in the journal, International Journal of Environmental Research and Public Health, and has been formatted according to journal guidelines.

Note: This chapter has been published in the journal, International Journal of Environmental Research and Public Health, and has been formatted according to journal guidelines.

Effect attenuation in the relationship between pediatric ED visits and satellite-based $PM_{2.5}$ exposure

I. Abstract

Background: Emergency department visits for respiratory issues have been associated with $PM_{2.5}$ concentrations. However, discrepancies exist between different studies in the literature.

Objective: This study considers the impact of different gap-filled and ungap-filled satellite-based exposure models on the OR between $PM_{2.5}$ exposure and pediatric ED visits for 3 possible outcomes, asthma or wheeze, otitis media, and upper respiratory infection.

Methods: We compare odds ratios calculated for three possible outcomes using three different, but related, satellite-based exposure models for $PM_{2.5}$, an ungap-filled model that leaves missing observations missing, and two gap-filled exposure models, one that accounts for the influence of cloud-cover on $PM_{2.5}$ concentrations and one that does not account for cloud-cover. We additionally examine results stratified on cloudiness.

Results: The three exposure models produced different results for the exposure, with the cloud-based exposure model producing slightly lower concentrations, on average, than the ungap-filled and no cloud gap-filled exposure models. When examining odds ratio estimates for each of the three outcomes, we identified statistically significant associations between satellite estimates and emergency department visits for asthma or wheeze, otitis media, and upper respiratory tract infection. Ungap-filled odds ratio estimates were biased towards the null for the outcomes asthma or wheeze and otitis media and unbiased for upper respiratory infection. When results were stratified on cloudiness we observed effect attenuation among ungap-filled ORs, only on cloudy days.

Conclusion: Gap-filling a satellite model is important to prevent effect attenuation in the resulting OR estimates calculated from an exposure model. However, the method used to gap-fill is less important.

II. Introduction

Emergency department (ED) visits for respiratory issues have been associated with air pollution episodes, often, like mortality, affecting the most vulnerable, children and elderly adults with pre-existing respiratory issues. Seminal work on the relationship between ED visits and air pollution concentrations in elderly adults has identified a 1-2% increase in ED visits for heart failure that is associated with increases in $PM_{2.5}$ concentrations of 10 $\mu g/m^3$. [1] Pediatric populations, however, are no less vulnerable to morbidity resulting from air pollution. The literature lacks large-scale studies on the association between ED visits for various causes and air pollution concentrations in pediatric populations. However, regional studies have found associations between air pollution concentrations and upper respiratory symptoms [2], asthma exacerbation [3] [4] [5], pneumonia [6], and bronchitis [7]. However, given the patchwork nature of the existing studies on this topic, discrepancies remain between studies regarding the strength of the association. These discrepancies undermine the strength of the existing literature, making biases inherent in different study designs and exposure measurement methods important to root out.

Strickland et al. examined the associations between pediatric emergency department (ED) visits for six possible health outcomes and exposure to $PM_{2.5}$. [8] The authors identified a sensitivity in the odds ratios (OR) between pediatric emergency department (ED) visits and exposure estimates that was dependent on the proportion of missing observations in the satellite model. [8] This is a significant finding because satellite models often have many missing observations due to cloud cover and high surface reflectance. [9]

$PM_{2.5}$ levels under these conditions are likely to differ from conditions observed when observations are not missing. [10] [11] This non-random missingness in satellite-derived $PM_{2.5}$ exposure estimates has the potential to bias study results in unpredictable ways.

This study investigates sensitivity in odds ratios calculated from satellite-based exposure measurements to missing satellite observations. We compare three sets of odds ratios calculated between $PM_{2.5}$ and pediatric ED visits for three adverse health outcomes, i.e. asthma/wheeze, otitis media, and upper respiratory infection. Two of the three sets of odds ratios (ORs) use a satellite-based model that has been gap-filled, or where the missing observations have been imputed, to represent the exposure, while the third uses an ungap-filled satellite model. The first set of gap-filled ORs uses a gap-filled exposure model that assumes the missing observations are missing at random, while the second set of ORs uses a gap-filled exposure model that assumes the missing observations are missing as a result of cloud cover. The resulting OR estimates and confidence interval sizes are then compared to identify changes resulting from whether cloud-driven missingness in a satellite model is treated in a model and whether it makes a difference if the gap-filling is treated as a random or non-random event.

III. Methods – Data

a. Health data

The health dataset consists of ZIP code-level data on pediatric ED visits in the US state of Georgia from January 1st 2002 through June 30th, 2010 for a total of over 8 million ED visits from 150 hospitals. This dataset, and the analysis of ICD-9 codes for case definitions were previously described by Strickland et al. [8] Briefly, ICD-9 codes 493 or 786.07 in any diagnosis field was determined to be asthma/wheeze, primary codes 381 and

382 were defined as otitis media (OM), and primary codes 460-465 and 477 as upper respiratory infection (URI) if the codes for asthma/wheeze were also not present.

Over the time period from 2002-2010, a total of 429,199 ED visits for asthma or wheeze were recorded in the state of Georgia. In addition to these visits, over 1 million, 1,021,685, ED visits for URI were recorded, additionally the state recorded 548,197 for OM. We additionally restricted to ED visits that occurred between January 1st, 2003 and December 31st 2005, to correspond to the period of availability of the exposure data. After restricting the time period the number of ED visits for each outcome dropped to 137,912 for asthma/wheeze, 365,541 for URI, and 199,856 for OM.

Cases were additionally categorized by cloudiness. ZIP codes and days with less than or equal to 20% cloudy observations categorized as 'clear,' ZIP codes and days with greater than or equal to 80% cloudy observations categorized as 'cloudy,' and ZIP codes and days with 20-80% cloudy observations categorized as 'partially cloudy.' After categorization by cloudiness a total of 107,793 URI cases were categorized as partially cloudy, while 58,836 were categorized as clear, and 165,818 were categorized as cloudy. For asthma or wheeze, 42,668 were partially cloudy, 64,065 were cloudy, and 20,775 were clear. For OM, 58,688 were partially cloudy, 92,533 were cloudy, and 29,943 were clear.

b. Exposure model inputs

We utilized 1 km AOD retrieved by the Multi-Angle Implementation of Atmospheric Correction (MAIAC) algorithm based on the measurements of the Moderate Resolution Imaging Spectroradiometer (MODIS) aboard the Aqua and Terra satellites as a major predictor of our $PM_{2.5}$ exposure model. [12] For the basic satellite model, this information was combined with meteorological information from the nearest National Land Data Assimilation System (NLDAS) [13] and North American Regional Reanalysis

(NARR) [14] model pixels and matched in time to the overpass time for Aqua and Terra separately. Meteorological information pulled from NLDAS included the precipitation rate, the percentage of precipitation that was convective, temperature, humidity, short wave radiation downwards, long wave radiation downwards, and wind speed. Meteorological information pulled from NARR included the planetary boundary layer (PBL) height, and relative humidity. Daily counts of fires within a 25 km radius were also taken from the Aqua and Terra MODIS fire products (M*D14_L2). [15] From a global 2x2.5 degree run of the 10.1 GEOS-Chem chemical transport model incorporating mechanisms for secondary organic aerosols, we included the percentage of sulfate molecules contained in the PBL, calculated using equation 1 and the modeled $PM_{2.5}$ concentration. [16] In equation 1, the percentage of sulfate molecules contained in the PBL at each pixel and overpass, p_k, is calculated by summing the product of the mixing ratio of sulfate, x, air density, y, and box height, z, at that pixel in each level to the PBL height, and dividing by the product of x, y, and z summed over the entire vertical column, composed of n layers.

$$p_k = \sum_{i=1}^{PBL} x_{ik} y_{ik} z_{ik} \Big/ \sum_{j=1}^{n} x_{jk} y_{jk} z_{jk} \qquad \text{Equation 1}$$

From the National Land Cover Database (NLCD) we included the percentage of impervious surface area in each MAIAC pixel. [17] From Census TIGER database we extracted the distance from each MAIAC pixel polygon to the nearest primary or secondary road. [18] We additionally included elevation from the 3D elevation program (3DEP) national elevation product [19], and counts of $PM_{2.5}$ point sources from the National Emissions Inventory 2008 [20]. For the cloud gap-filling model we incorporated information from the Terra and Aqua MODIS cloud (M*D06_L2) [21] and location products (M*D03_L2), converting the 1x1 km cloud AOD (COD) swath product to the

1x1 km MAIAC grid using inverse distance interpolation (IDW) and the 5x5 km cloud emissivity swath product to the 1x1 km MAIAC grid using reconstructed Thiessen polygons. [22] Finally, models were fit to $PM_{2.5}$ concentrations measured at EPA ground monitors within the study area. [23]

IV. Methods – Exposure models

Both the no cloud and cloud gap-filled satellite models start from the same AOD-$PM_{2.5}$ model, and differ in how they fill in the $PM_{2.5}$ observations where and when AOD is missing. This model, a linear mixed effects model represented by equation 2, relates MAIAC AOD values to ground-level concentrations of $PM_{2.5}$, as measured at EPA ground monitors, with random slopes for AOD, temperature, RH, and percentage of sulfate molecules in the PBL, and a random intercept for each day in the time series.

$$PM_{2.5,st} = (b_0 + b_{0,t}) + (b_1 + b_{1,t})AOD_{st} + (b_2 + b_{2,t})p_{st} + (b_3 + b_{3,t})Temperature_{st} + (b_4 + b_{4,t})RH_{st} + b_5 WindSpeed_{st} + b_6 PBLheight_{st} + b_7 Elevation_s + b_8 PercentImpervious_s + b_9 NEI2008_s + b_{10} DistRoads_s + b_{11} FireCount_s + b_{12} LocalRoadLength_s + b_{13}(DistRoads_s * LocalRoadLength_s) + b_{14}(Temperature_{st} * RH_{st}) + \epsilon_{st}(b_{0,t} b_{1,t} b_{2,t}) \sim N[(0,0,0), \psi]$$

Equation 2

In equation 2, $PM_{2.5}$ at each location, s, and time, t, is modeled as a function of intercepts, normal (b_0) and day-specific ($b_{0,t}$), with fixed ($b_{1\text{-}4}$) and random ($b_{1\text{-}4,t}$) slopes for AOD, the percentage of sulfate molecules in the PBL, p, Temperature and RH; fixed slopes, $b_{5\text{-}14}$, for wind speed, PBL height, elevation, percent impervious surface area, counts from the NEI 2008 within a buffer of 25 km, the distance to nearest road, fire counts within a 25 km radius, length of local roads, interaction between temperature and RH, and interaction terms between distance to major roads and local road length. We then fit a second stage

Generalized Additive Model (GAM), equation 3, over the residuals from equation 2 at each location and month, smoothing results over space.

$$PM_{2.5_{resi_{sm}}} = \alpha + s(X_s, Y_s)_m + s(PercentImpervious_s) + s(Elevation) + \varepsilon_{sm}$$

Equation 3

In equation 3, $PM_{2.5}$ residuals at each location, s, and month, m, are regressed on a spatial spline of the projected X and Y locations of each point and spatial splines of the percent impervious surface area and elevation at each location, plus the random error, ε.

a. No cloud gap-filled satellite model

We adapt the model presented in Kloog et al (2014) to predict $PM_{2.5}$ concentrations on each day at locations where AOD was not available. This model, presented in equation 4, is a generalized additive model (GAM) with the mean $PM_{2.5}$ from all monitors in the study area on that day, a smooth function of latitude and longitude, and a random intercept for each cell.

$$PredPM_{ij} = (\alpha + u_i) + (\beta_1 + v_i)MPM_j + s(X_i, Y_i) + \varepsilon_{ij}$$ Equation 4

In equation 4 the predicted PM, PredPM, at each location, i, and time point, j, is modeled as a function of intercepts for the entire study area, α, and each grid cell, u_i, and slopes for the mean $PM_{2.5}$ concentration, MPM overall, β_1, and at each location, v_i, plus a smooth function of the latitude and longitude, $s(X_i, Y_i)$.

b. Cloud gap-filled satellite model

Finally, for the cloud gap-filling model, we adapt the no cloud gap-filling model, adding additional meteorological and cloud parameters to better predict $PM_{2.5}$ concentrations when AOD is missing. In this GAM model, represented by equation 5, the following predictors were additionally included; Cloud AOD (COD), cloud emissivity (CE), Temperature (Temp), Convective precipitation (CPrec), modeled $PM_{2.5}$ from GEOS-Chem

(PM25), shortwave radiation downwards (SWIR), longwave radiation downwards (LWIR), elevation, percentage of impervious surface area (PImperv), PBL height (PBLh), Fire counts within a 25 km buffer (FireCounts), indicator for NEI 2008 source emissions (NEI2008), and distance to the nearest primary or secondary road (DistRds).

$$
\begin{aligned}
PredPM_{ij} = (\alpha + u_i) + (\beta_1 + v_i)MPM_j + s(X_i, Y_i) + s\left(COD_{ij}\right) + \beta_2 CE_{ij} \\
+ s\left(Temperature_{ij}\right) + s\left(CPrec_{ij}\right) + s\left(PM25_{ij}\right) + s\left(SWIR_{ij}\right) \\
+ s\left(LWIR_{ij}\right) + s(Elevation_i) + s(PImperv_i) + s\left(PBLh_{ij}\right) \\
+ s\left(FireCounts_{ij}\right) + \beta_3 NEI2008_i + \beta_4 DistRds_i \\
+ s\left(Temperature_{ij}, RH_{ij}\right) + s\left(COD_{ij}, CE_{ij}\right) \\
+ c\left(CPrec_{ij}, WindSpeed_{ij}\right) + s\left(PM25_{ij}, LWIR_{ij}\right) \\
+ s\left(PM25_{ij}, SWIR_{ij}\right) + \varepsilon_{ij}
\end{aligned}
$$

Equation 5

In equation 5, the predicted PM, PredPM at each location, i, and time point, j, is modeled as in equation 4, plus the addition of 18 parameters.

V. Methods – Epidemiology models

Exposure estimates for daily $PM_{2.5}$ produced from the No cloud and Cloud gap-filled and ungap-filled satellite models were aggregated to daily ZIP code level estimates, with ZIP codes defined according to the 2010 Census TIGER definitions. [18] These ZIP code-level daily estimates of $PM_{2.5}$ concentration were then paired with daily counts of ED visits for asthma/wheeze, otitis media, and upper respiratory infection, and case-crossover models with stratification by ZIP code year, and month were used to obtain OR estimates between ED visits for each of the three outcomes and the three exposure estimates. Case-crossover models included a number of variables to control for residual within-month and

seasonal confounding. We included cubic polynomials for same day temperature, humidity and day of year as well as indicators for day of week, warm season, holiday and lag holiday. We additionally included interaction terms between the warm season indicator and temperature, humidity, day of week, holiday and lag holiday.

We also conducted sensitivity analyses to investigate the impact of effect modification by cloudiness and existence of an ungap-filled $PM_{2.5}$ estimate. To accomplish this we followed the same methodology as the above, also matching cases to control days based off of cloudiness and existence of an ungap-filled $PM_{2.5}$ estimate. The same set of variables as were used in the main models was used to control for residual within-month and seasonal confounding.

Finally, we examined the effectiveness of the filtering technique used in Strickland et al [8], where to prevent weakening of effect estimates resulting from missing AOD observations in the exposure model, ZIP codes and days where less than 30% of the exposure observations were valid were screened out from the analysis. We screened ungap-filled estimates using this same method.

VI. Results

Ten-fold cross-validation R^2 estimates were 0.78 for the ungap-filled satellite model, 0.74 for the cloud gap-filled satellite model, and 0.70 for the no cloud gap-filled satellite model. These results, reported in table 1, indicate model fits that are comparable to reported results for similar models in the southeast. [24] [25] Examining relative differences at the daily level between the no cloud and cloud models reveals a slight negative average relative difference, indicating that most locations had slightly lower estimates under the cloud than the no cloud model. A few exceptions, such as near roads and in locations with $PM_{2.5}$

emissions from NEI 2008 are visible in figure 1, below, which maps these average relative differences at each location.

ZIP code level concentrations of $PM_{2.5}$ averaged 13.5 $\mu g/m^3$ under the ungap-filled model. Under the No cloud gap-filled model, concentrations averaged 13.6 $\mu g/m^3$, and under the cloud gap-filled model concentrations averaged 12.9 $\mu g/m^3$. Reflecting the lower average concentrations in the cloud gap-filled exposure model, ZIP code level concentrations are lower across the state, but particularly in the southern part of the state, relative to the no cloud gap-filled model. Again, some exceptions exist, primarily along road networks where differences between the cloud and no cloud gap-filled models are strongest (see figure 1). These differences aside, spatial patterns in the three exposure layers at the zip code level are fairly similar.

After aggregation to ZIP codes, concentrations followed the same general pattern, see table 2, averaging 13.48 $\mu g/m^3$ for the ungap-filled model, 13.58 $\mu g/m^3$ for the no cloud gap-filled model, and 12.87 $\mu g/m^3$ for the cloud gap-filled model. A number of ZIP codes, 200,607, were missing ungap-filled estimates, however concentrations were similar between the ungap-filled and no cloud gap-filled, while 475 were missing cloud gap-filled estimates.

Strickland et al. found statistically significant associations for asthma or wheeze and upper respiratory infection, with odds ratios of 1.013 (1.003, 1.023) for asthma or wheeze and 1.015 (1.008, 1.022) for upper respiratory infection. [8] Using the same dataset, albeit restricted to 2003-2005, we observed statistically significant associations, see table 3, for both of these outcomes, as well as for otitis media, under both gap-filled exposure models. Under the ungap-filled exposure model we observed statistically significant results for asthma or wheeze and URI only. Our estimates, even the ungap-filled estimates which would best approximate the Strickland et al. values, are all higher than the original odds

ratios. This is likely a function of the difference in time period between the two studies, even though the same underlying data is used.

We expected to observe that ungap-filled OR estimates would be attenuated towards the null relative to gap-filled estimates, with the cloud gap-filled estimates having the least attenuation and the smallest confidence intervals. We did observe, for the outcomes asthma or wheeze and OM, OR estimates under the ungap-filled satellite model were attenuated towards the null, relative to estimates from the gap-filled satellite models. Confidence interval sizes are also slightly smaller for the gap-filled estimates than for the ungap-filled estimates, a result of including additional cases in the gap-filled results. For the other outcome, URI, ungap-filled estimates were comparable to gap-filled estimates.

The sensitivity analysis results, where estimates were broken down by cloudiness to look for effect modification between the groups, are laid out in figure 3. All three exposure models produce comparable odds ratios under clear and partially cloudy conditions, when cloudcover is less than 80% of a ZIP code on a given day. However, under cloudy conditions, the ungap-filled exposure estimates are attenuated towards the null, relative to the gap-filled estimates. In the case of OM, this attenuation is enough to make the difference between a significant estimate and a non-significant estimate. In the case of OM, we also see some effect modification on cloudy days relative to clear and partially cloudy days, where cloudy effect estimates are significantly higher and exclude the null whereas clear and partially cloudy estimates all include the null.

After screening of ungap-filled exposure estimates where more than 30% of pixels in a given ZIP code on a given day were missing, OR estimates were weaker than before screening for all three outcomes and had larger confidence intervals. For asthma or wheeze, OR values dropped from 1.027 (1.010; 1.044) to 1.021 (0.993; 1.050) and became non-

significant as confidence interval sizes increased. For otitis media, OR estimates dropped from 1.008 (0.994; 1.023) without screening down to 1.004 (0.980; 1.029) with screening. Upper respiratory infection followed the same pattern, decreasing from 1.031 (1.021; 1.042) to 1.028 (1.010; 1.046) with screening

VII. Discussion

We observed statistically significant associations between daily no cloud and cloud gap-filled satellite-based $PM_{2.5}$ exposure estimates at the zip code level and asthma or wheeze, URI, and OM. These findings are broadly in keeping with the existing literature. Pediatric respiratory issues are broadly known to be associated with $PM_{2.5}$ concentrations. [26] Upper respiratory infection, and asthma or wheeze fall into this category. Otitis media, has been shown to be associated with extremely high air pollution exposures (e.g. Household smoke), but associations with ambient levels of air pollutants are inconsistent in the literature. [27] [28]

We observed that ORs for asthma or wheeze and OM were attenuated towards the null when ungap-filled estimates were used, relative to when cloud or no cloud gap-filled estimates were used. This was what we expected to observe, given non-differential exposure misclassification on a continuous outcome. In the sensitivity analysis we broke down results by cloudiness, confirming attenuation towards the null amongst cloudy observations for all three outcomes. This attenuation results from a combination of exposure misclassification and inclusion of additional cloudy cases in the dataset. Exposure misclassification results as ZIP codes and days with estimates from the ungap-filled model may be biased relative to gap-filled estimates since observations were only made over clear locations and observations made under cloudy locations tend to be lower on average. Additional cloudy cases are added into the dataset as ZIP codes and days which do not have an ungap-filled

estimates gain estimates under the gap-filled models. In the case of OM, there is also some evidence of effect modification by cloudiness. For this outcome, only gap-filled cloudy days are associated with an increase in ED visits as a result of same day $PM_{2.5}$ exposure, and all other estimates cross over the null.

Limitations of this study include possible error in the assignment of ambient air pollutant concentrations. Children spend a large amount of their daytime at locations which are not the residence, such as at a school or daycare center. These alternative locations may not be located in the same ZIP code as the residence leading to misclassification of exposure levels. However, since this type of misclassification would have been non-differential relative to the outcome, results should be biased towards the null. Additionally, in this case, all three exposure models would have been equally affected.

Finally, we did not investigate confounding by co-pollutants. This is a potential limitation of the study as clear sky days are also associated with increases in ozone, which has been reported to exacerbate ED visits for asthma. [30] It is possible that confounding from other pollutants could have affected our results. However, this bias, particularly that from ozone should have resulted in an association with $PM_{2.5}$ under clear skies that was higher than that under cloudy skies, effectively causing effect modification by cloudiness. Given the inconclusive results of our sensitivity analysis, it is likely that multi-pollutant models would be revealing in this case. Moreover, the additional uncertainty involved with characterizing ozone concentrations in the context of using multiple exposure models for $PM_{2.5}$ would have complicated the analysis.

VIII. Conclusions

We found statistically significant associations between PM2.5 and pediatric ED visits for asthma or wheeze, upper respiratory infection, and otitis media. Futhermore, we observed that ungap-filled satellite-based estimates were biased towards the null, relative to gap-filled satellite-based estimates, to the extent that different conclusions would have been reached in the case of otitis media. When results were broken down by cloudiness we additionally observed effect attenuation in estimates from the ungap-filled models under cloudy conditions. This attenuation in the results comes from a combination of increased study power via the addition of additional case-days with gap-filled but no ungap-filled exposure estimates and exposure misclassification in the ungap-filled estimates. We did not, however, identify significant differences between the two gap-filling methods, finding, instead, that the cloud and no cloud gap-filling models are roughly equivalent from an epidemiology standpoint. However, these results highlight the importance of gap-filling when using satellite-based models to represent the exposure.

References

1. Dominici, F.; Peng, R.D.; Bell, M.L.; Pham, L.; McDermott, A.; Zeger, S.L.; Samet, J.M. Fine particulate air pollution and hospital admission for cardiovascular and respiratory diseases. Jama 2006, 295, 1127-1134.

2. von Mutius, E.; Sherrill, D.; Fritzsch, C.; Martinez, F.; Lebowitz, M. Air pollution and upper respiratory symptoms in children from east germany. European Respiratory Journal 1995, 8, 723-728.

3. McConnell, R.; Berhane, K.; Gilliland, F.; London, S.J.; Vora, H.; Avol, E.; Gauderman, W.J.; Margolis, H.G.; Lurmann, F.; Thomas, D.C. Air pollution and bronchitic

symptoms in southern california children with asthma. Environmental health perspectives 1999, 107, 757.

4. O'connor, G.T.; Neas, L.; Vaughn, B.; Kattan, M.; Mitchell, H.; Crain, E.F.; Evans, R.; Gruchalla, R.; Morgan, W.; Stout, J. Acute respiratory health effects of air pollution on children with asthma in us inner cities. Journal of Allergy and Clinical Immunology 2008, 121, 1133-1139. e1131.

5. Sheppard, L.; Levy, D.; Norris, G.; Larson, T.V.; Koenig, J.Q. Effects of ambient air pollution on nonelderly asthma hospital admissions in seattle, washington, 1987-1994. Epidemiology 1999, 23-30.

6. Ilabaca, M.; Olaeta, I.; Campos, E.; Villaire, J.; Tellez-Rojo, M.M.; Romieu, I. Association between levels of fine particulate and emergency visits for pneumonia and other respiratory illnesses among children in santiago, chile. Journal of the Air & Waste Management Association 1999, 49, 154-163.

7. Barnett, A.G.; Williams, G.M.; Schwartz, J.; Neller, A.H.; Best, T.L.; Petroeschevsky, A.L.; Simpson, R.W. Air pollution and child respiratory health: A case-crossover study in australia and new zealand. American journal of respiratory and critical care medicine 2005, 171, 1272-1278.

8. Strickland, M.; Hao, H.; Hu, X.; Chang, H.; Darrow, L.; Liu, Y. Pediatric emergency visits and short-term changes in pm2. 5 concentrations in the us state of georgia. Environmental health perspectives 2015.

9. Belle, J.; Liu, Y. Evaluation of aqua modis collection 6 aod parameters for air quality research over the continental united states. Remote Sensing 2016, 8, 815.

10. Belle, J.H.; Chang, H.H.; Wang, Y.; Hu, X.; Lyapustin, A.; Liu, Y. The potential impact of satellite-retrieved cloud parameters on ground-level pm2. 5 mass and

composition. International journal of environmental research and public health 2017, 14, 1244.

11. Yu, C.; Di Girolamo, L.; Chen, L.; Zhang, X.; Liu, Y. Statistical evaluation of the feasibility of satellite-retrieved cloud parameters as indicators of pm2. 5 levels. Journal of Exposure Science and Environmental Epidemiology 2015, 25, 457-466.

12. Lyapustin, A.; Wang, Y.; Laszlo, I.; Kahn, R.; Korkin, S.; Remer, L.; Levy, R.; Reid, J. Multiangle implementation of atmospheric correction (maiac): 2. Aerosol algorithm. Journal of Geophysical Research: Atmospheres 2011, 116.

13. Mitchell, K.E.; Lohmann, D.; Houser, P.R.; Wood, E.F.; Schaake, J.C.; Robock, A.; Cosgrove, B.A.; Sheffield, J.; Duan, Q.; Luo, L. The multi-institution north american land data assimilation system (nldas): Utilizing multiple gcip products and partners in a continental distributed hydrological modeling system. Journal of Geophysical Research: Atmospheres 2004, 109.

14. Mesinger, F.; DiMego, G.; Kalnay, E.; Mitchell, K.; Shafran, P.C.; Ebisuzaki, W.; Jović, D.; Woollen, J.; Rogers, E.; Berbery, E.H. North american regional reanalysis. Bulletin of the American Meteorological Society 2006, 87, 343-360.

15. Justice, C.; Giglio, L.; Korontzi, S.; Owens, J.; Morisette, J.; Roy, D.; Descloitres, J.; Alleaume, S.; Petitcolin, F.; Kaufman, Y. The modis fire products. Remote Sensing of Environment 2002, 83, 244-262.

16. Bey, I.; Jacob, D.J.; Yantosca, R.M.; Logan, J.A.; Field, B.D.; Fiore, A.M.; Li, Q.; Liu, H.Y.; Mickley, L.J.; Schultz, M.G. Global modeling of tropospheric chemistry with assimilated meteorology: Model description and evaluation. Journal of Geophysical Research: Atmospheres 2001, 106, 23073-23095.

17. Fry, J.A.; Xian, G.; Jin, S.; Dewitz, J.A.; Homer, C.G.; LIMIN, Y.; Barnes, C.A.; Herold, N.D.; Wickham, J.D. Completion of the 2006 national land cover database for the conterminous united states. Photogrammetric engineering and remote sensing 2011, 77, 858-864.

18. Marx, R.W. The tiger system: Automating the geographic structure of the united states census. Government publications review 1986, 13, 181-201.

19. Arundel, S.; Phillips, L.; Lowe, A.; Bobinmyer, J.; Mantey, K.; Dunn, C.; Constance, E.; Usery, E. Preparing the national map for the 3d elevation program–products, process and research. Cartography and Geographic Information Science 2015, 42, 40-53.

20. Rao, V.; Tooly, L.; Drukenbrod, J. 2008 national emissions inventory: Review, analysis and highlights; 2013.

21. Platnick, S.; Meyer, K.G.; King, M.D.; Wind, G.; Amarasinghe, N.; Marchant, B.; Arnold, G.T.; Zhang, Z.; Hubanks, P.A.; Holz, R.E. The modis cloud optical and microphysical products: Collection 6 updates and examples from terra and aqua. IEEE Transactions on Geoscience and Remote Sensing 2017, 55, 502-525.

22. Turner, R. Deldir: Delaunay triangulation and dirichlet (voronoi) tessellation. R package version 0.0-8. URL http://cran. r-project. org/web/packages/deldir 2009.

23. EPA. Aqs data mart. https://aqs.epa.gov/aqsweb/documents/data_mart_welcome.html (03/31),

24. Lee, M.; Koutrakis, P.; Coull, B.; Kloog, I.; Schwartz, J. Acute effect of fine particulate matter on mortality in three southeastern states from 2007–2011. Journal of Exposure Science and Environmental Epidemiology 2016, 26, 173.

25. Hu, X.; Waller, L.A.; Lyapustin, A.; Wang, Y.; Al-Hamdan, M.Z.; Crosson, W.L.; Estes, M.G.; Estes, S.M.; Quattrochi, D.A.; Puttaswamy, S.J. Estimating ground-level pm

2.5 concentrations in the southeastern united states using maiac aod retrievals and a two-stage model. Remote Sensing of Environment 2014, 140, 220-232.

26. EPA, D. Integrated science assessment for particulate matter. US Environmental Protection Agency Washington, DC 2009.

27. Heinrich, J.; Raghuyamshi, V.S. Air pollution and otitis media: A review of evidence from epidemiologic studies. Current allergy and asthma reports 2004, 4, 302-309.

28. Girguis, M.S.; Strickland, M.J.; Hu, X.; Liu, Y.; Chang, H.H.; Kloog, I.; Belanoff, C.; Bartell, S.M.; Vieira, V.M. Exposure to acute air pollution and risk of bronchiolitis and otitis media for preterm and term infants. Journal of exposure science & environmental epidemiology 2017, 1.

29. Malig, B.J.; Pearson, D.L.; Chang, Y.B.; Broadwin, R.; Basu, R.; Green, R.S.; Ostro, B. A time-stratified case-crossover study of ambient ozone exposure and emergency department visits for specific respiratory diagnoses in california (2005–2008). Environmental health perspectives 2016, 124, 745.

30. Gent, J.F.; Triche, E.W.; Holford, T.R.; Belanger, K.; Bracken, M.B.; Beckett, W.S.; Leaderer, B.P. Association of low-level ozone and fine particles with respiratory symptoms in children with asthma. Jama 2003, 290, 1859-1867.

Conclusion

This dissertation has focused on missing observations in satellite retrievals of aerosol optical depth (AOD) and the impact of these missing observations on our ability to make accurate estimates of $PM_{2.5}$ concentrations, as well as downstream impacts on our ability to estimate health impacts for this pollutant. In the introduction, we introduced the field of air pollution epidemiology, going over the basics of what $PM_{2.5}$ is and how it has been associated with human health in the past. In chapter 1, we evaluated the coverage and accuracy in the 10 and 3 km AOD products from NASA, some based off of the dark target (DT) algorithm, and some based off of the deep blue (DB) algorithm. We found that, while all four of the products evaluated were highly accurate, coverage only averaged around 30% in the United States. This leaves around 70% of all AOD observations missing. We additionally examined the impact of including lower-confidence retrievals for AOD in a model relating AOD to $PM_{2.5}$, finding that the gains in coverage associated with these noisier observations outweighed the loss of accuracy. Finally, we examined a number of potential sources of bias in AOD retrievals, namely, land cover type, scattering angle, solar zenith angle, sensor zenith angle, normalized difference vegetation index (NDVI), and total column precipitable water (TCPW), finding some amount of bias from all sources. Of particular interest were positive biases in AOD that was associated with developed land, shrub land, high scattering angles, low solar zenith angles, summer months, and low or high NDVI and TCPW. All four products were more susceptible to bias in the Western US than in the Eastern US. Of the four products surveyed, the 10 km DB product was most robust to bias from all sources.

In chapter 2, we characterized the missing data problem, showing that cloud-cover alters $PM_{2.5}$ concentrations beneath the cloud via changes in associated meteorological conditions, wet deposition during precipitation events, and light blockage. We identified negative associations between $PM_{2.5}$ concentrations and relative humidity (RH), planetary boundary layer height (PBL height), and wind speed, which we understood as coming from, respectively, changes in the rate of photooxidation of hydrocarbons, additional area available for vertical mixing, and increased rates of dry deposition and vertical and horizontal mixing. We additionally identified changes in speciation that occur under clouds as a result of light blockage. Namely, thick afternoon clouds are associated with decreases in the sulfate component of $PM_{2.5}$, while thick morning clouds were associated with increases in the organic carbon component of $PM_{2.5}$. Precipitation was associated with a general decrease in $PM_{2.5}$ concentrations, as well as with changes in speciation, with indications that soluble components of $PM_{2.5}$ were more likely to be deposited to the surface than non-soluble components, such as OC. We additionally demonstrated that gap-filling methods that account for cloud-cover produce estimated concentrations and spatial patterns of concentrations that are different from those obtained without gap-filling or by using a gap-filling method that doesn't account for the impact of cloud-cover.

In chapter 3, we examined the impact of different satellite gap-filling techniques on odds ratio estimates for the relationship between pediatric ED visits for asthma or wheeze, upper respiratory infection and otitis media and $PM_{2.5}$ concentrations. We found that when the satellite model was left ungap-filled, meaning that missing AOD observations were left missing in the final $PM_{2.5}$ estimates, odds ratios were attenuated towards the null for asthma or wheeze and otitis media, relative to odds ratios obtained when using any gap-filling technique. We further examined OR estimates stratified on

cloudiness, defining clear as having less than 20% cloud, partially cloudy as having between 20% and 80% and cloudy as having greater than 80% cloud. In stratified analyses, ungap-filled effect estimates were attenuated towards the null relative to estimates that use gap-filled exposure models.

Our results highlight the problem of missing observations in satellite retrievals, demonstrating the importance of handling these observations and imputing any missing values, when estimating $PM_{2.5}$ concentrations, particularly if these estimates are used in the context of determining human health impacts.

Figures and Tables

Chapter 1: Evaluation of Aqua MODIS collection 6 AOD parameters for air quality research over the continental United States

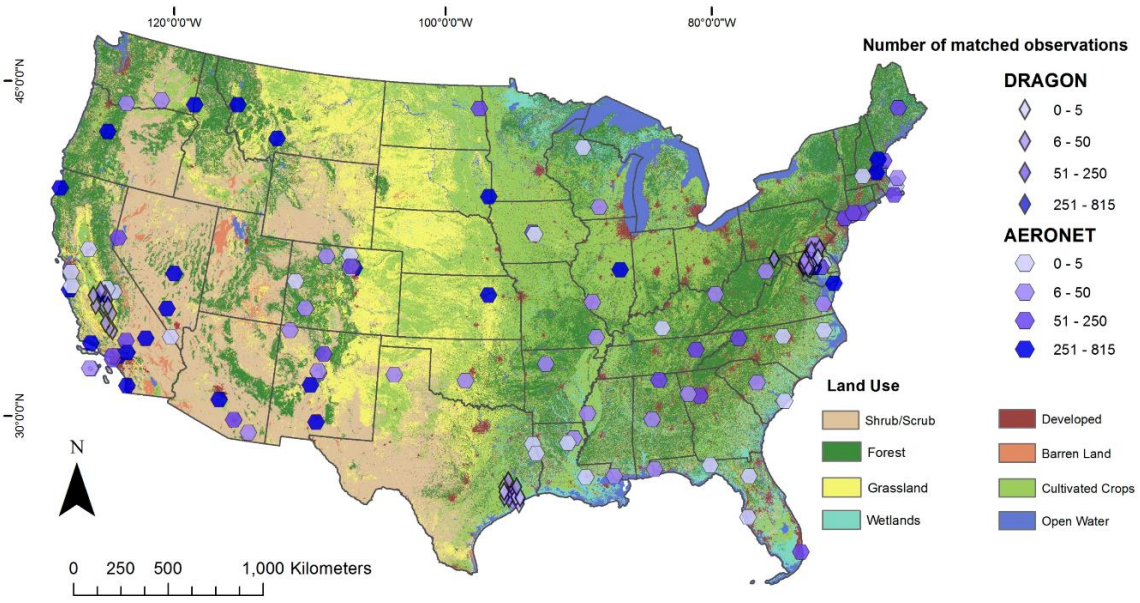

Chapter 1.Figure 1. Spatial distribution of AERONET (hexagons) and DRAGON (diamonds) sites over the study period from 1 January 2004 to 31 December 2013. The color of the symbols represents the number of collocations at each site.

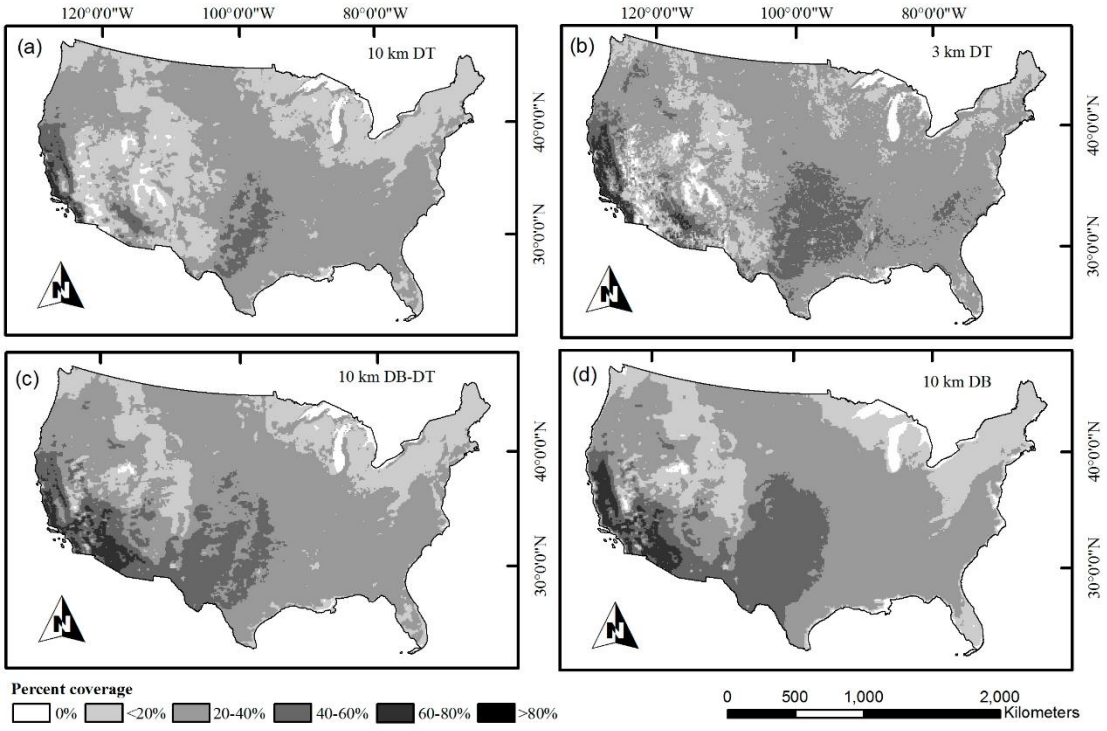

Chapter 1.Figure 2. Mean coverage statistics for high confidence AOD retrievals in the CONUS for 10 km DT (a); 3 km DT (b); 10 km DB-DT (c); and 10 km DB (d). Coverage is calculated as the percentage of days between 1 January 2004 and 31 December 2013 with a valid MODIS retrieval from Aqua.

AOD Parameter	Coverage % (QAC 3 Only)	Coverage % (QAC 1, 2, 3)
3 km DT	28.2	28.9
10 km DT	24.3	32.8
10 km DB-DT	29.7	31.1
10 km DB	28.9	49.6

Chapter 1.Table 1. Coverage statistics for both QAC 3 retrievals only, and for all AOD retrievals. Coverage is calculated as the percentage of days with a valid Aqua retrieval for each AOD parameter.

Region	QAC	Parameter	N	Error	Intercept	Slope	R	% Above EE	% Below EE	% Inside EE
West	1	3 km DT	546	0.02	0.02	1.03	0.86	9.0	0.9	90.1
		10 km DT	1487	0.04	0.05	1.46	0.58	43.4	1.6	55.0
		10 km DB-DT	482	0.01	0.01	1.06	0.85	7.3	1.5	91.3
		10 km DB	10603	0.04	0.07	1.01	0.52	42.0	2.0	55.9
	2	10 km DT	2577	0.08	0.08	1.30	0.58	58.1	2.4	39.6
		10 km DB-DT	1321	0.01	0.03	0.95	0.47	27.0	3.3	69.6
		10 km DB	2316	0.01	0.04	0.90	0.62	27.8	3.4	68.9
	3	3 km DT	6251	0.06	0.06	1.41	0.64	48.9	2.5	48.6
		10 km DT	7814	0.02	0.03	0.98	0.71	25.3	5.6	69.1
		10 km DB-DT	11590	0.01	0.01	1.01	0.73	17.3	5.1	77.6
		10 km DB	10662	−0.00	0.02	0.75	0.63	11.2	5.9	82.9
East	1	3 km DT	883	0.02	0.04	0.80	0.79	12.6	4.6	82.8
		10 km DT	1322	0.02	0.02	1.19	0.82	26.6	5.6	67.8
		10 km DB-DT	440	0.00	0.04	0.50	0.71	3.9	8.4	87.7
		10 km DB	7019	0.05	0.08	0.84	0.76	36.4	1.0	62.7
	2	10 km DT	1538	0.04	0.02	1.26	0.88	37.1	6.1	56.8
		10 km DB-DT	16	0.13	0.17	0.42	0.21	62.5	0.0	37.5
		10 km DB	368	0.05	0.09	0.70	0.73	39.1	1.4	59.5
	3	3 km DT	5616	0.01	−0.01	1.24	0.89	16.0	7.6	76.4
		10 km DT	6409	0.00	−0.01	1.18	0.92	10.8	8.4	80.9
		10 km DB-DT	6750	0.00	−0.01	1.17	0.91	11.7	7.5	80.8
		10 km DB	6617	0.01	0.03	0.79	0.80	10.5	2.6	86.9

N: number of collocations. Error: $\tau M - \tau A$ The intercept, slope, and correlation coefficient (r) are calculated using a linear regression model relating MODIS to AERONET AOD values. The error envelope is defined as $\pm(0.05 + 0.15)\tau A$.

Chapter 1.Table 2. Performance statistics for each AOD parameter.

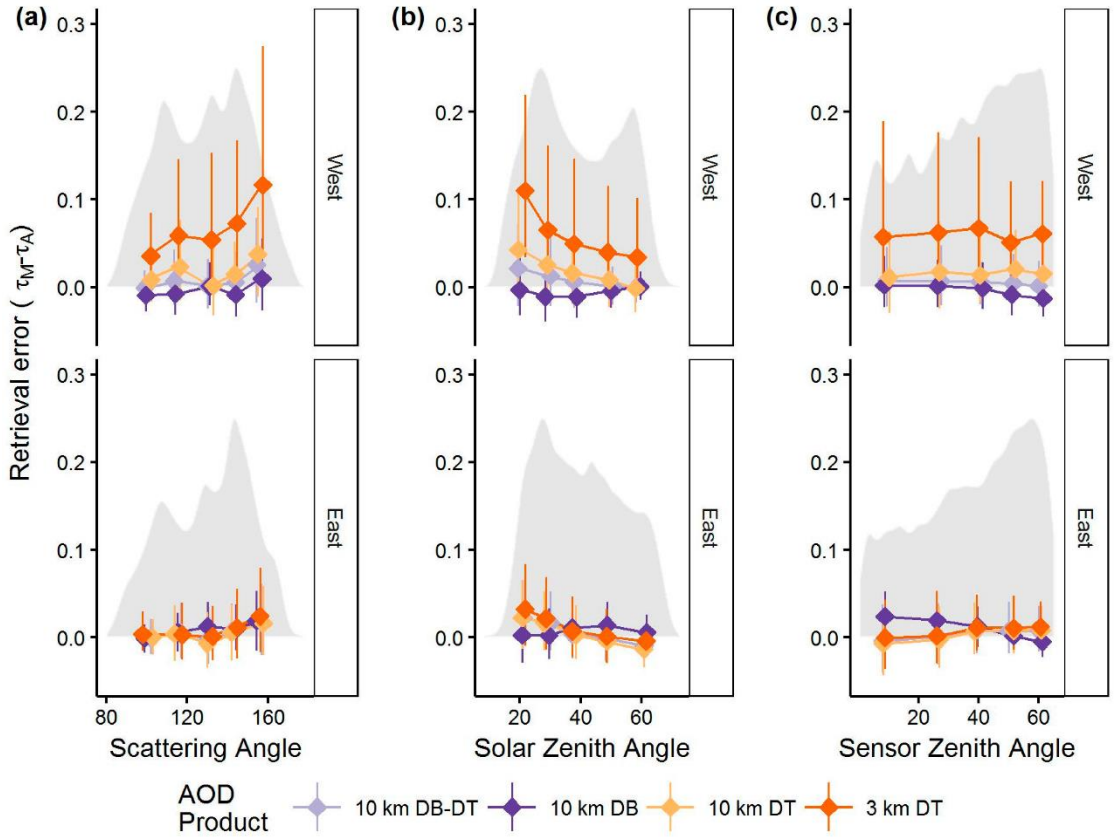

Chapter 1.Figure 3. The dependence of AOD retrieval error and distributions of values for scattering angle (a); solar zenith angle (b); and sensor zenith angle (c). Median error (points) and the IQR (vertical line ranges from 25th to 75th percentile) is shown within quintiles. The distribution of values is shown in the background in gray and represents proportional frequency, where 0.25 on the y-axis represents the most frequent value in the category.

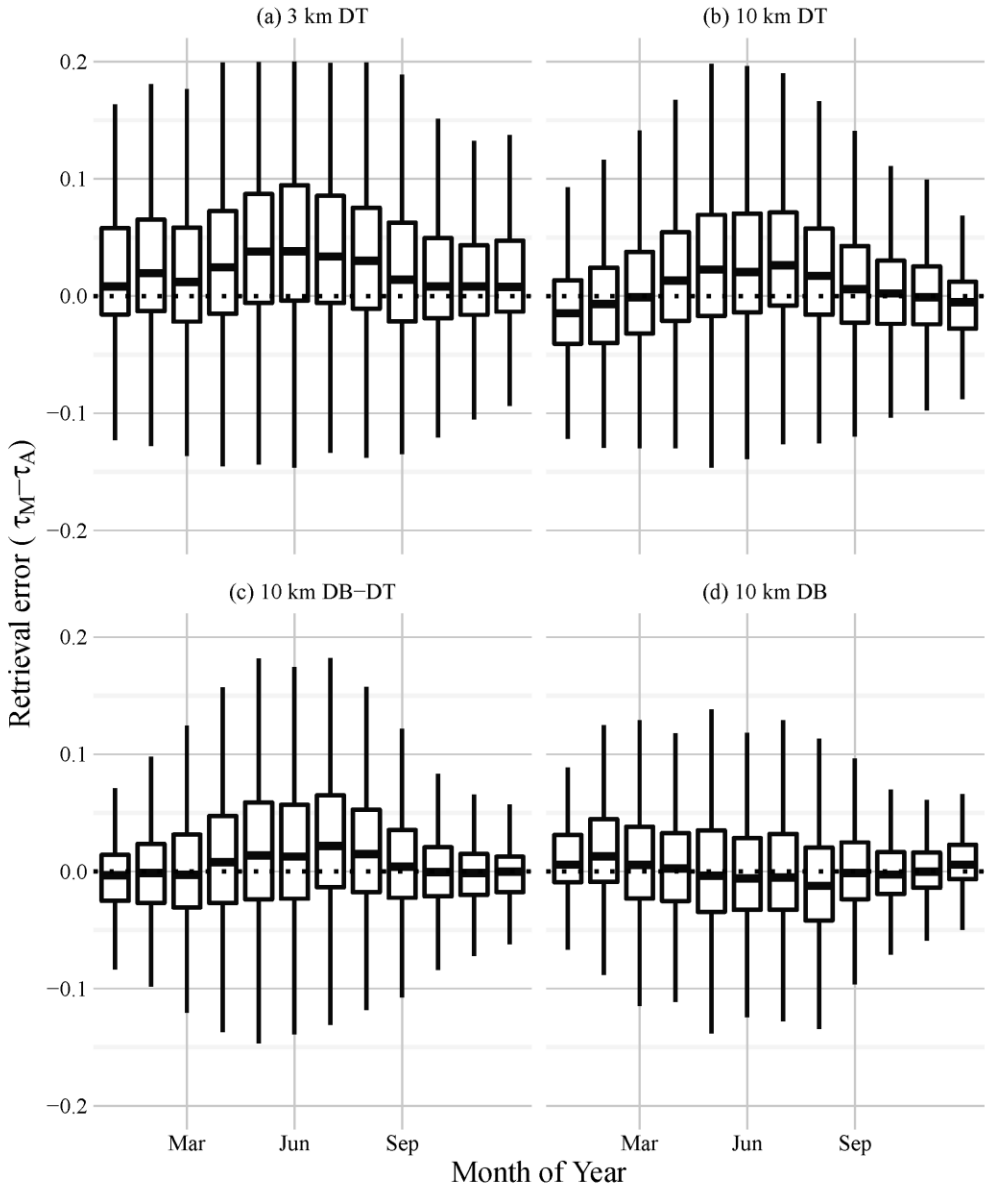

Chapter 1.Figure 4. Boxplot showing the distribution of retrieval errors in MODIS AOD relative to AERONET, for each month of the year, for 3 km DT (a); 10 km DT (b); 10 km DB-DT (c); and 10 km DB (d). For each box, the midline represents the median, upper, and lower hinges represent the 25th and 75th percentiles, whiskers extend out to 5th and 95th percentiles.

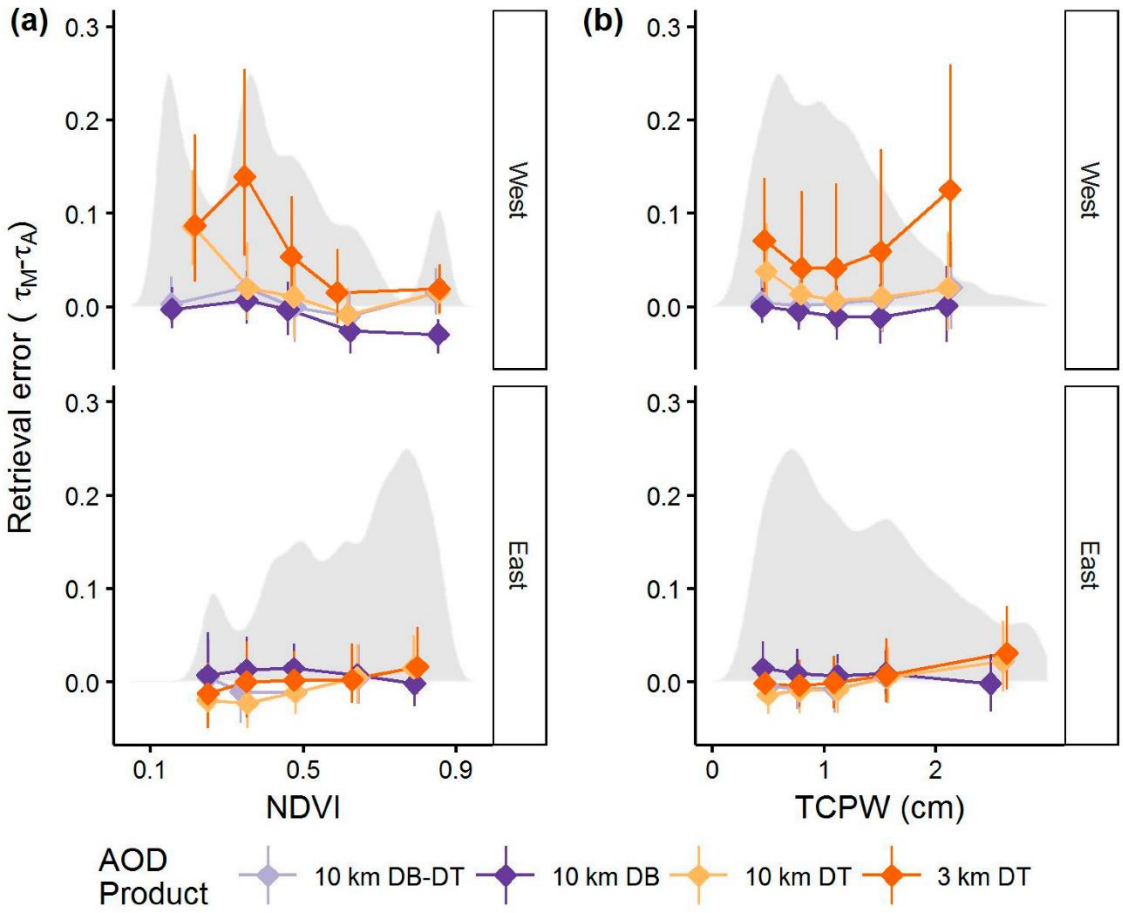

Chapter 1.Figure 5. Dependence of AOD retrieval errors and distributions of values in QAC 3 MODIS AOD for NDVI (a) and TCPW (b). Median AOD retrieval error (dots) and the IQR (vertical line ranges from 25th percentile to 75th) is shown within quintiles of NDVI, and total column precipitable water. The density distribution of values is shown in the background in gray and represents proportional frequency, where 0.25 on the y-axis represents the most frequent value in the category.

Parameter	QAC 3 only			Best of QAC 1, 2, and 3			Filtered & Corrected AOD		
	N	R^2	Fixed Slope	N	R^2	Fixed Slope	N	R^2	Fixed Slope
3 km DT	10,438	0.76	14.4	10,438	0.76	14.4	9680	0.75	20.2
10 km DT	8994	0.72	20.4	11,511	0.77	16.1	10,593	0.75	23.4
10 km DB-DT	8994	0.72	20.4	8994	0.72	20.4	8457	0.71	25.7
10 km DB	8560	0.80	31.2	14,706	0.83	11.7	13,448	0.83	16.7

Chapter 1.Table 3. Performance statistics for each AOD parameter in the Atlanta case study.

Chapter 2: The potential impact of satellite-retrieved cloud parameters on ground-level PM2.5 mass and composition

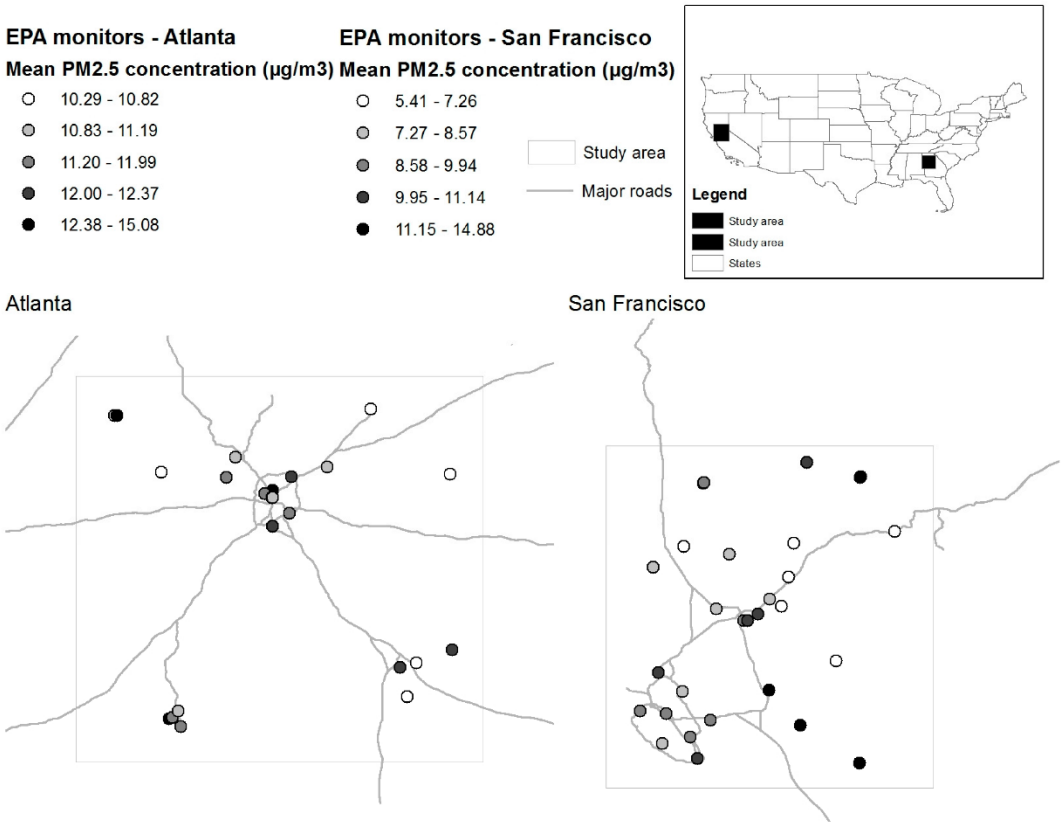

Chapter 2.Figure 1. Study site definitions and Environmental Protection Agency (EPA) ground monitor distributions within the two study areas. Mean PM2.5 concentrations over the study period are displayed for each monitor.

Study site and season		No. of observations	Mean $PM_{2.5}$ ($\mu g/m^3$)	Median $PM_{2.5}$ ($\mu g/m^3$)
San Francisco	Total	23,357	9.5	7.0
	Winter	6393	13.6	10.2
	Spring	5739	6.0	5.5
	Summer	5173	8.1	6.5
	Fall	6052	9.8	7.9
Atlanta	Total	26,369	11.7	10.7
	Winter	6124	10.2	9.2
	Spring	6731	11.7	10.6
	Summer	6677	13.9	12.8
	Fall	6837	10.9	10.2

Chapter 2.Table 1A. Descriptive results for total gravimetric mass

Study site and season		No. of observations	Nitrate *	Sulfate *	Organic Carbon (OC) *
San Francisco	Total	2853	19.7 (2.5)	16.5 (1.3)	47.6 (5.3)
	Winter	722	28.5 (5.3)	7.0 (1.0)	52.0 (8.5)
	Spring	675	17.9 (1.2)	20.5 (1.3)	42.5 (2.9)
	Summer	724	15.2 (1.1)	24.6 (1.6)	43.7 (3.5)
	Fall	732	17.4 (2.2)	14.1 (1.3)	51.9 (6.0)
Atlanta	Total	2410	6.7 (0.7)	32.6 (3.4)	46.5 (5.1)
	Winter	570	11.9 (1.2)	27.3 (2.6)	48.2 (5.0)
	Spring	628	6.8 (0.7)	34.5 (3.6)	45.4 (5.3)
	Summer	607	3.3 (0.3)	37.0 (4.4)	43.4 (4.9)
	605	5.3 (0.5)	31.1 (3.1)	49.2 (5.0)	605
* Values are presented as % total mass (species mass in μg/m3).					

Chapter 2.Table 1B. Descriptive results for species fractions

Observation Category			Atlanta		San Francisco	
			Aqua	Terra	Aqua	Terra
Total gravimetric mass	Matches with MAIAC	All matches	21,700	21,359	19,388	19,390
		Matches with AOD missing	14,470 (67%)	13,050 (61%)	7922 (41%)	7927 (41%)
		Cloud	14,460	13,046	7733	7693
	Including MODIS cloud and RUC/RAP information	Definitively uncloudy	9 (<1%)	2 (<1%)	95 (1%)	178 (2%)
		Possibly cloudy	5860 (41%)	3556 (27%)	2355 (30%)	4326 (56%)
		Cloud—uncertain phase	1100 (8%)	1994 (15%)	1124 (15%)	800 (10%)
		Cloud—Ice cloud	2725 (19%)	3210 (25%)	2397 (31%)	1530 (20%)
		Cloud—Water cloud	4719 (33%)	4269 (33%)	1929 (25%)	1050 (14%)
Speciated Mass Fractions	Matches with MAIAC	All matches	1997	1982	2385	2394
		Matches with AOD missing	1313 (66%)	1192 (60%)	868 (36%)	908 (38%)
		Cloud	1313	1192	868	908
	Including MODIS cloud and RUC/RAP information	Definitively uncloudy	0 (0%)	0 (0%)	0 (0%)	0 (0%)
		Possibly cloudy	464 (35%)	480 (40%)	254 (29%)	458 (50%)
		Cloud—uncertain phase	100 (8%)	141 (12%)	114 (13%)	98 (11%)
		Cloud—Ice cloud	286 (22%)	253 (21%)	252 (29%)	204 (22%)
		Cloud—Water cloud	459 (35%)	311 (26%)	248 (29%)	147 (16%)

Chapter 2.Table 2. Categorization of observations using Multi-Angle Implementation of Atmospheric Correction (MAIAC), then MODIS cloud and rapid update cycle (RUC)/RAPid refresh (RAP) information.

Model R^2 Estimates		Possibly Cloudy	Ice Clouds	Water Clouds
Atlanta	Terra	0.56	0.71	0.74
	Aqua	0.57	0.69	0.73
San Francisco	Terra	0.47	0.60	0.64
	Aqua	0.45	0.54	0.56

Chapter 2.Table 3. Model R^2 estimates

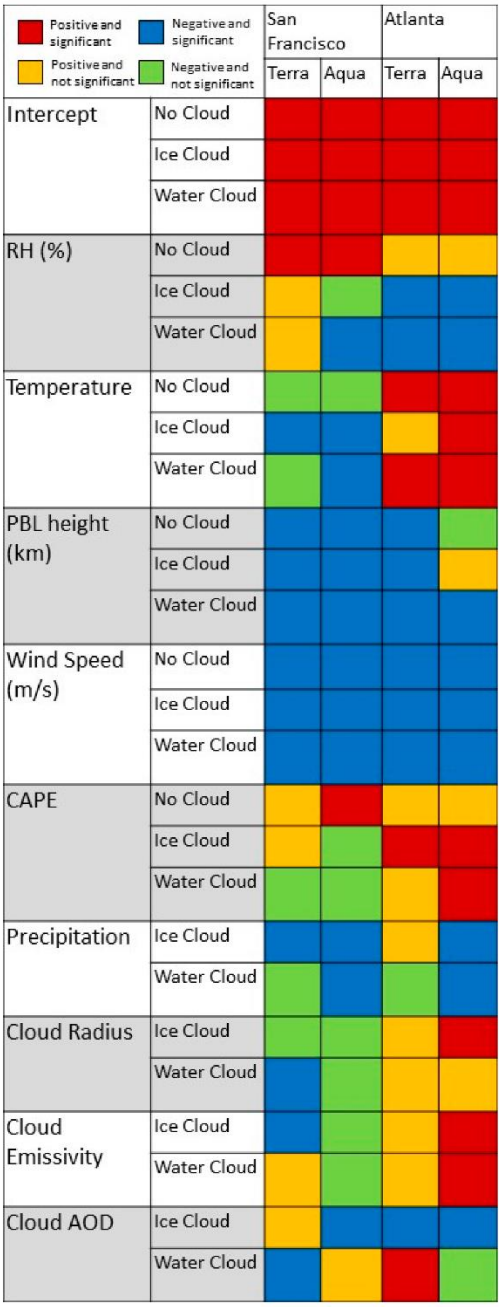

Chapter 2.Figure 2. Effect estimate directions and significance for no cloud, ice cloud, and water cloud models. Each estimate is colored according to its direction (positive or negative) and significance (0.05 level). Excepting the intercepts, a positive estimate means an increase in that variable is associated with an increase in PM2.5 concentrations, a negative estimate with a decrease in concentrations.

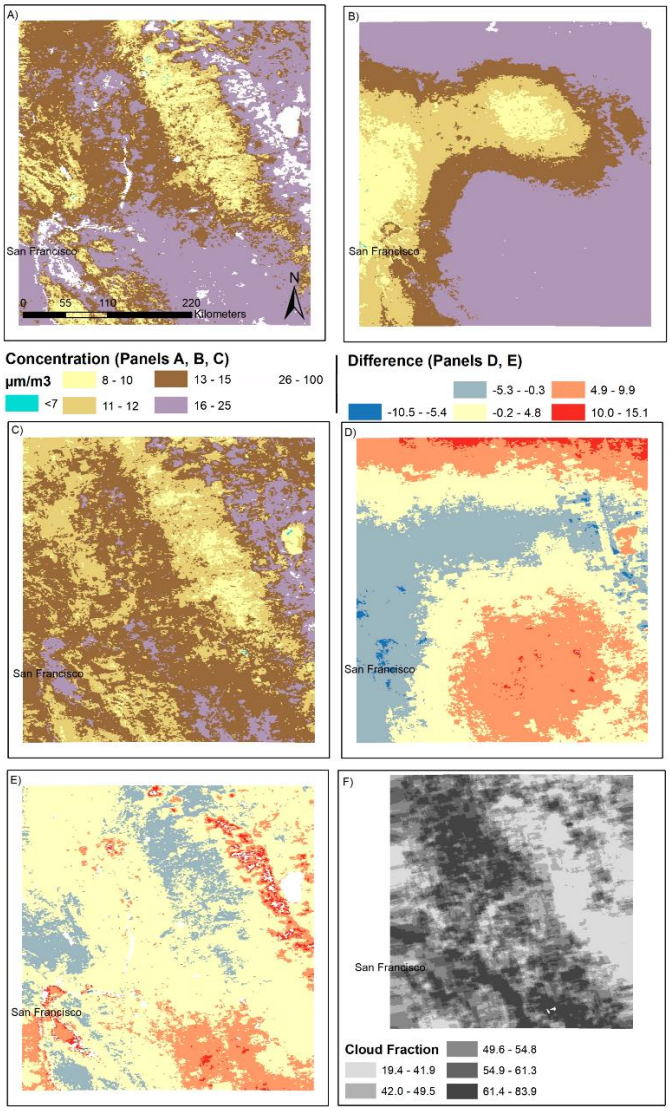

Chapter 2.Figure 3. Case study results in San Francisco for January 2012. Results presented are mean concentrations in µg/m3 over the month of January for: (A) un-gap-filled surface (Equation (2)); (B) Harvard model gap-filled surface (Equations (2) and (3)); (C) Cloud gap-filled surface (Equations (1) and (2)); (D) the difference between the Harvard gap-filled and Cloud gap-filled results at the monthly level; (E) the difference between the ungap-filled and Cloud gap-filled results at the monthly level; and (F) the fraction of days with a water or ice cloud, as detected by the MODIS M*D06 cloud product.

Effect attenuation in the relationship between pediatric ED visits and satellite-based PM2.5 exposure

	Ungap-filled	No cloud gap-filled	Cloud gap-filled
CV R^2	0.78	0.70	0.74

Chapter 3.Table 1 – CV R2 values for each of the three exposure models

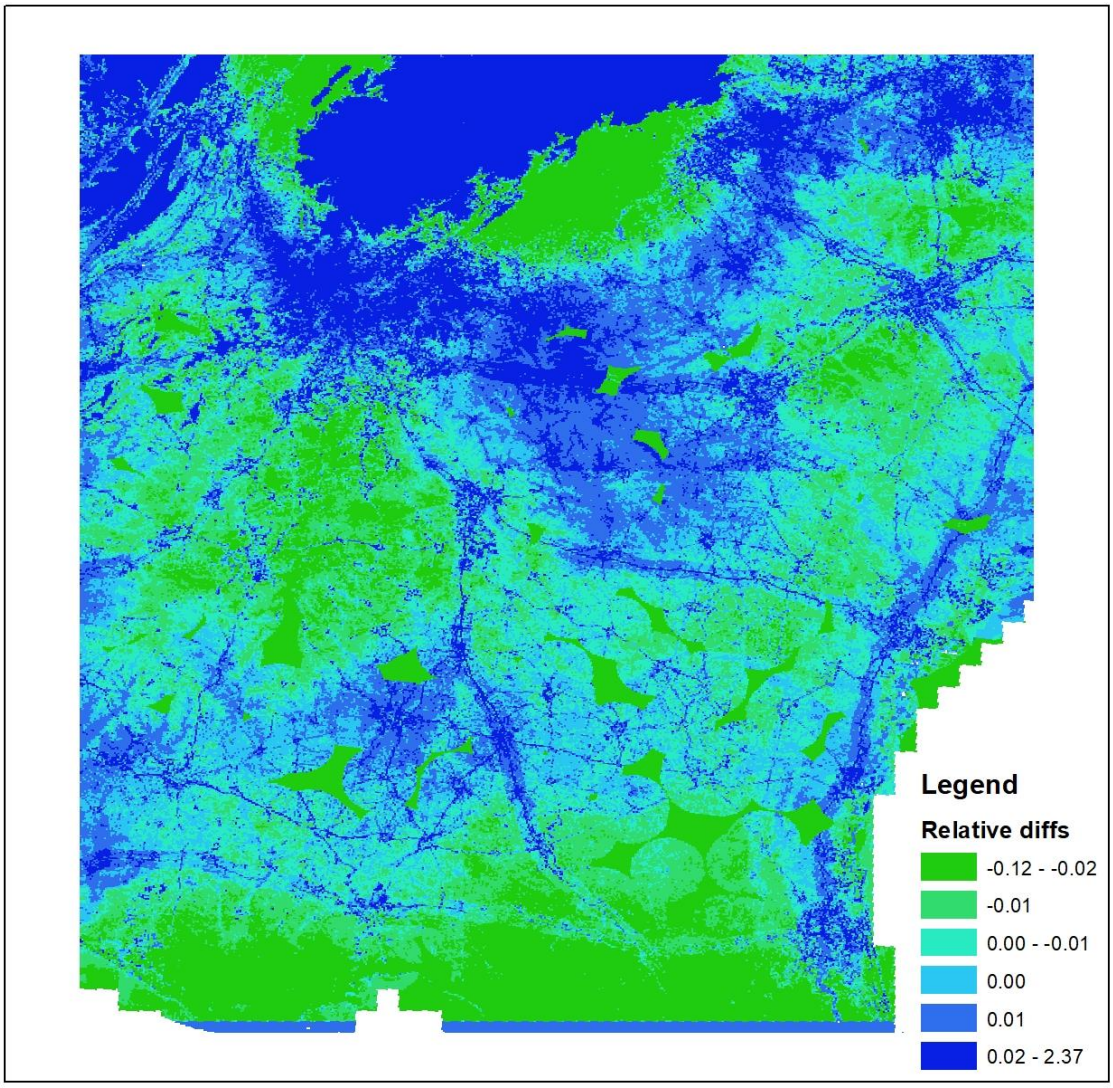

Chapter 3.Figure 1 – 2003-2005 average of daily relative differences between the cloud and no cloud models over the 1 km MAIAC prediction grid

Exposure Model	N	Minimum	P_{25}	P_{50}	Mean	P_{75}	Maximum
Ungap-filled	558,385	2.0	9.51	12.76	13.48	16.38	71.55
No cloud gap-filled	758,992	2.0	9.73	12.76	13.58	16.63	48.11
Cloud gap-filled	758,557	2.0	8.8	11.92	12.87	15.92	52.41

Chapter 3.Table 2 - ZIP code level exposure estimate distributions for the three different exposure models

Outcome group	Ungap-filled model	No cloud model	Cloud model
Asthma or wheeze	1.027 (1.010, 1.044)	1.040 (1.026, 1.055)	1.041 (1.026, 1.056)
Otitis Media	1.008 (0.994, 1.023)	1.024 (1.012, 1.037)	1.023 (1.011, 1.036)
Upper respiratory infection	1.031 (1.021, 1.042)	1.038 (1.029, 1.047)	1.032 (1.023, 1.042)

Chapter 3.Table 3 - Odds ratios per 10 μg/m3 increase in same-day PM2.5 concentrations for ED visits for 6 pediatric health outcomes in Georgia. Odds ratios (ORs) and confidence intervals (CIs), presented as OR (95% CI)

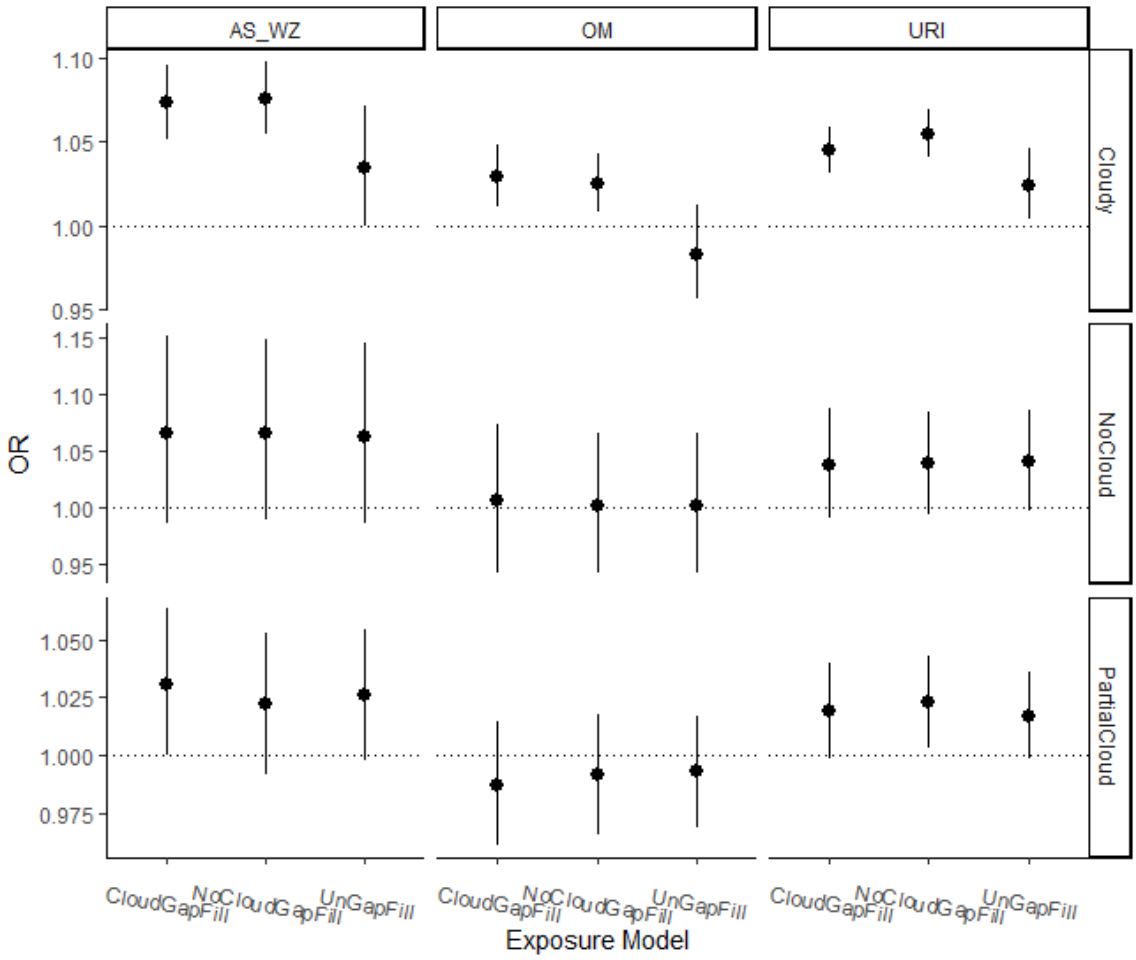

Chapter 3.Figure 2 - Odds ratios per 10 microgram/m^3 increase in same-day PM2.5 concentrations and ED visits for 3 pediatric health outcomes in Georgia under cloudy, partially cloudy (PartialCloud), and clear conditions (NoCloud)